

Supporting Information

Practical chromatography-free synthesis of 2-iodo-*N,N*-diisopropylferrocenecarboxamide and further transformations

William ERB,* Thierry ROISNEL and Vincent DORCET

Univ Rennes, CNRS, ISCR (Institut des Sciences Chimiques de Rennes) – UMR 6226, F-35000 Rennes, France.

Table of contents

Pictures of large scale reactions mixtures and TLC	S2
Crystallography	S7
NMR Spectra	S13
Selected NOESY correlations observed by 2D NMR	S76
HPLC Chromatograms	S77
References	S80

Pictures of large scale reactions mixtures and TLC

Synthesis of ferrocenecarboxylic acid (3)

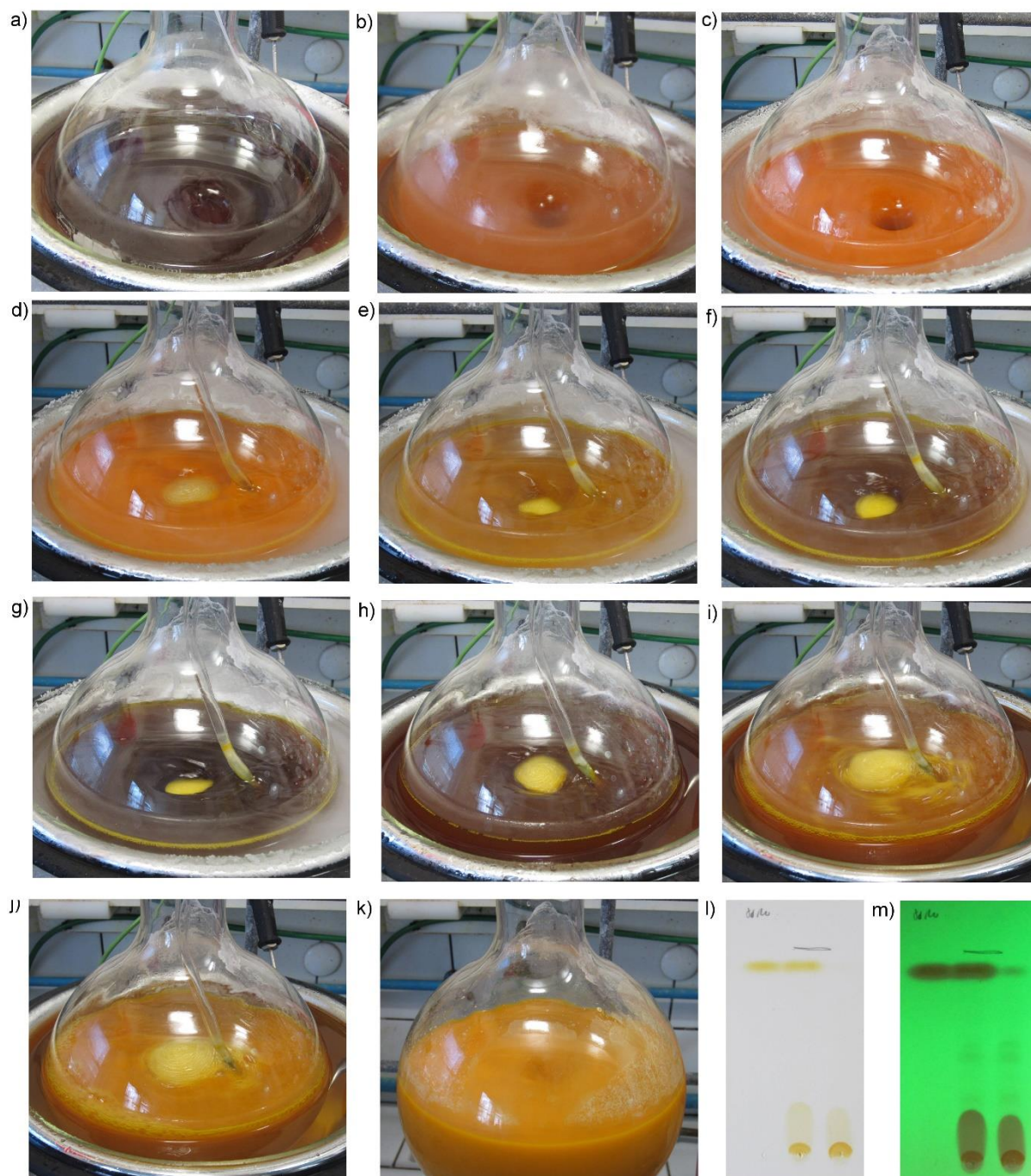


Figure 1. a) Reaction mixture before addition of *t*BuLi; b) Reaction mixture during addition of *t*BuLi; c) Reaction mixture 1 h after addition of *t*BuLi; d) Reaction mixture at the beginning of CO₂ bubbling; e-g) Reaction mixture during CO₂ bubbling; h-i) Reaction mixture warming to rt; j) Reaction mixture warming to rt; k) Reaction mixture when reaction is complete; l) TLC under visible light, PET/EtOAc (80:20); m) TLC under UV light, PET/EtOAc (80:20).

Synthesis of *N,N*-diisopropylferrocenecarboxamide (1)

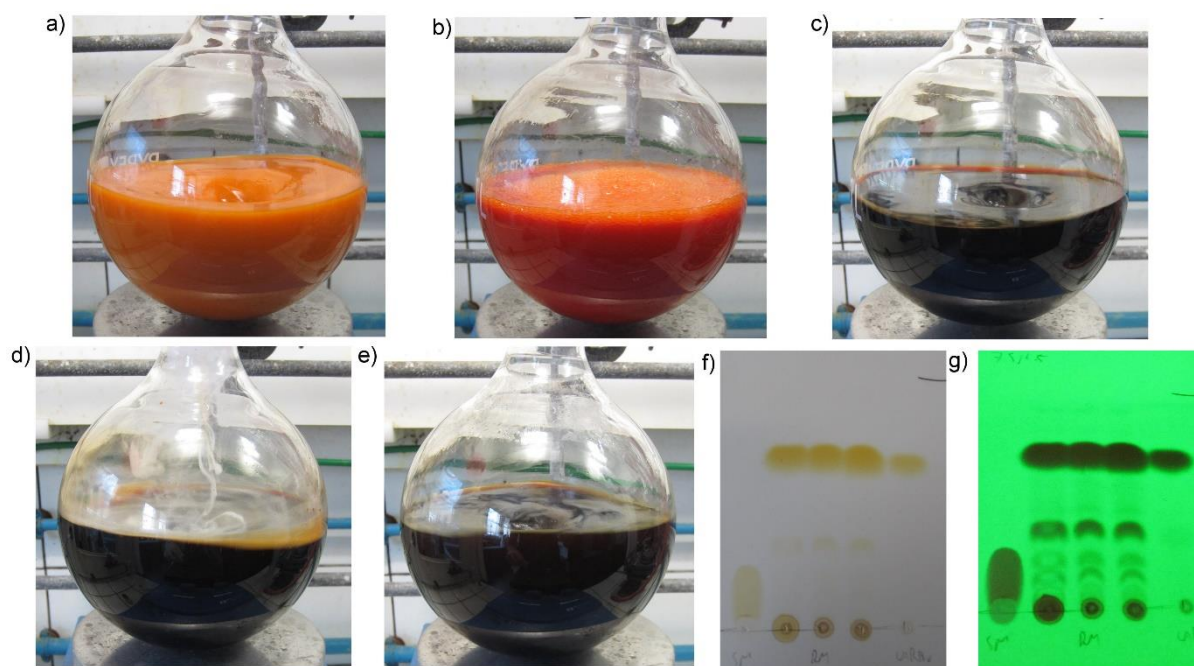


Figure 2. a) Reaction mixture before addition of oxalyl chloride; b) Reaction mixture during and after addition of oxalyl chloride; c) Reaction mixture 30 min after addition of oxalyl chloride; d) Reaction mixture during addition of diisopropylamine; e) Reaction mixture 30 min after addition of diisopropylamine; f) TLC under visible light, PET/EtOAc (75:25); g) TLC under UV light, PET/EtOAc (75:25).

Synthesis of (\pm)-2-iodo-*N,N*-diisopropylferrocenecarboxamide ((\pm)-2) by using *n*BuLi-TMEDA

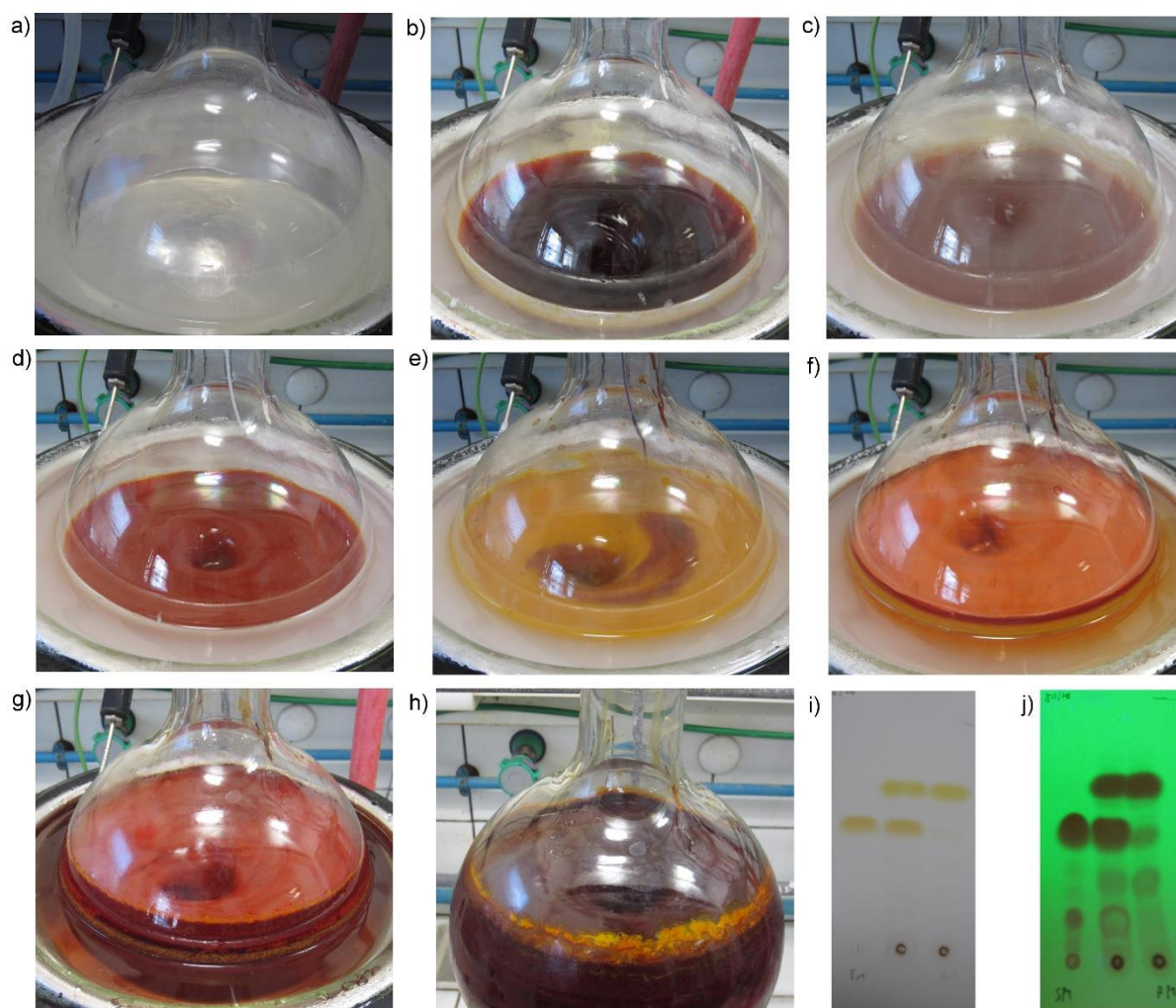


Figure 3. a) The *n*BuLi/TMEDA chelate solution; b) Reaction mixture 1 h after addition of **1**; c-e) Reaction mixture during addition of iodine; f) Reaction mixture after addition of iodine; g-h) Reaction mixture upon warming to rt; i) TLC under visible light, PET/EtOAc (80:20); j) TLC under UV light, PET/EtOAc (80:20).

Synthesis of (\pm)-2-iodo-*N,N*-diisopropylferrocenecarboxamide ((\pm)-2) by using LiTMP-ZnCl₂

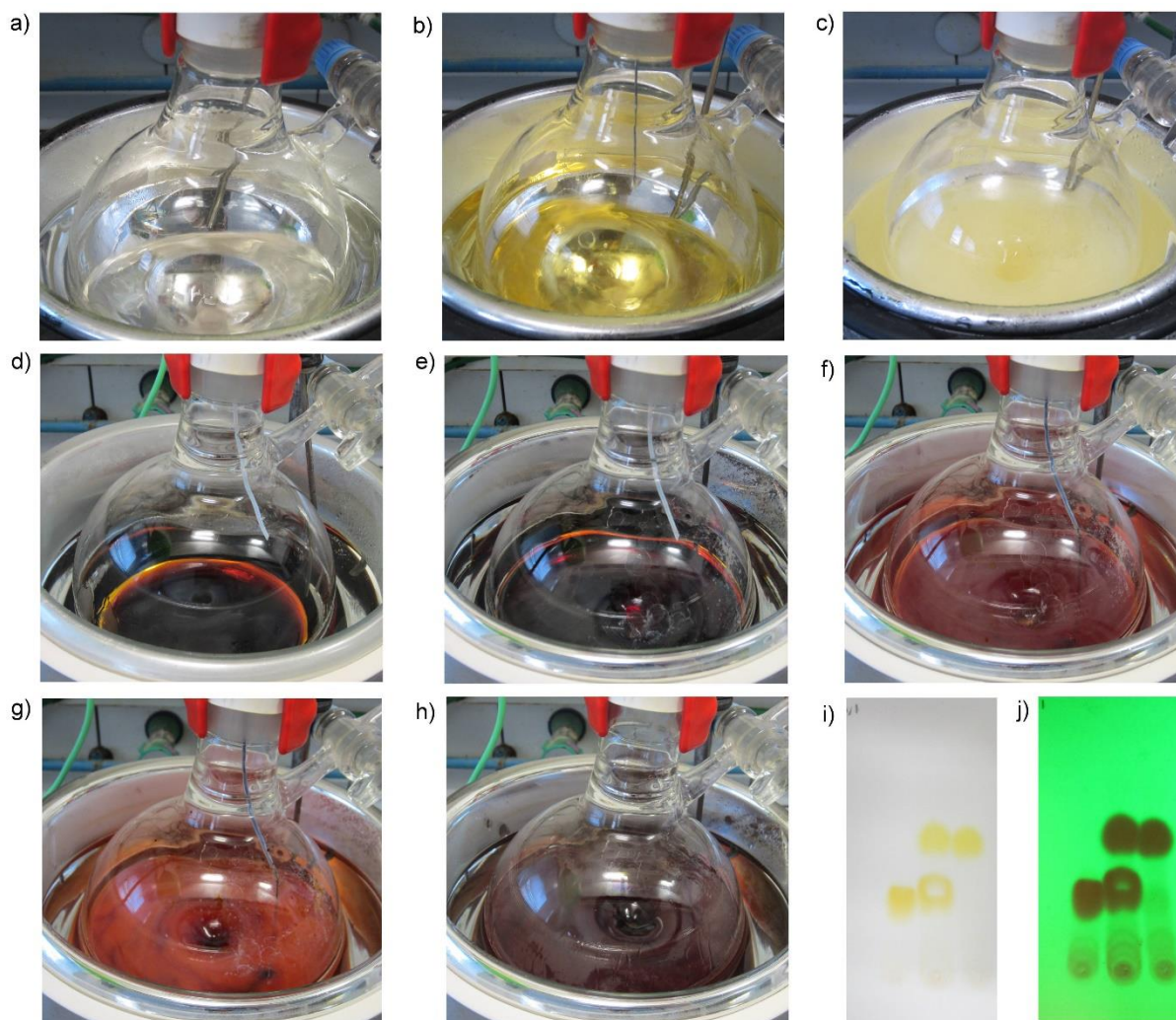


Figure 4. a) The TMPH solution in THF; b) Reaction mixture upon addition of *n*BuLi; c) Reaction mixture 10 min after addition of *n*BuLi; d) The compound **1** and ZnCl₂ solution in THF; e) Reaction mixture 2 h after addition of LiTMP solution; f-g) Reaction mixture upon addition of iodine in solution in THF; h) Reaction mixture after addition of iodine; i) TLC under visible light, PET/EtOAc (90:10); j) TLC under UV light, PET/EtOAc (90:10).

Synthesis of (*S_p*)-2-iodo-*N,N*-diisopropylferrocenecarboxamide ((*S_p*)-2)

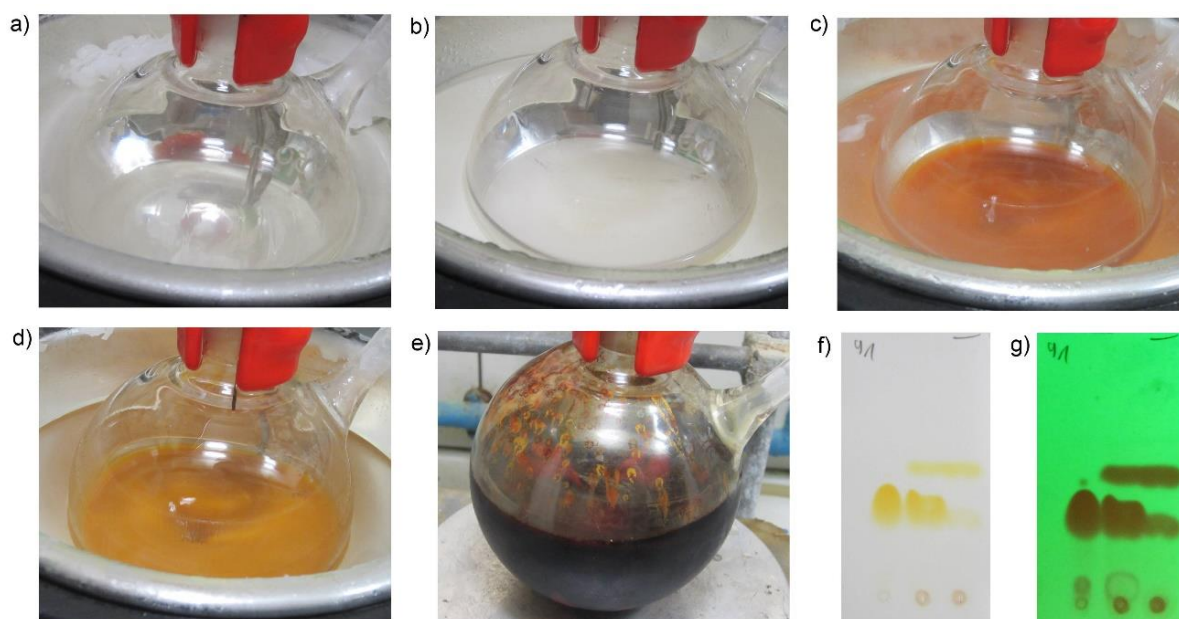


Figure 5. a) The (+)-sparteine surrogate solution; b) The *n*BuLi/(+)-sparteine surrogate chelate solution; c) Reaction mixture 1 h after addition of **1**; d) Reaction mixture during addition of iodine; e) Reaction mixture once at rt; f) TLC under visible light, PET/EtOAc (90:10); g) TLC under UV light, PET/EtOAc (90:10).

Crystallography

For (S_p)-2, (\pm)-4, (\pm)-5, (\pm)-6, (\pm)-7, (\pm)-9, (\pm)-10, (\pm)-11, (\pm)-13, (\pm)-14 and (\pm)-17, the X-ray diffraction data were collected using D8 VENTURE Bruker AXS diffractometer at the temperature given in the crystal data. The samples were studied with monochromatized Mo-K α radiation ($\lambda = 0.71073 \text{ \AA}$). The structure was solved by dual-space algorithm using the *SHELXT* program,¹ and then refined with full-matrix least-square methods based on F^2 (*SHELXL*).² All non-hydrogen atoms were refined with anisotropic atomic displacement parameters. H atoms were finally included in their calculated positions and treated as riding on their parent atom with constrained thermal parameters. The molecular diagrams were generated by MERCURY (version 3.9).

Crystal data for (S_p)-2. $C_{17}H_{22}FeINO$, $M = 439.10$, $T = 150 \text{ K}$; orthorhombic $P 2_1 2_1 2_1$ (I.T.#19), $a = 11.317(2)$, $b = 13.283(3)$, $c = 23.793(6) \text{ \AA}$, $V = 3576.4(15) \text{ \AA}^3$. $Z = 8$, $d = 1.631 \text{ g.cm}^{-3}$, $\mu = 2.568 \text{ mm}^{-1}$. A final refinement on F^2 with 7918 unique intensities and 334 parameters converged at $\omega R(F^2) = 0.1162$ ($R(F) = 0.0537$) for 5744 observed reflections with $I > 2\sigma(I)$. CCDC 1898624.

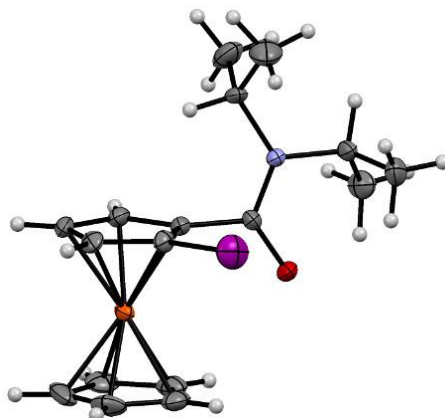


Figure 6. Molecular structure of compound (S_p)-2 (thermal ellipsoids shown at the 30% probability level).

Crystal data for (\pm)-4. $C_{23}H_{27}FeNO$, $M = 389.30$, $T = 150 \text{ K}$; monoclinic $P 2_1/n$ (I.T.#14), $a = 14.9375(19)$, $b = 18.213(2)$, $c = 15.7162(19) \text{ \AA}$, $\beta = 111.799(4)^\circ$, $V = 3969.9(9) \text{ \AA}^3$. $Z = 8$, $d = 1.303 \text{ g.cm}^{-3}$, $\mu = 0.770 \text{ mm}^{-1}$. A final refinement on F^2 with 9016 unique intensities and 477 parameters converged at $\omega R(F^2) = 0.0689$ ($R(F) = 0.0323$) for 7434 observed reflections with $I > 2\sigma(I)$. CCDC 1909912.



Figure 7. Molecular structure of compound (\pm)-4 (thermal ellipsoids shown at the 30% probability level).

Crystal data for (±)-5. $C_{24}H_{29}FeNO_2$, $M = 419.33$, $T = 150$ K; monoclinic $C c$ (I.T.#9), $a = 13.0954(12)$, $b = 21.838(2)$, $c = 7.2746(8)$ Å, $\beta = 90.262(4)$ °, $V = 2080.4(4)$ Å³. $Z = 4$, $d = 1.339$ g.cm⁻³, $\mu = 0.744$ mm⁻¹. A final refinement on F^2 with 4445 unique intensities and 241 parameters converged at $\omega R(F^2) = 0.0787$ ($R(F) = 0.0355$) for 4206 observed reflections with $I > 2\sigma(I)$. CCDC 1909910.

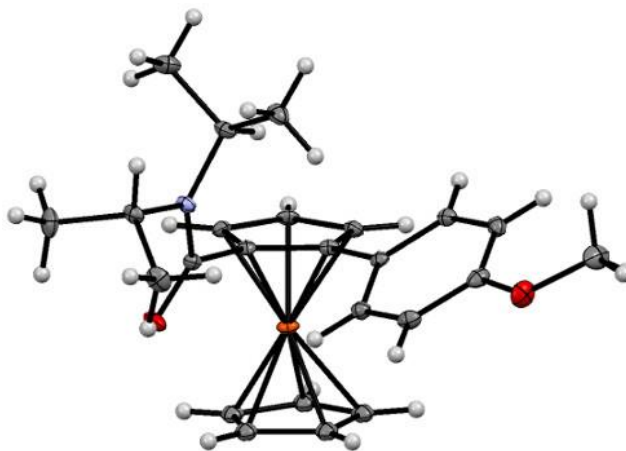


Figure 8. Molecular structure of compound (±)-5 (thermal ellipsoids shown at the 30% probability level).

Crystal data for (±)-6. $C_{25}H_{31}FeNO_3$, $M = 449.36$, $T = 150$ K; monoclinic $P 2_1/c$ (I.T.#14), $a = 10.5791(11)$, $b = 10.6613(11)$, $c = 19.8541(18)$ Å, $\beta = 91.090(4)$ °, $V = 2238.9(4)$ Å³. $Z = 4$, $d = 1.333$ g.cm⁻³, $\mu = 0.699$ mm⁻¹. A final refinement on F^2 with 5095 unique intensities and 277 parameters converged at $\omega R(F^2) = 0.0802$ ($R(F) = 0.0328$) for 4440 observed reflections with $I > 2\sigma(I)$. CCDC 1909911.

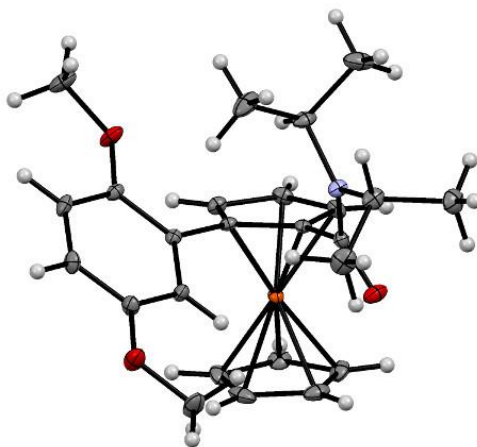


Figure 9. Molecular structure of compound (±)-6 (thermal ellipsoids shown at the 30% probability level).

Crystal data for (±)-7. $C_{27}H_{29}FeNO$, $M = 439.36$, $T = 150$ K; monoclinic $C 2/c$ (I.T.#15), $a = 32.567(4)$, $b = 7.4303(8)$, $c = 22.463(3)$ Å, $\beta = 125.311(4)$ °, $V = 4435.6(9)$ Å³. $Z = 8$, $d = 1.316$ g.cm⁻³, $\mu = 0.698$ mm⁻¹. A final refinement on F^2 with 5072 unique intensities and 275 parameters converged at $\omega R(F^2) = 0.1041$ ($R(F) = 0.0396$) for 4391 observed reflections with $I > 2\sigma(I)$. CCDC 1909914.

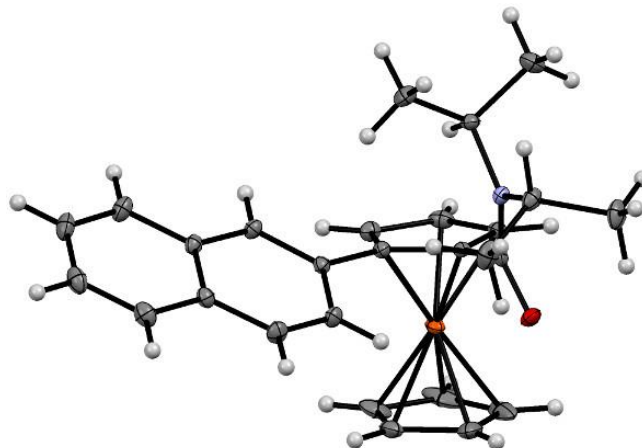


Figure 10. Molecular structure of compound (±)-7 (thermal ellipsoids shown at the 30% probability level).

Crystal data for (±)-9. $C_{23}H_{26}ClFeNO$, $M = 423.75$, $T = 150$ K; monoclinic $P 2_1/c$ (I.T.#14), $a = 14.084(2)$, $b = 10.914(2)$, $c = 13.538(2)$ Å, $\beta = 103.597(6)$ °, $V = 2022.7(6)$ Å³. $Z = 4$, $d = 1.392$ g.cm⁻³, $\mu = 0.890$ mm⁻¹. A final refinement on F^2 with 4556 unique intensities and 248 parameters converged at $\omega R(F^2) = 0.0888$ ($R(F) = 0.0373$) for 3764 observed reflections with $I > 2\sigma(I)$. CCDC 1909913.

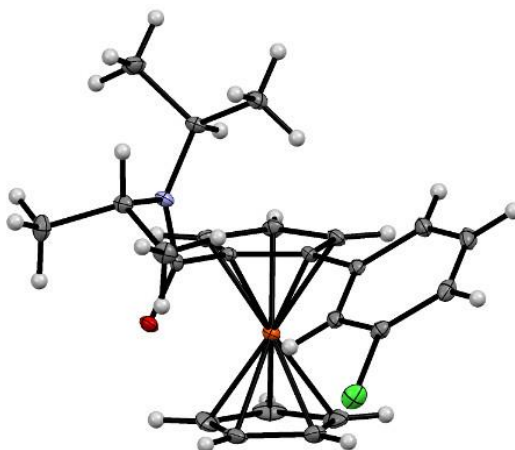


Figure 11. Molecular structure of compound (±)-9 (thermal ellipsoids shown at the 30% probability level).

Crystal data for (±)-10. $C_{24}H_{26}F_3FeNO$, $M = 457.31$, $T = 150$ K; monoclinic $P 2_1/n$ (I.T.#14), $a = 11.8596(11)$, $b = 10.9447(9)$, $c = 16.5793(15)$ Å, $\beta = 89.930(4)^\circ$, $V = 2152.0(3)$ Å³. $Z = 4$, $d = 1.411$ g.cm⁻³, $\mu = 0.741$ mm⁻¹. A final refinement on F^2 with 4888 unique intensities and 273 parameters converged at $\omega R(F^2) = 0.1613$ ($R(F) = 0.0667$) for 4028 observed reflections with $I > 2\sigma(I)$. CCDC 1909915.

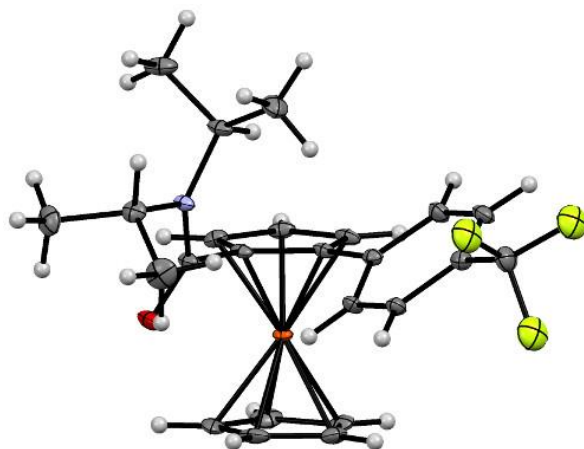


Figure 12. Molecular structure of compound (±)-10 (thermal ellipsoids shown at the 30% probability level).

Crystal data for (±)-11. $C_{24}H_{26}FFeNO_3$, $M = 451.31$, $T = 150$ K; triclinic $P -1$ (I.T.#2), $a = 13.1191(17)$, $b = 13.2958(15)$, $c = 14.9573(16)$ Å, $\alpha = 71.416(4)$, $\beta = 65.243(4)$, $\gamma = 89.744(4)^\circ$, $V = 2220.3(5)$ Å³. $Z = 4$, $d = 1.350$ g.cm⁻³, $\mu = 0.712$ mm⁻¹. A final refinement on F^2 with 10158 unique intensities and 494 parameters converged at $\omega R_F^2 = 0.1025$ ($R_F = 0.0415$) for 8397 observed reflections with $I > 2\sigma(I)$. CCDC 1909916.

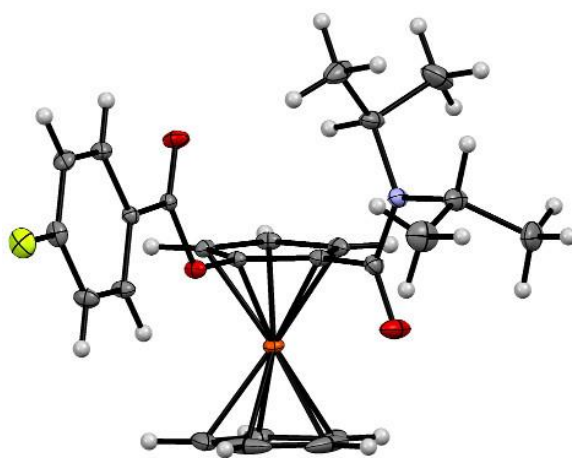


Figure 13. Molecular structure of compound (±)-11 (thermal ellipsoids shown at the 30% probability level).

Crystal data for (±)-13. $C_{26}H_{31}FeNO_3$, $M = 461.37$, $T = 150$ K; monoclinic $P 2_1/c$ (I.T.#14), $a = 13.6489(15)$, $b = 7.5313(6)$, $c = 22.135(2)$ Å, $\beta = 91.206(4)^\circ$, $V = 2274.9(4)$ Å³. $Z = 4$, $d = 1.347$ g.cm⁻³, $\mu = 0.690$ mm⁻¹. A final refinement on F^2 with 5174 unique intensities and 253 parameters converged at $\omega R_F^2 = 0.1510$ ($R_F = 0.0636$) for 3967 observed reflections with $I > 2\sigma(I)$. CCDC 1909919.

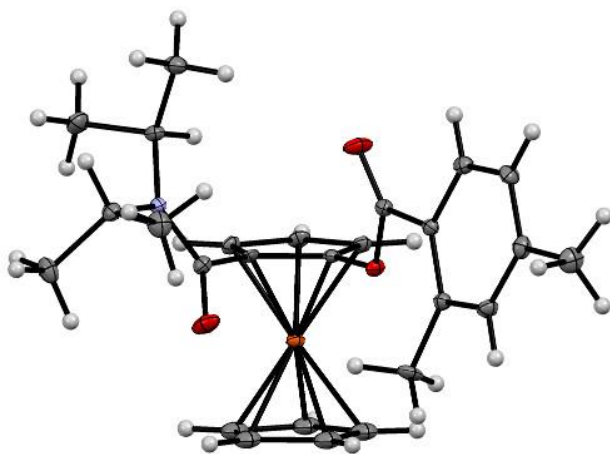


Figure 14. Molecular structure of compound (±)-13 (thermal ellipsoids shown at the 30% probability level).

Crystal data for (±)-14. $C_{26}H_{29}FeNO_5$, $M = 491.35$, $T = 150$ K; triclinic $P -1$ (I.T.#2), $a = 10.4904(12)$, $b = 11.0366(12)$, $c = 11.2048(11)$ Å, $\alpha = 93.771(4)$, $\beta = 108.488(4)$, $\gamma = 100.808(4)^\circ$, $V = 1197.5(2)$ Å³. $Z = 2$, $d = 1.363$ g.cm⁻³, $\mu = 0.666$ mm⁻¹. A final refinement on F^2 with 5501 unique intensities and 303 parameters converged at $\omega R_F^2 = 0.0838$ ($R_F = 0.0342$) for 4987 observed reflections with $I > 2\sigma(I)$. CCDC 1909918.

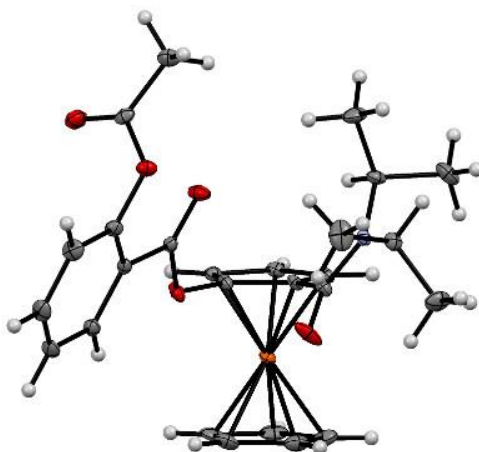


Figure 15. Molecular structure of compound (±)-14 (thermal ellipsoids shown at the 30% probability level).

Crystal data for (±)-16. C₂₈H₃₁Fe₂NO₃, *M* = 541.24, triclinic *P*-1 (I.T.#2), *a* = 7.3553(6), *b* = 10.6982(11), *c* = 15.9658(15) Å, α = 91.068(4), β = 93.064(3), γ = 103.447(3) °, *V* = 1219.5(2) Å³. *Z* = 2, *d* = 1.474 g.cm⁻³, μ = 1.220 mm⁻¹. A final refinement on *F*² with 5588 unique intensities and 311 parameters converged at ωR_F^2 = 0.0753 (*R*_F = 0.0274) for 4758 observed reflections with *I* > 2σ(*I*). CCDC 1909917.

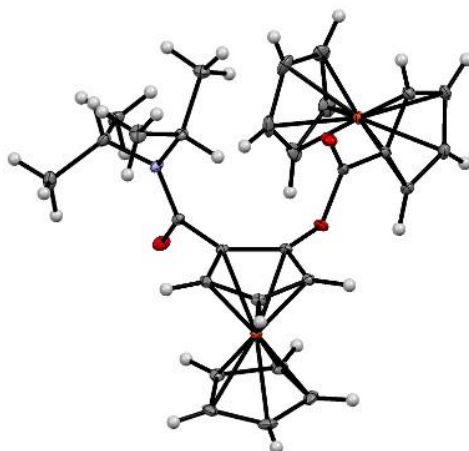
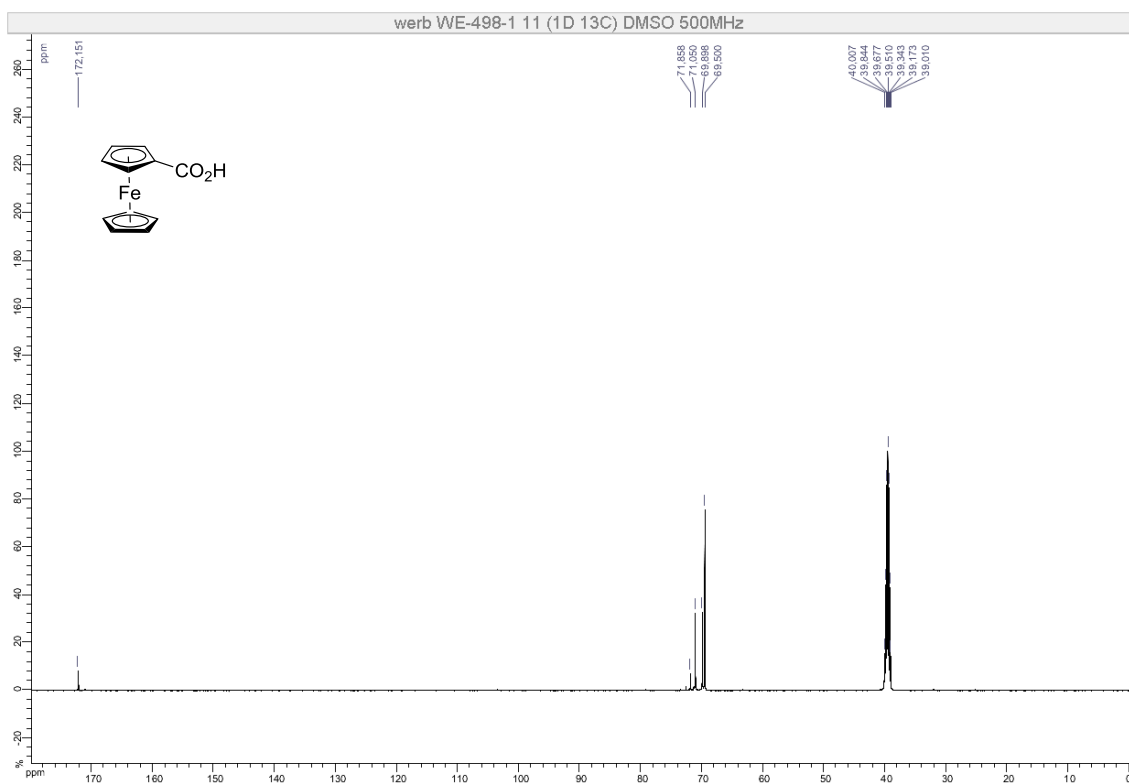
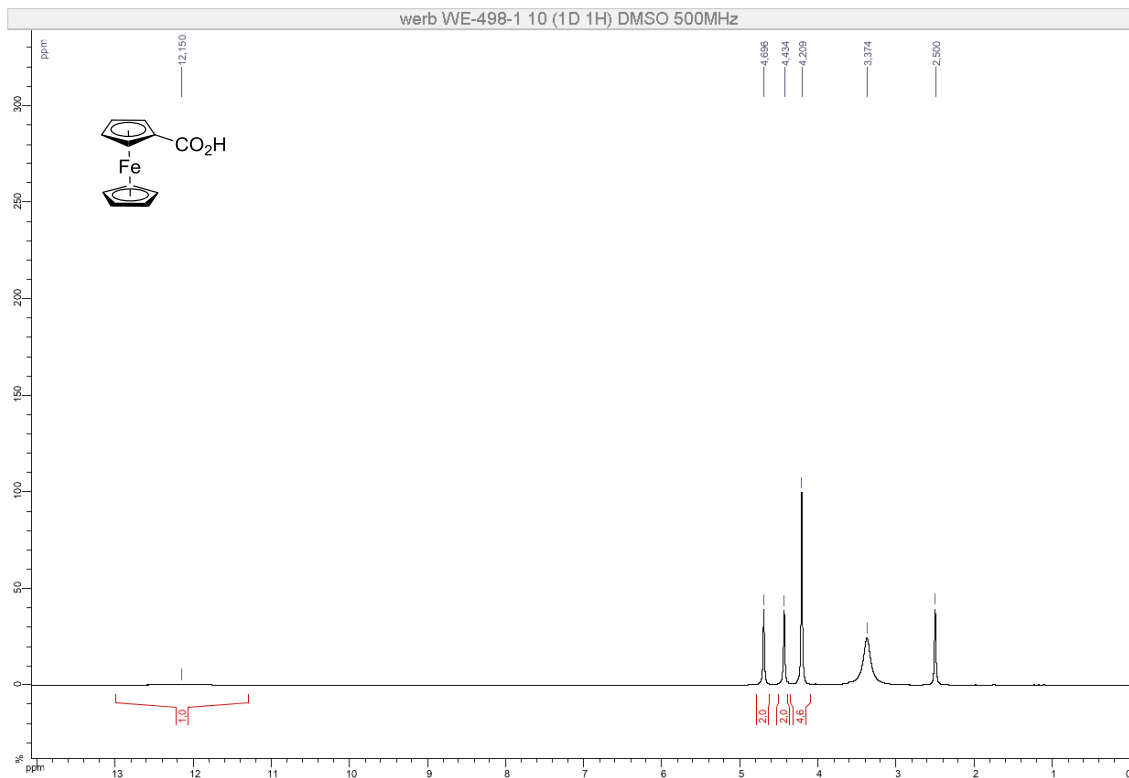
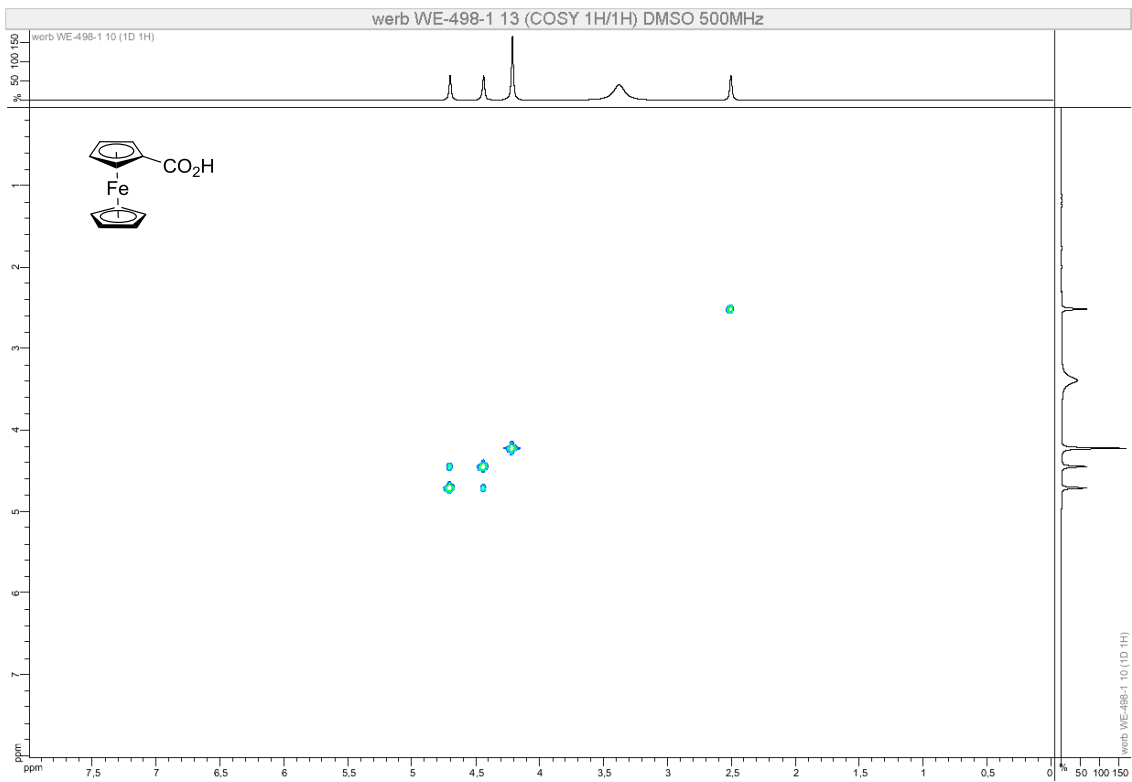
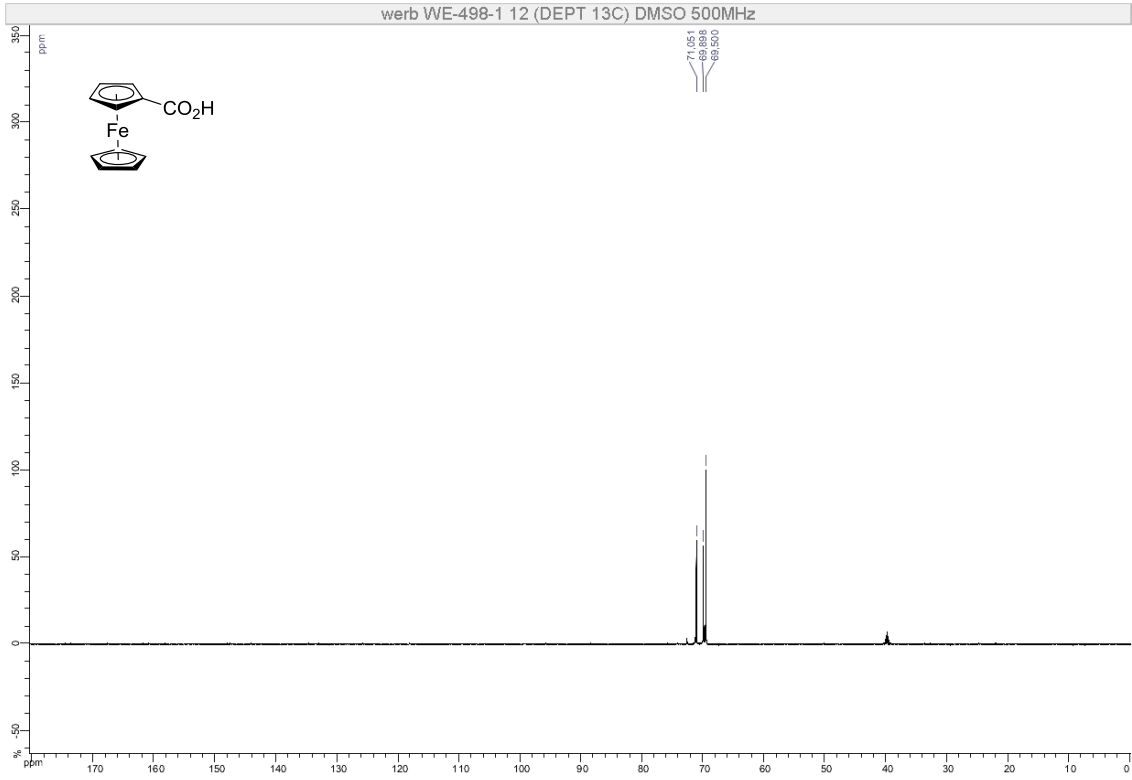


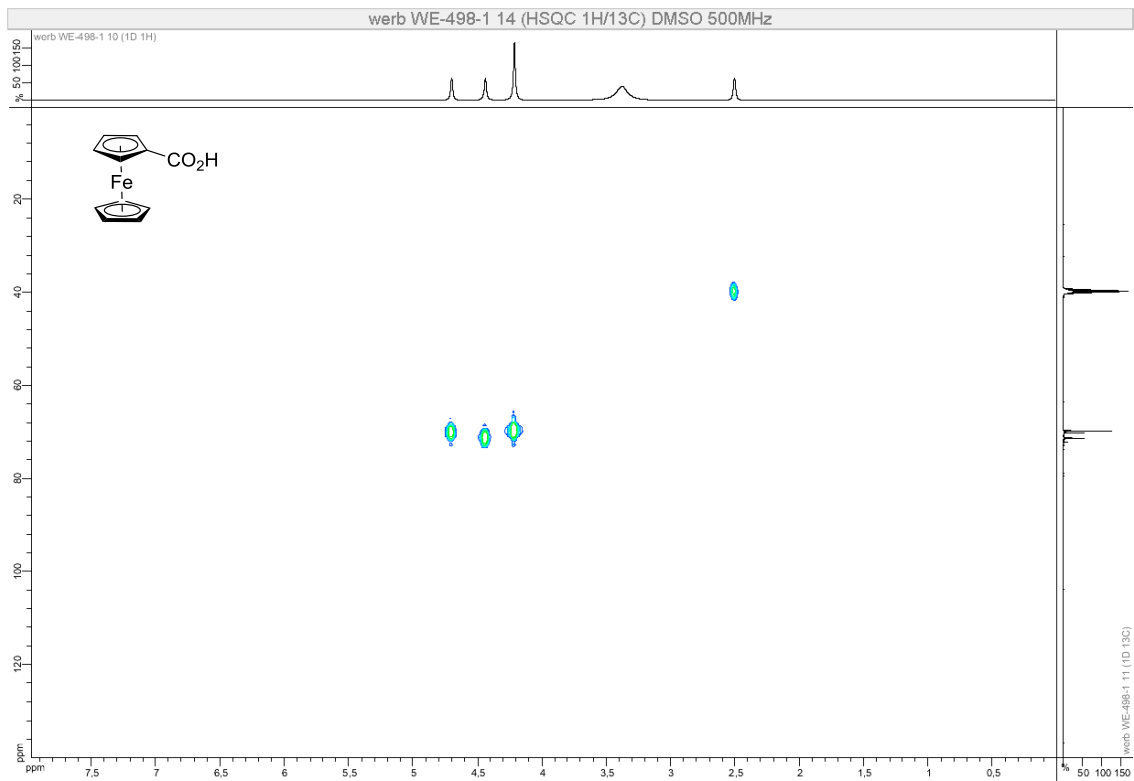
Figure 16. Molecular structure of compound (±)-16 (thermal ellipsoids shown at the 30% probability level).

NMR Spectra

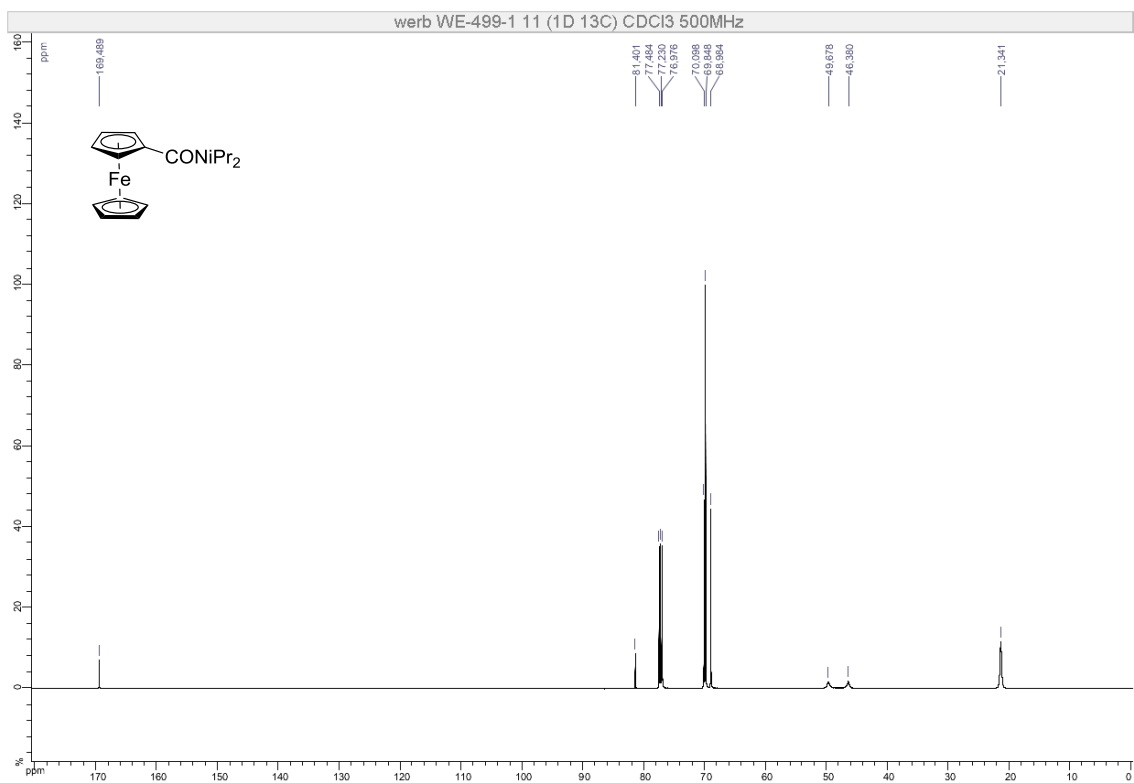
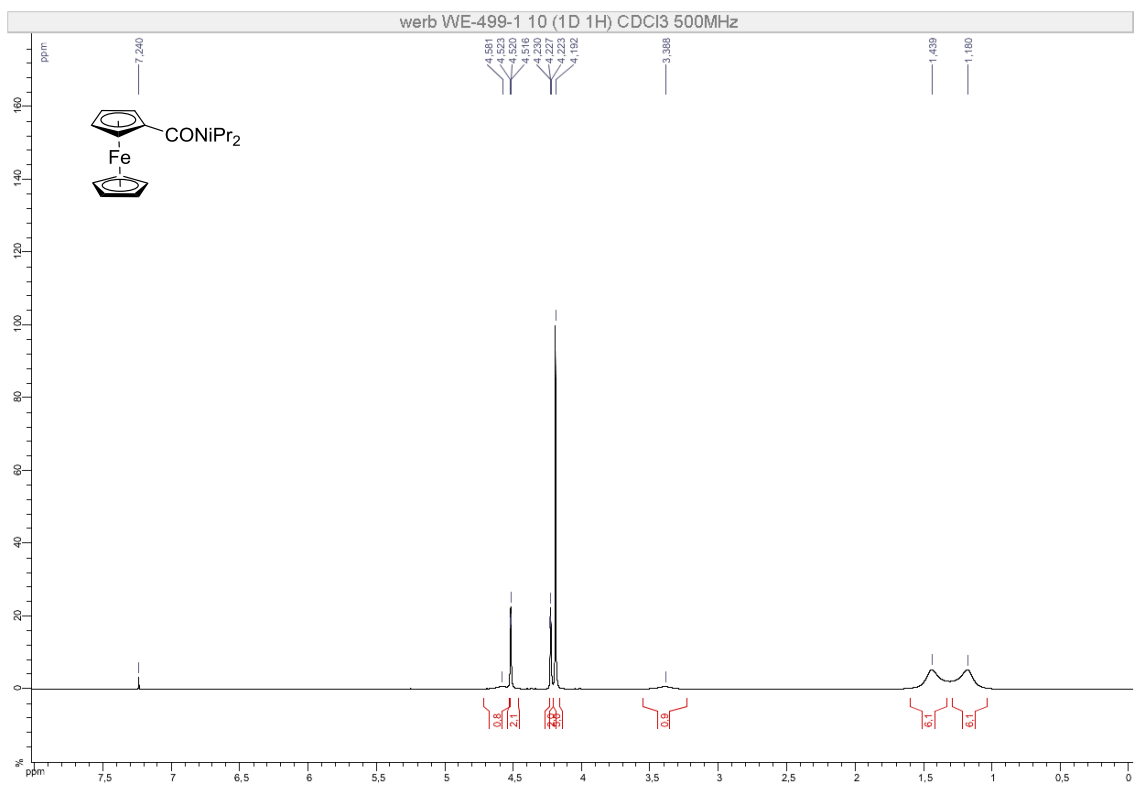
Compound 3

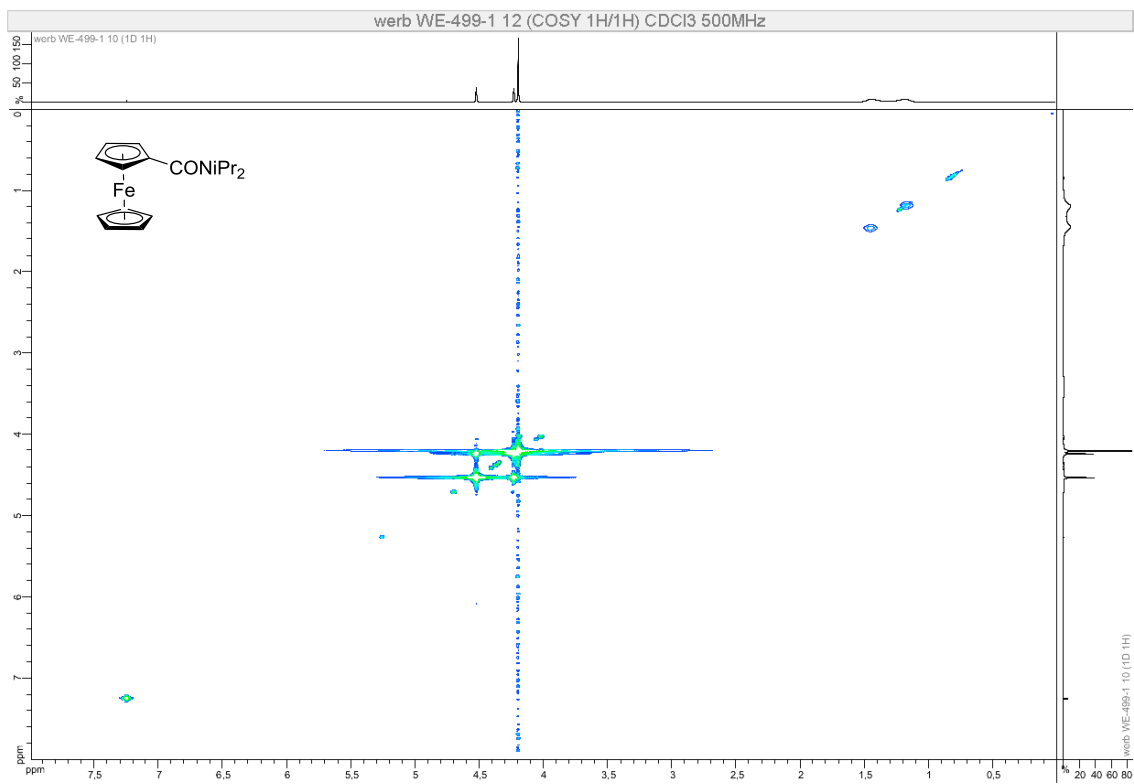
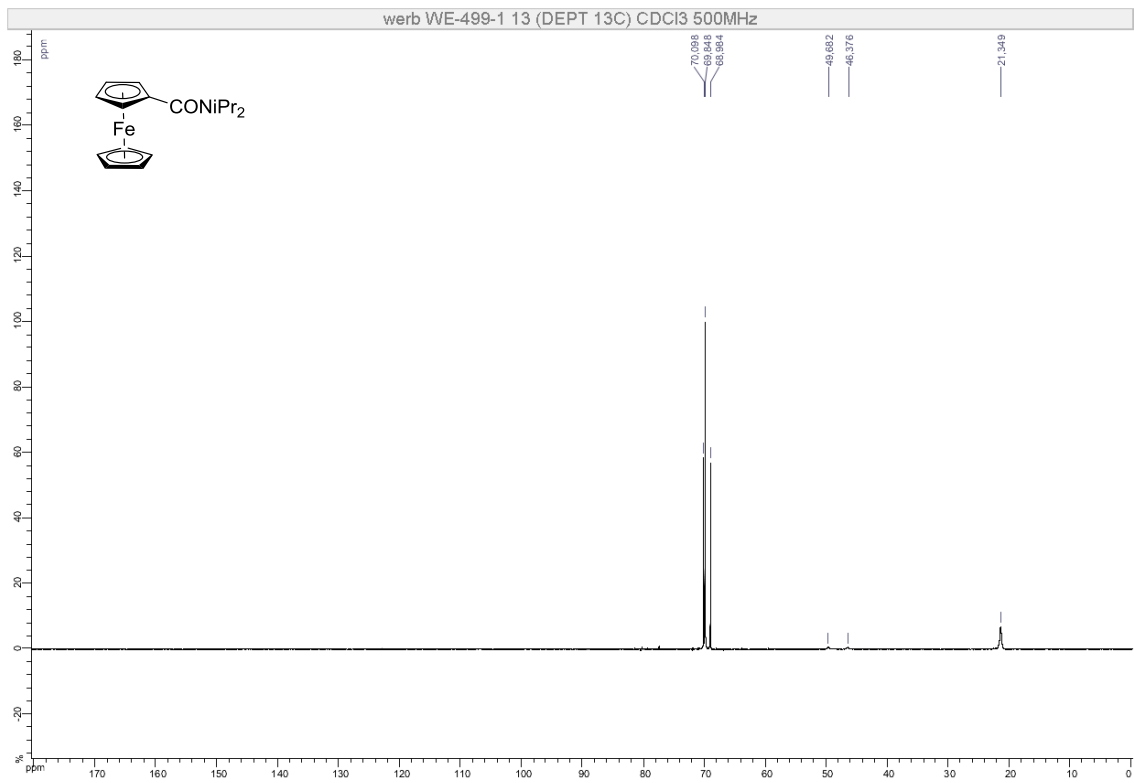


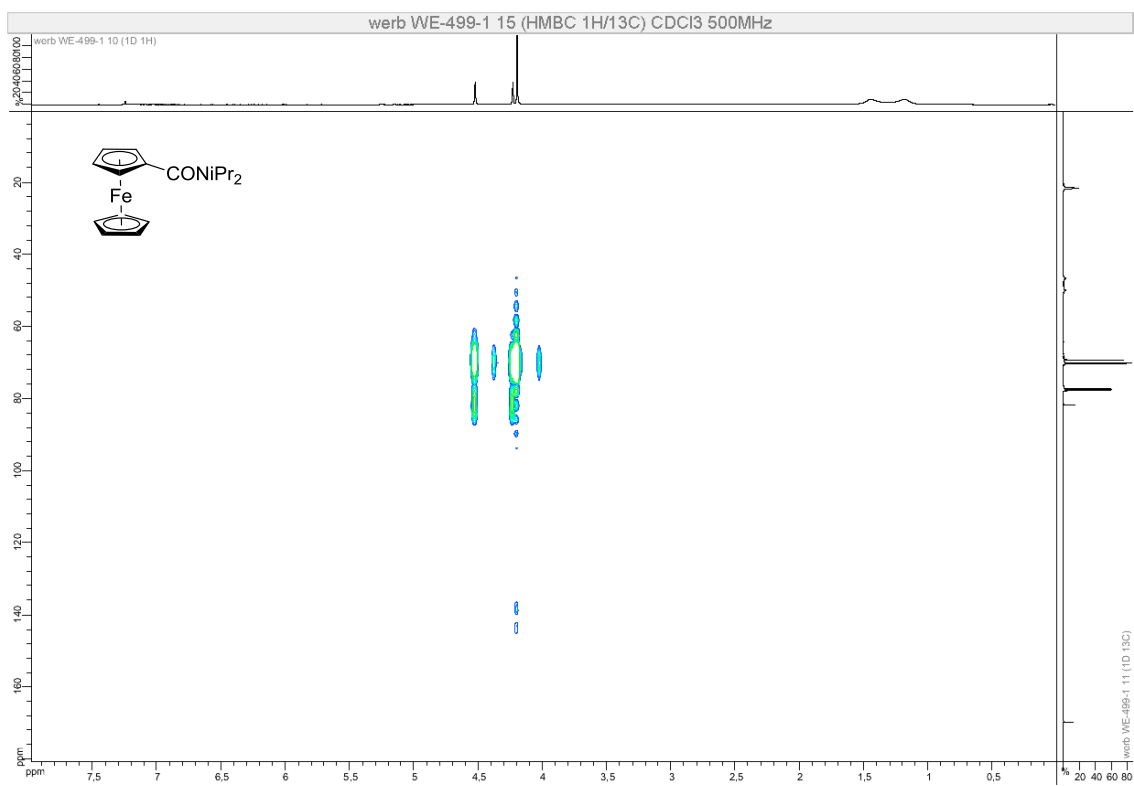
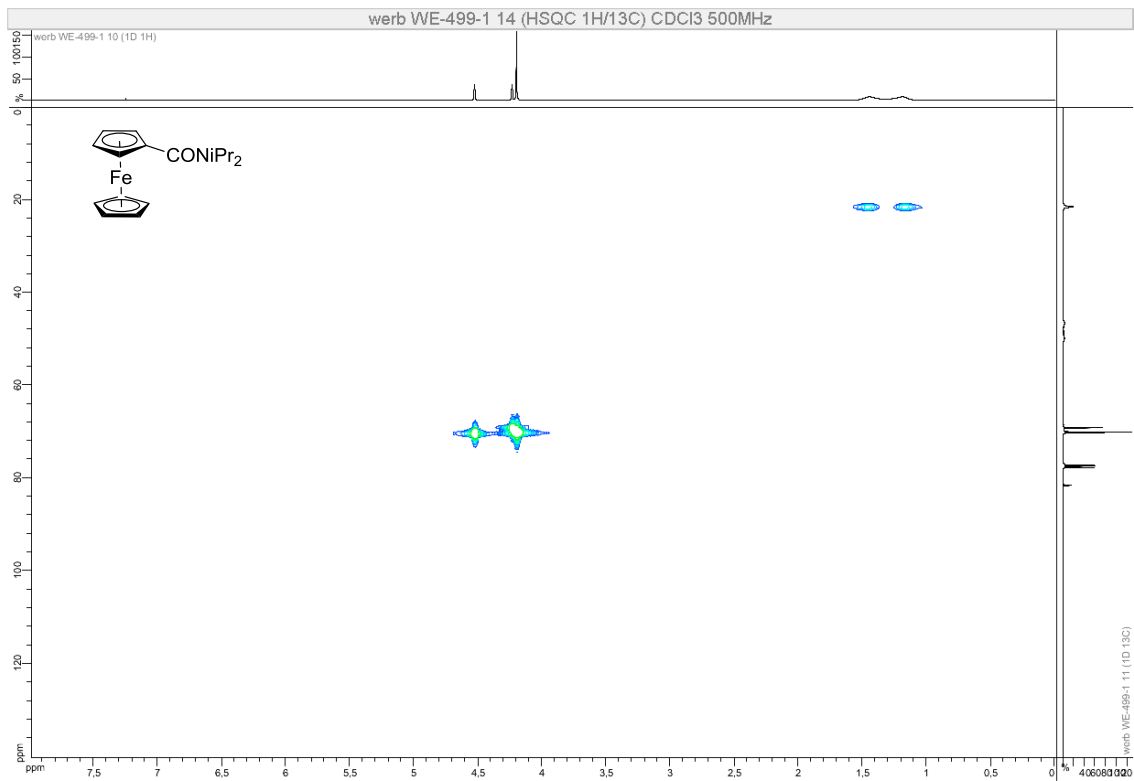


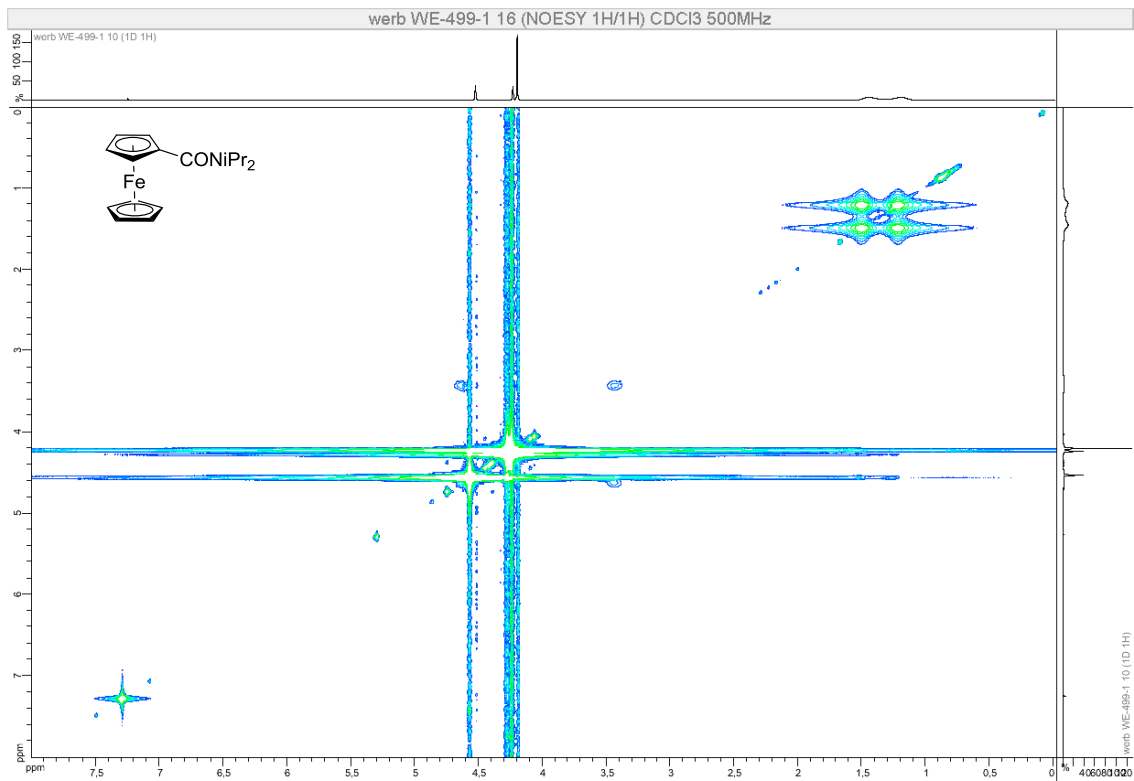


Compound 1

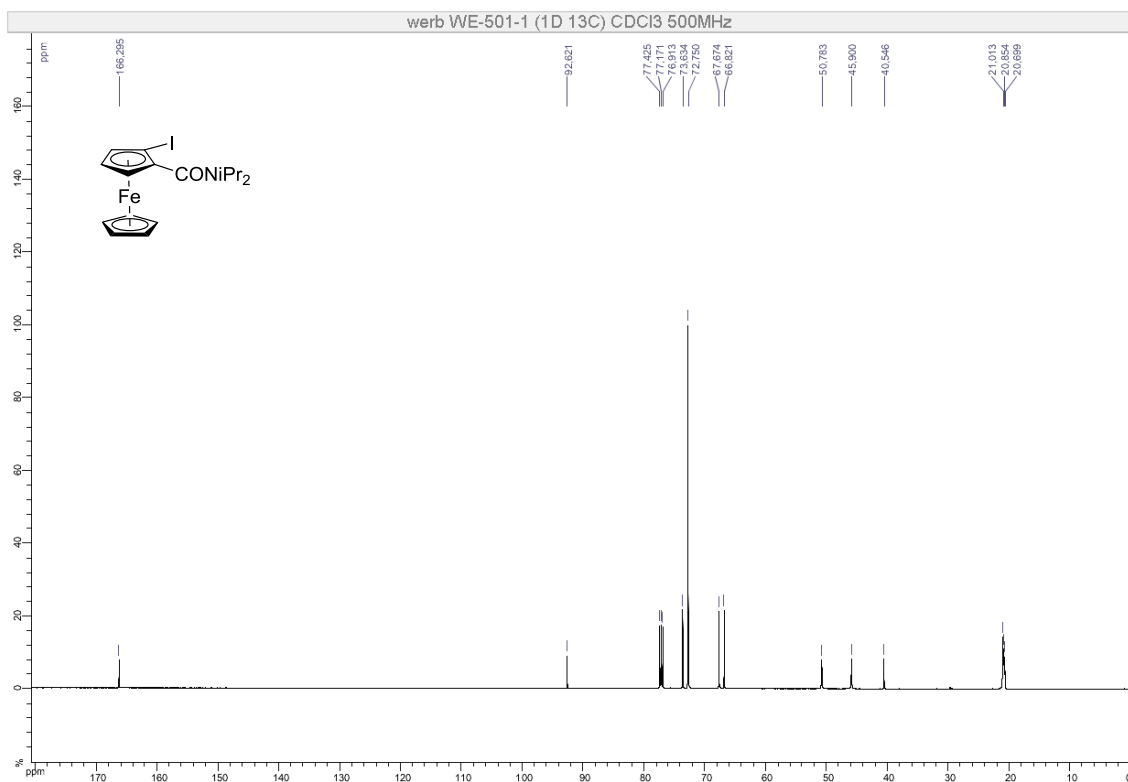
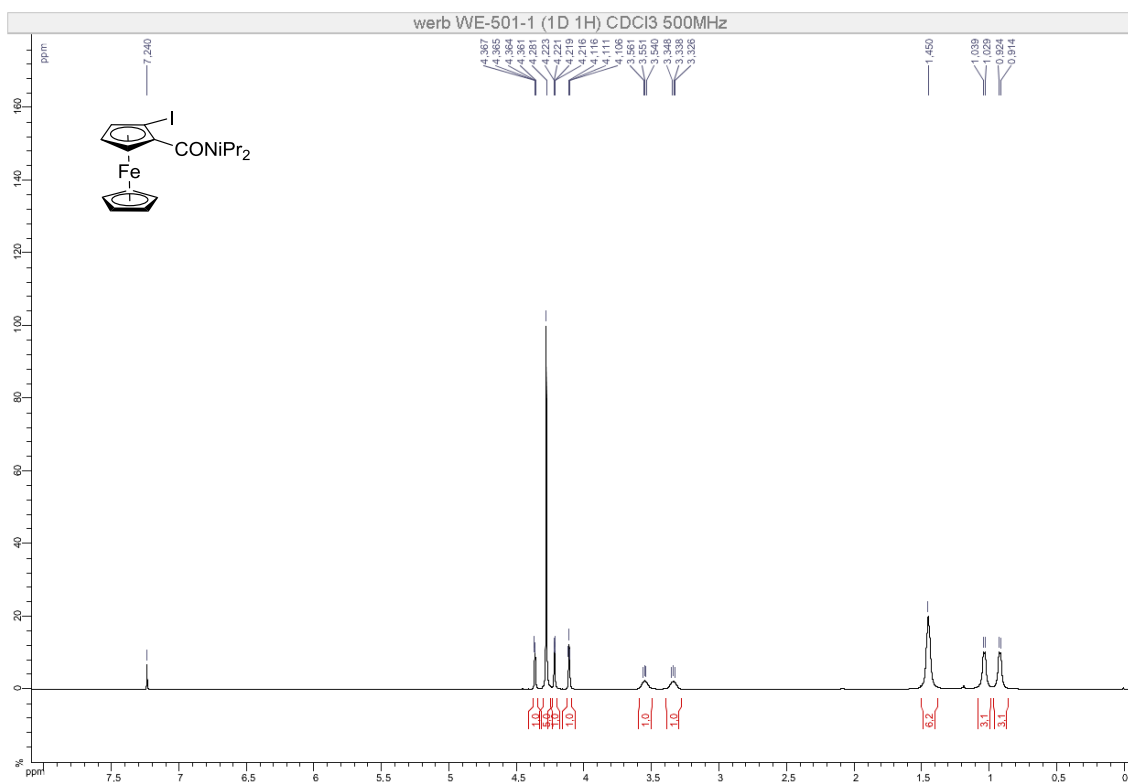


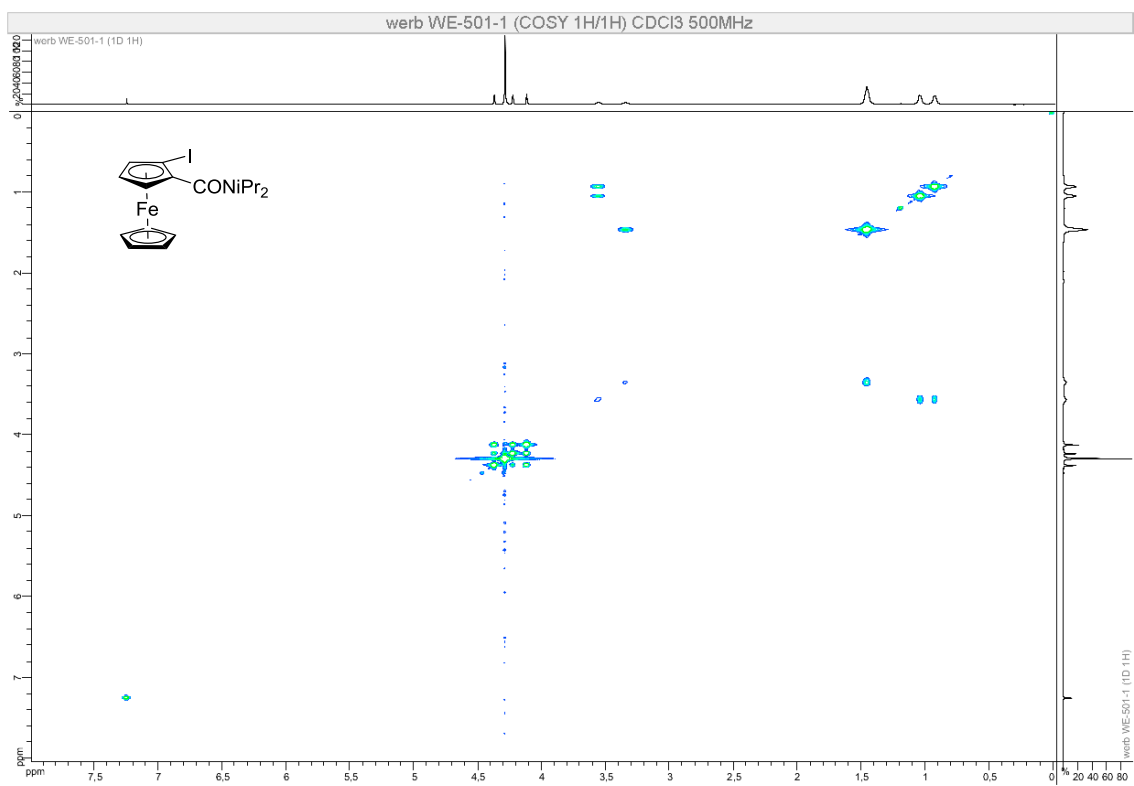
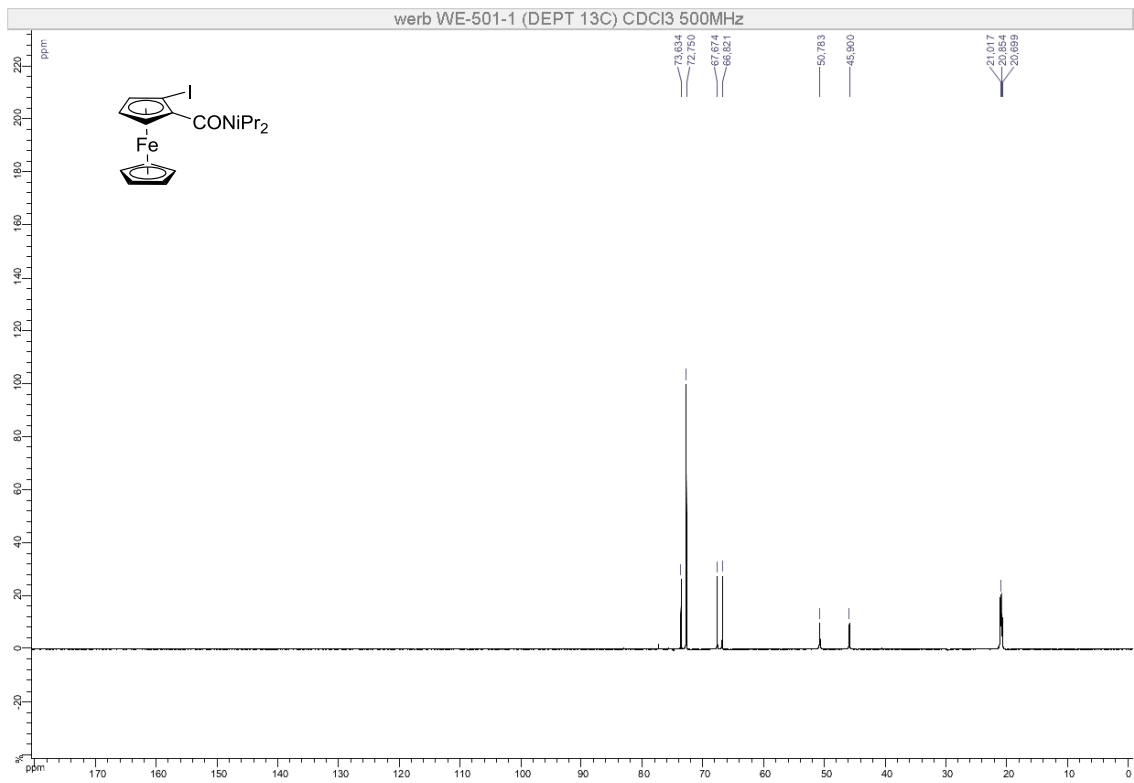


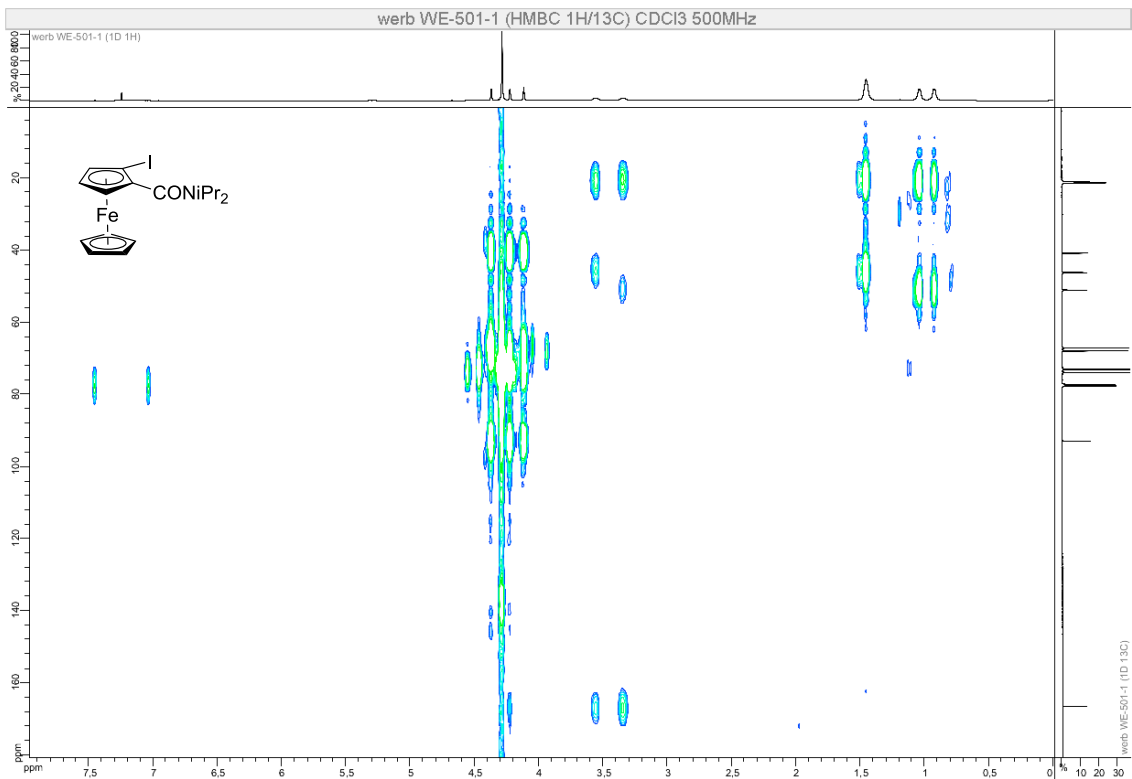
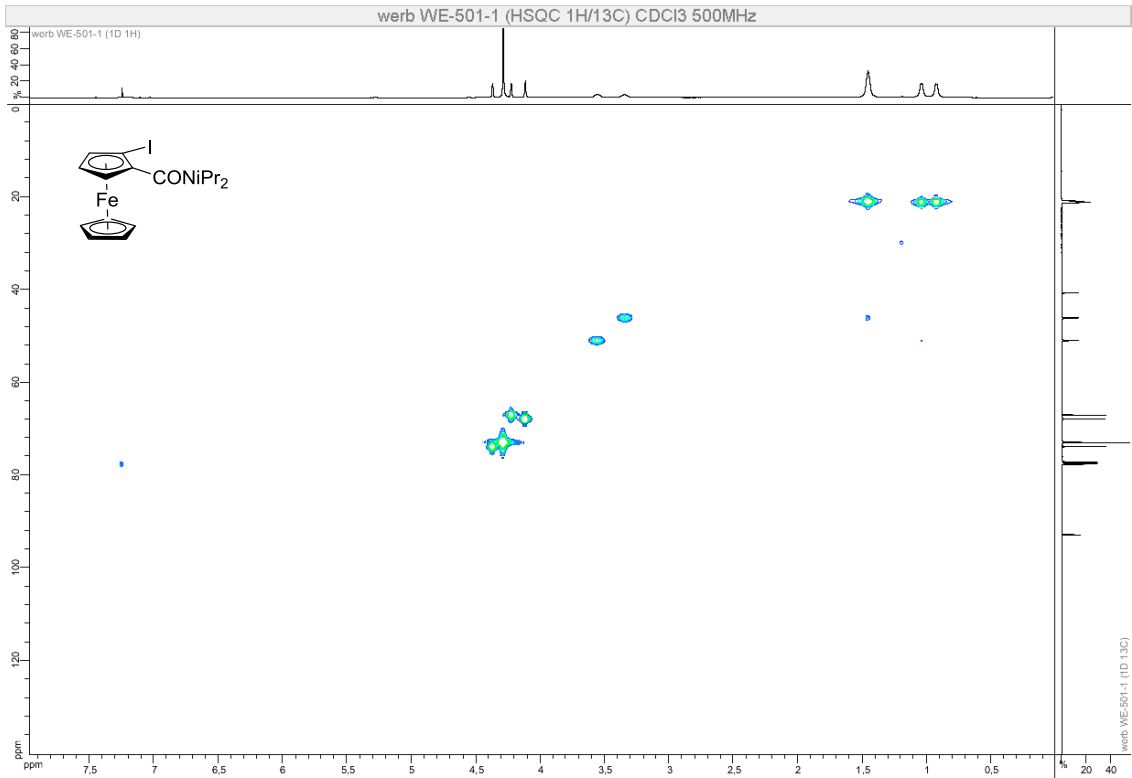




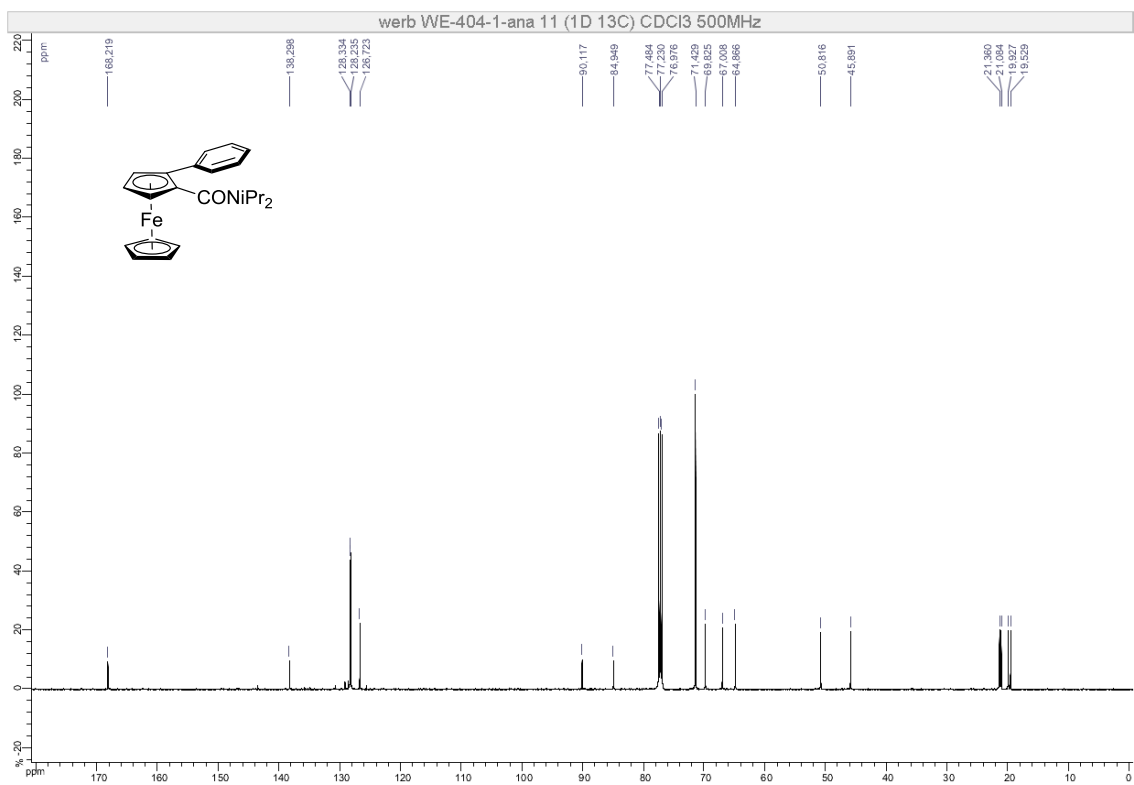
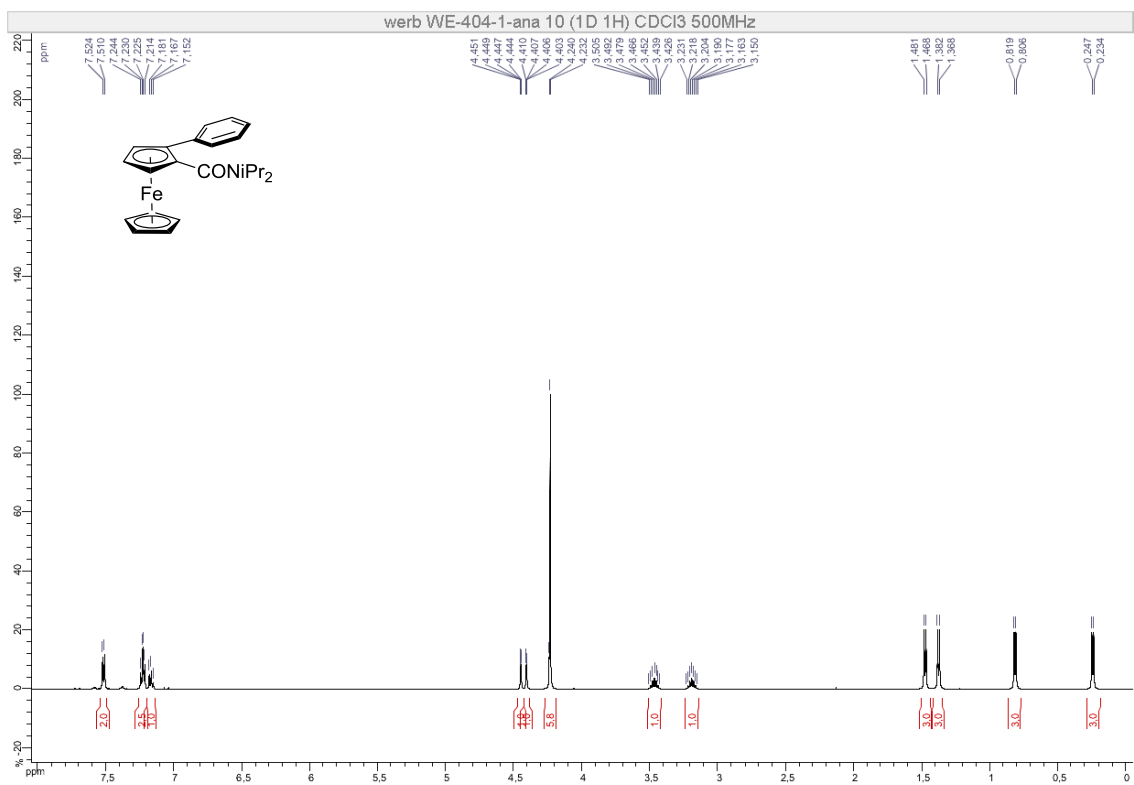
Compound (\pm)-2

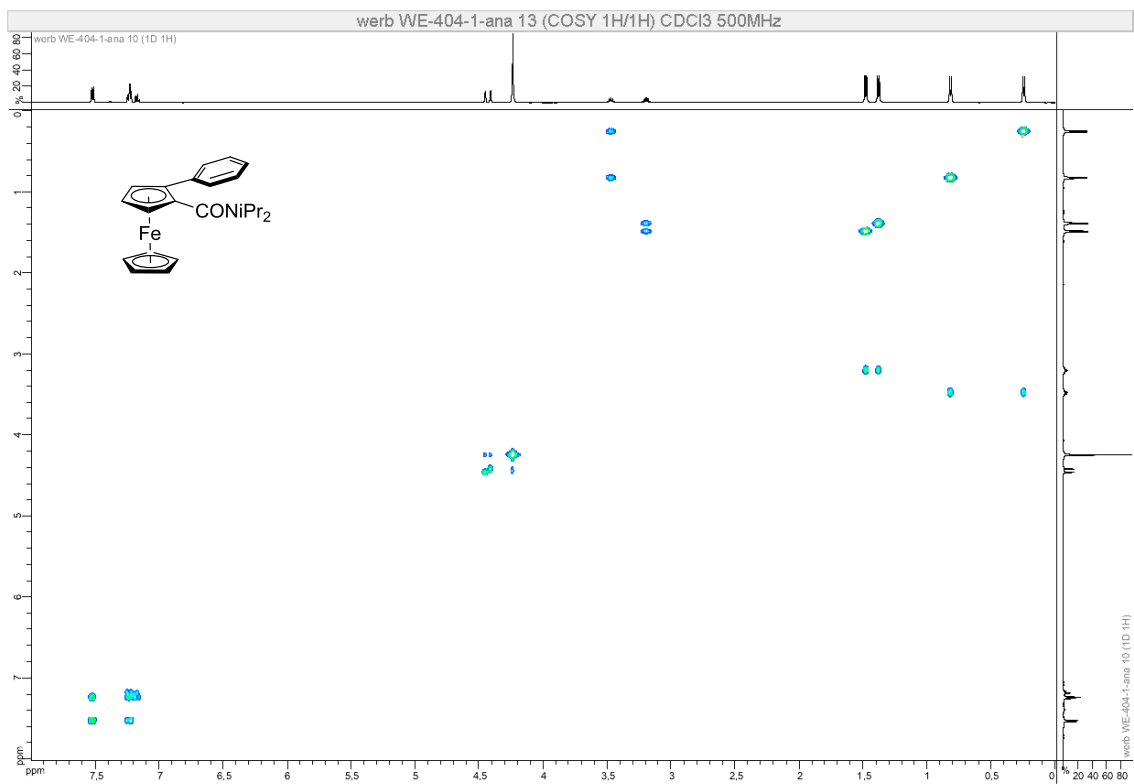
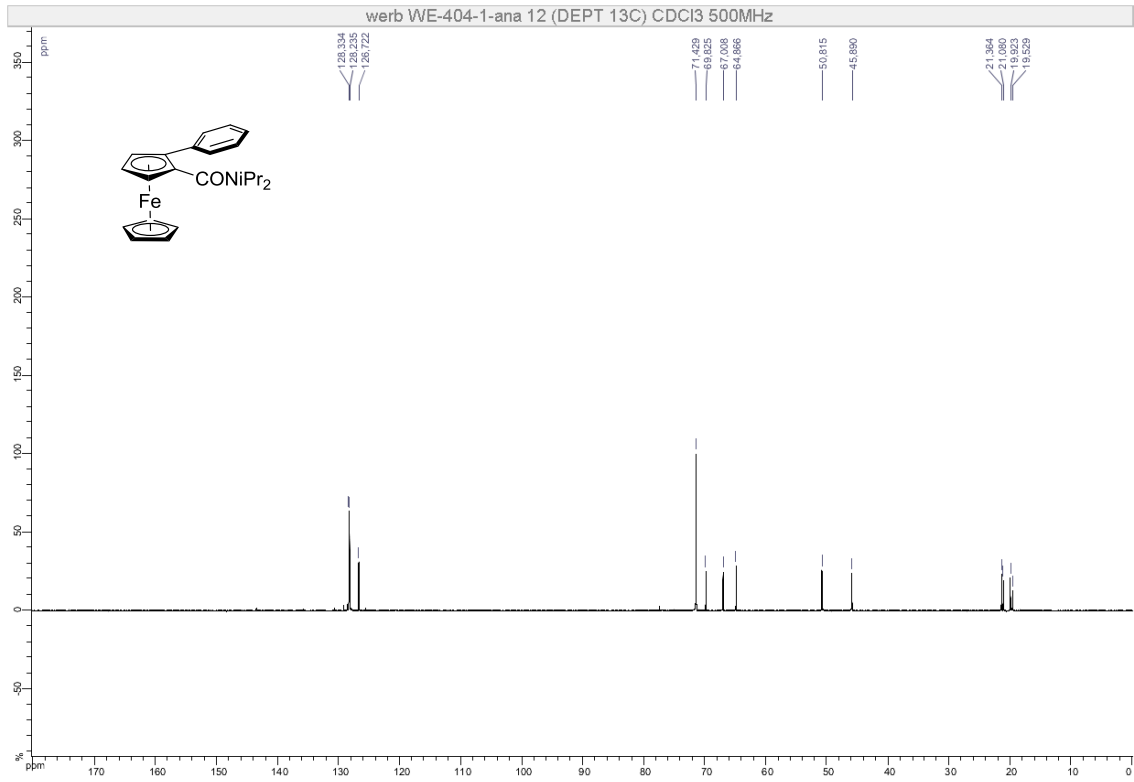


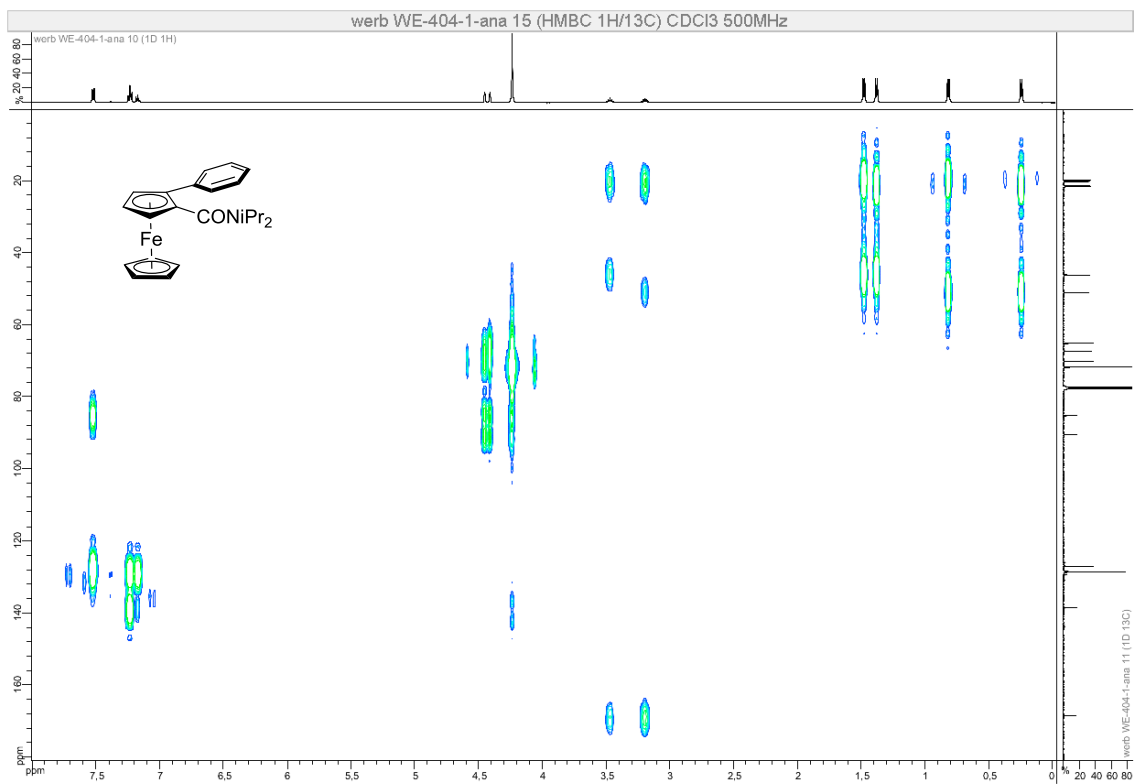
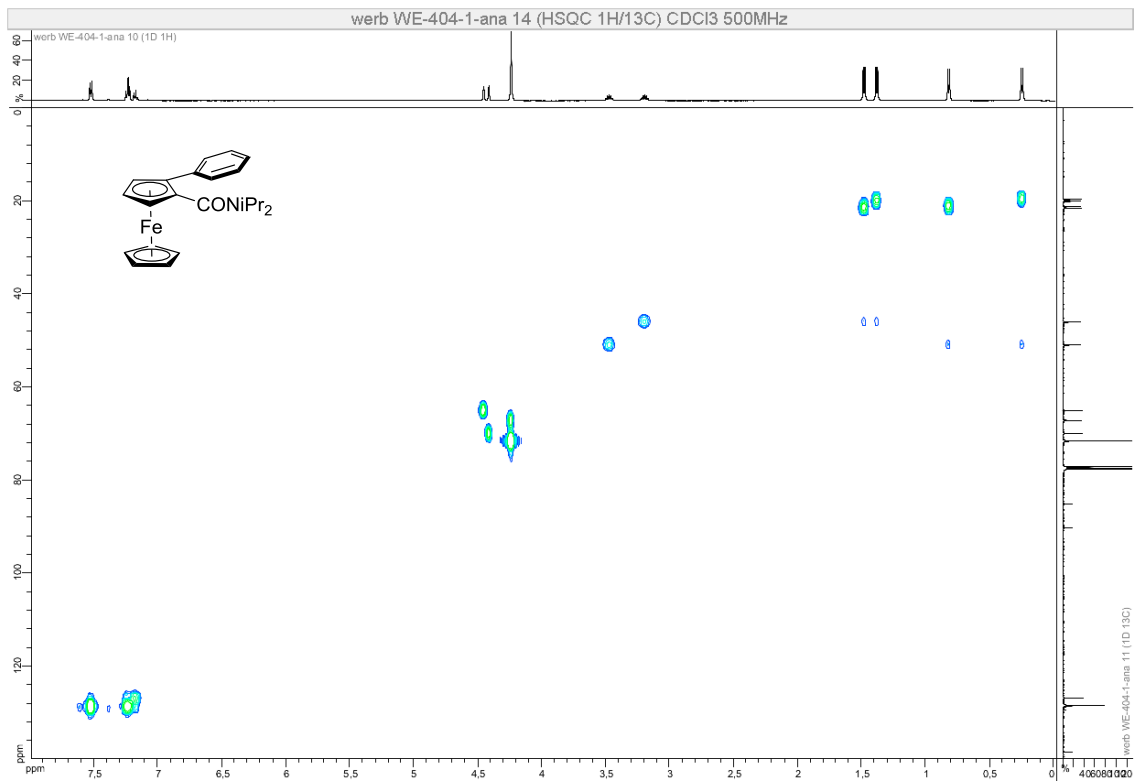


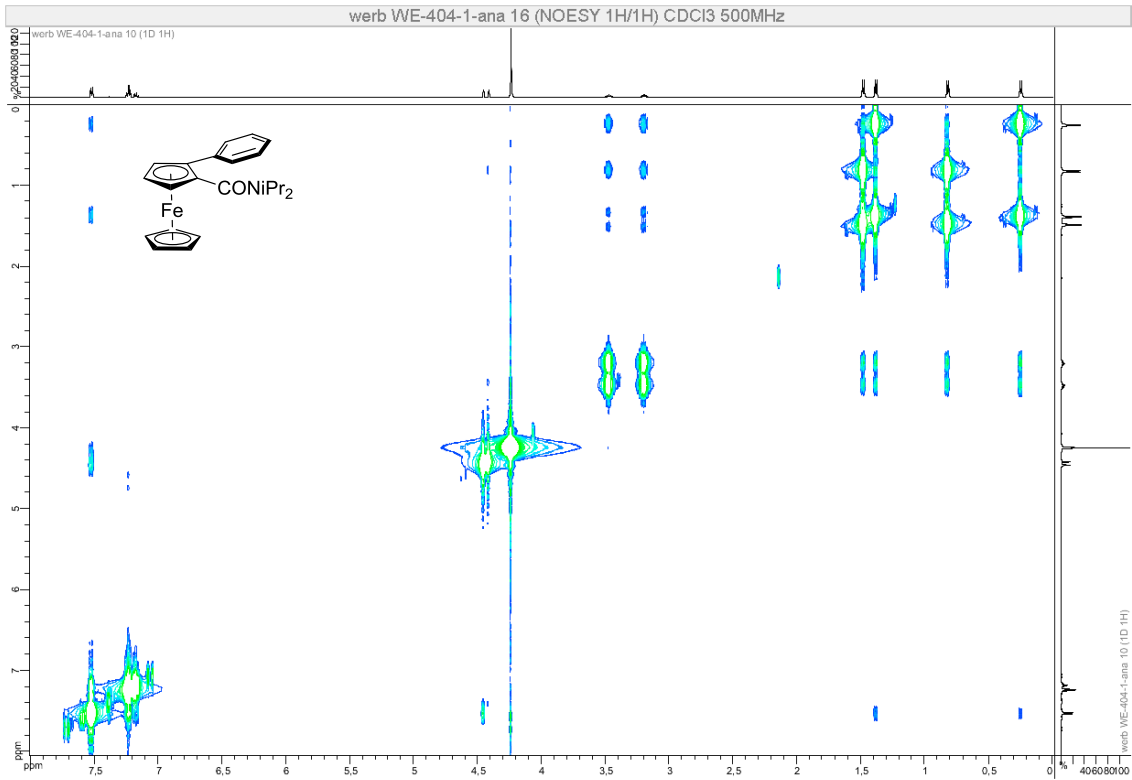


Compound (\pm)-4

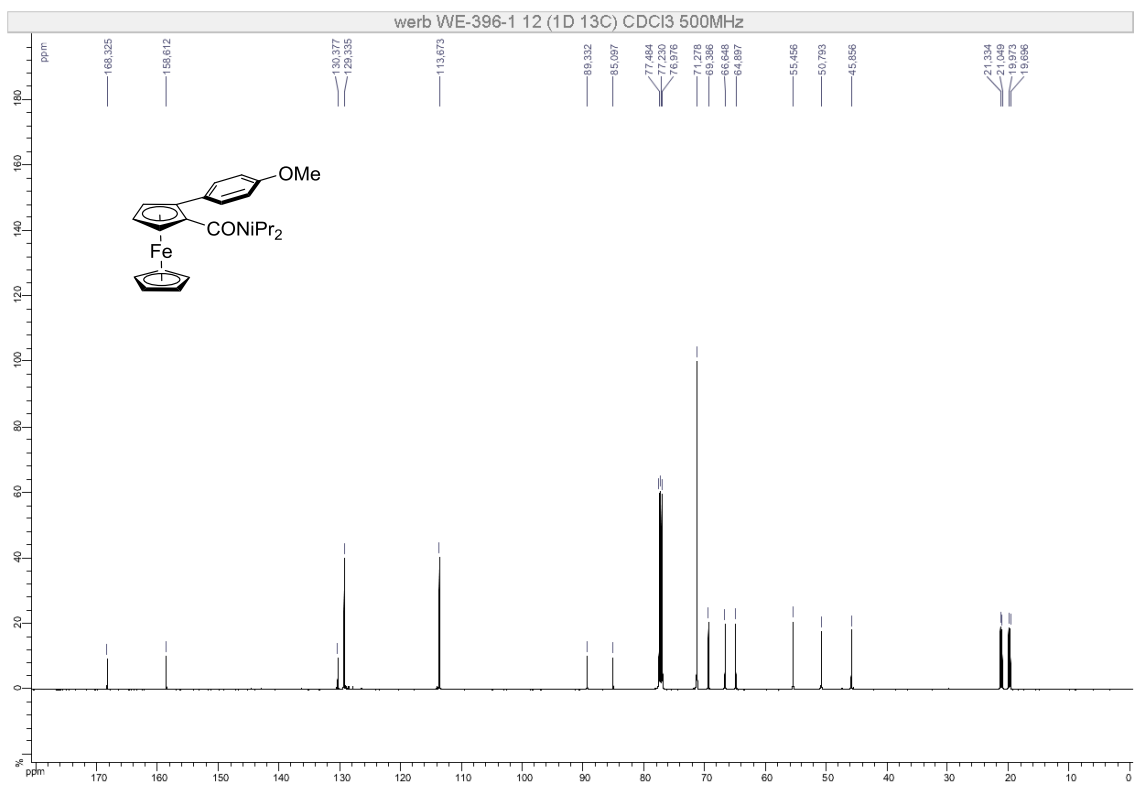
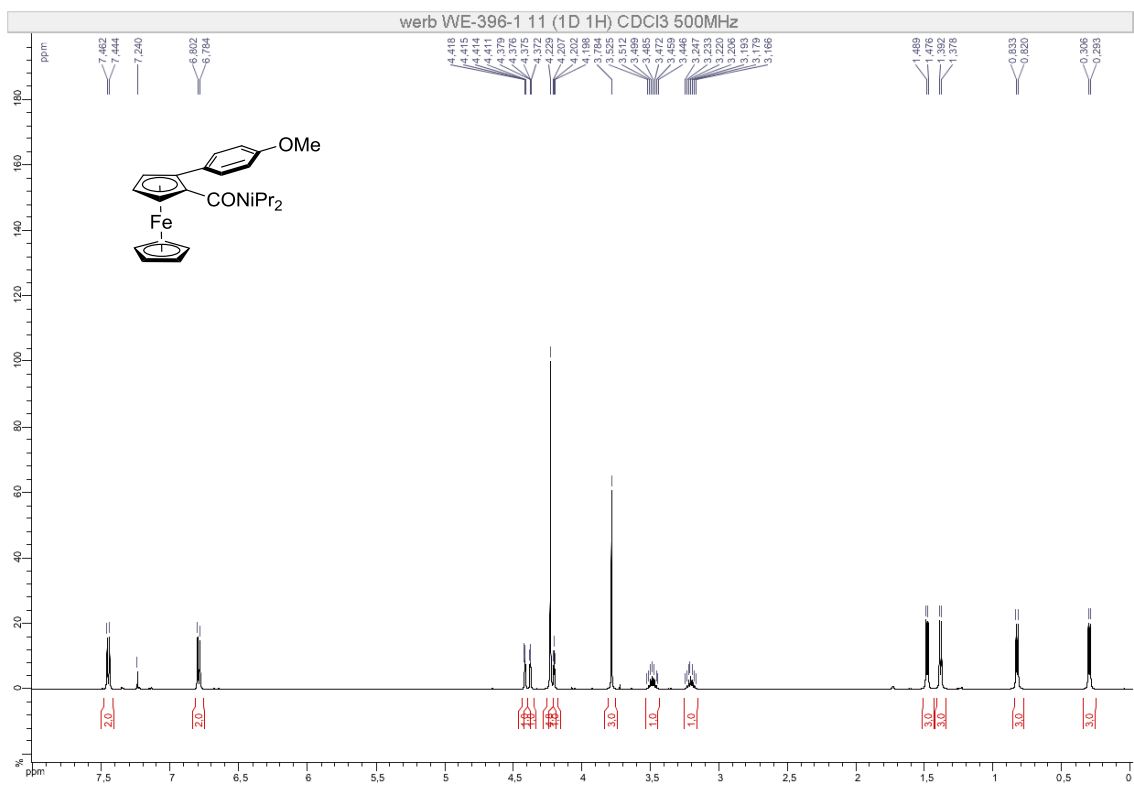


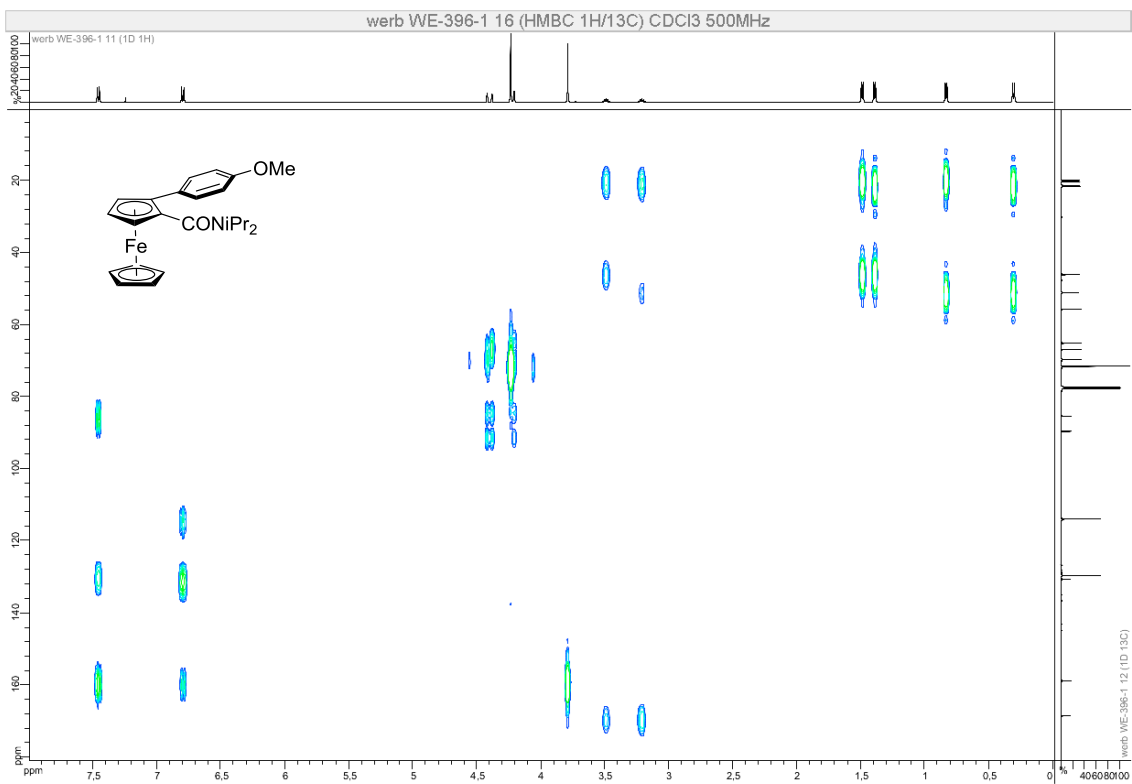
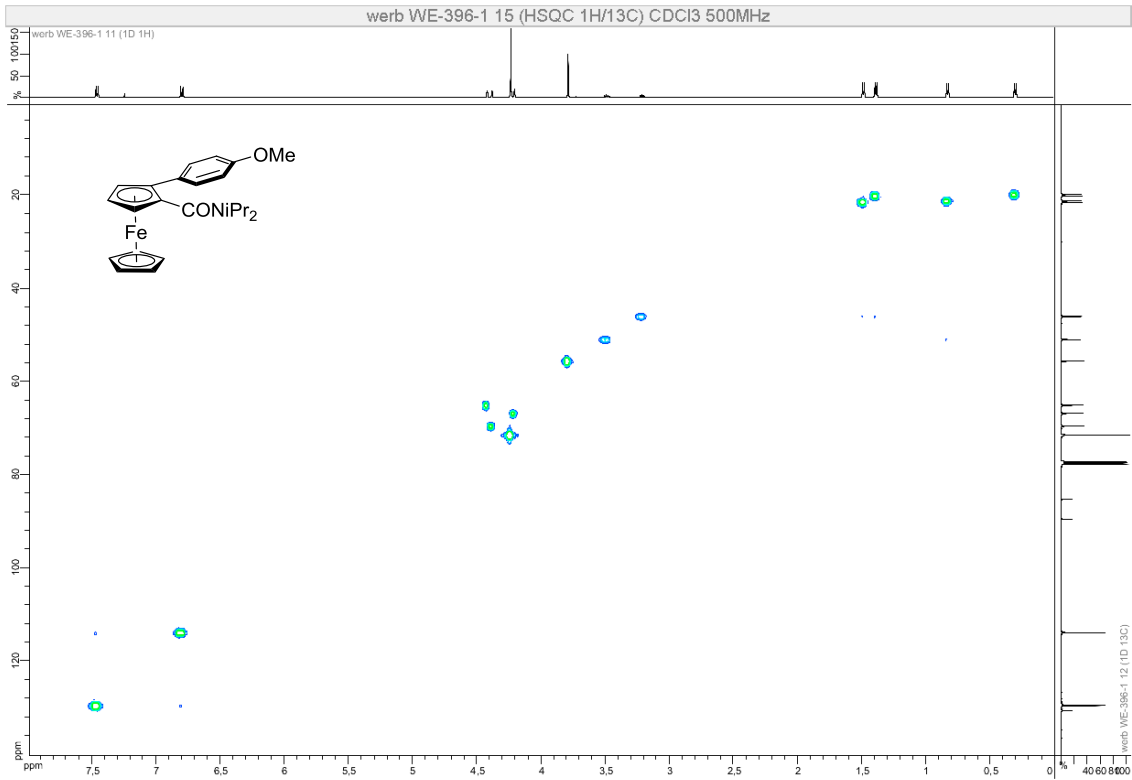


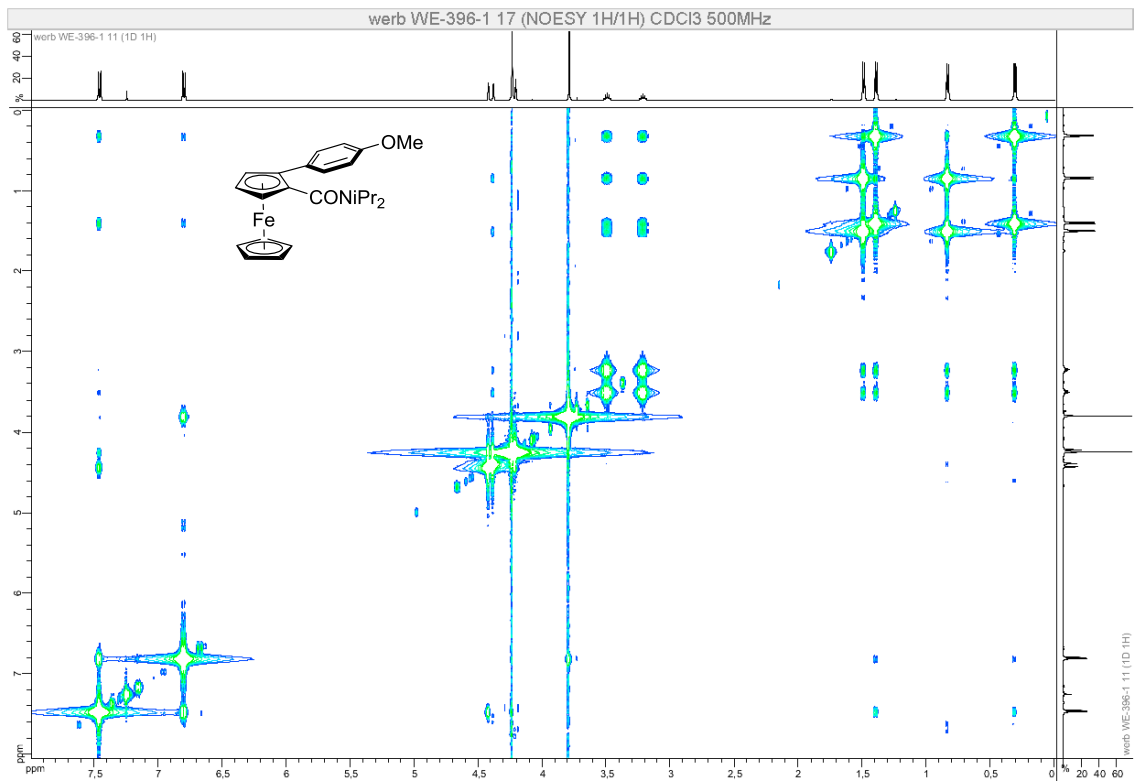




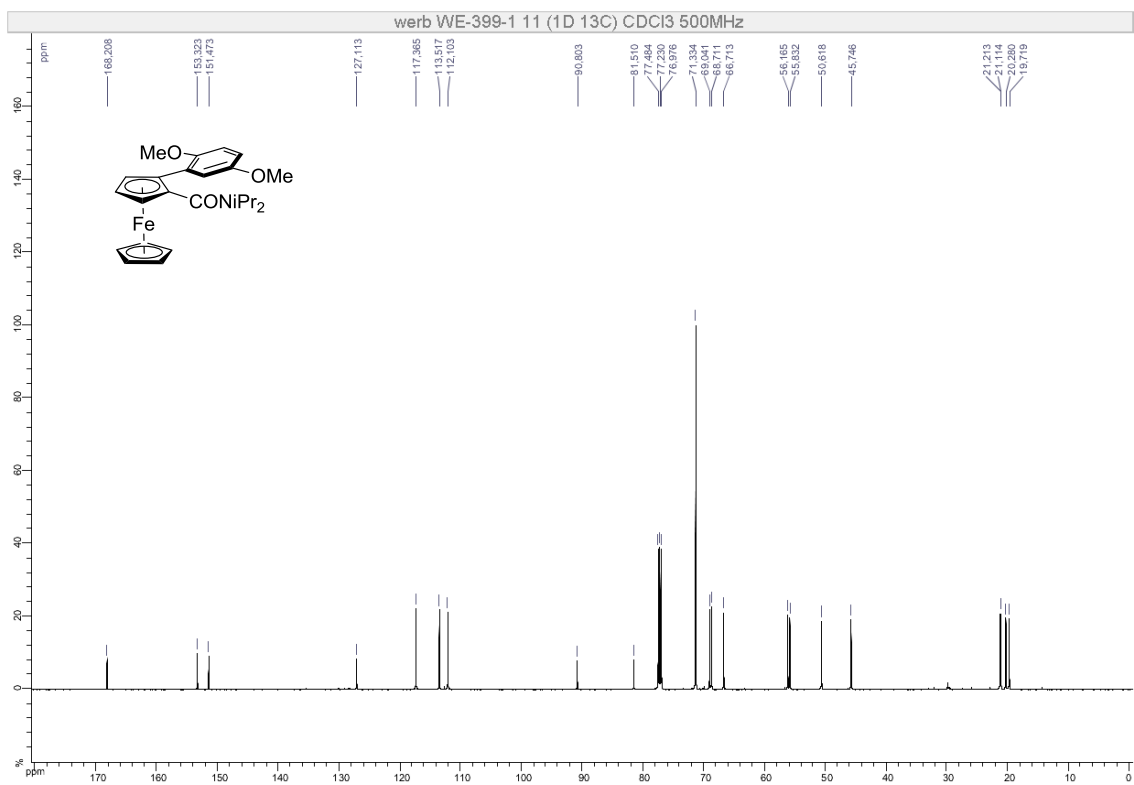
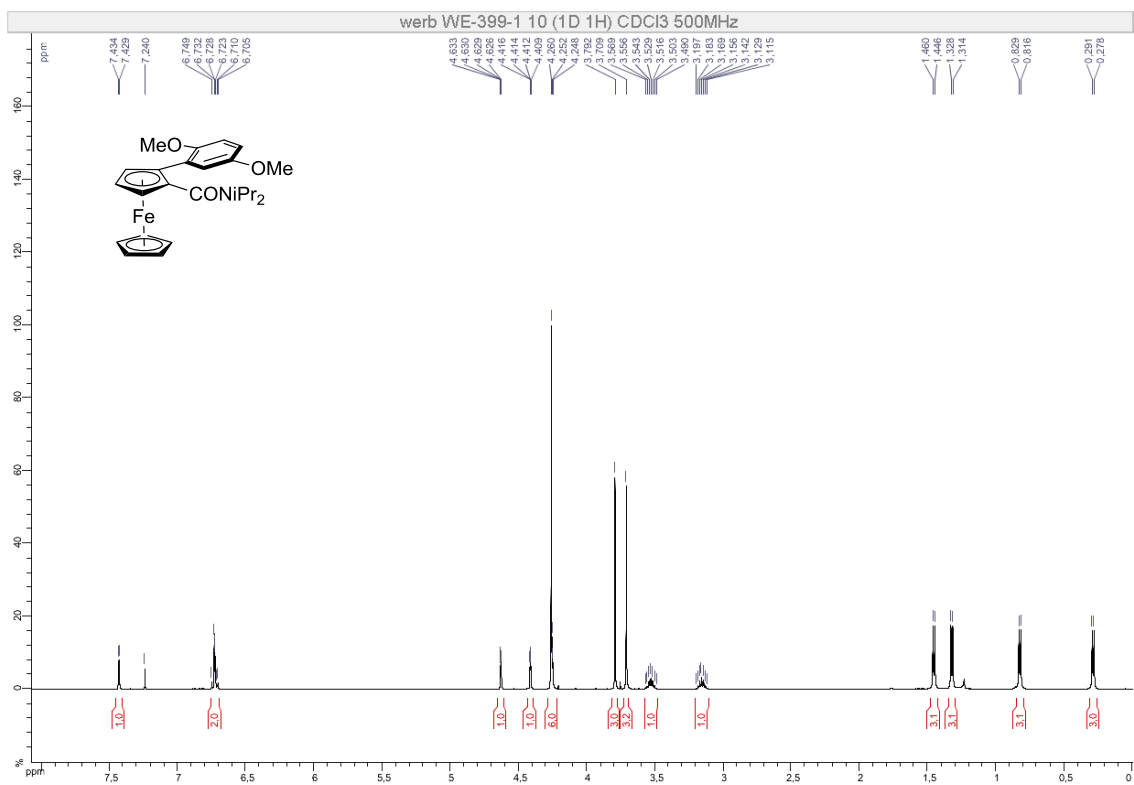
Compound (\pm)-5

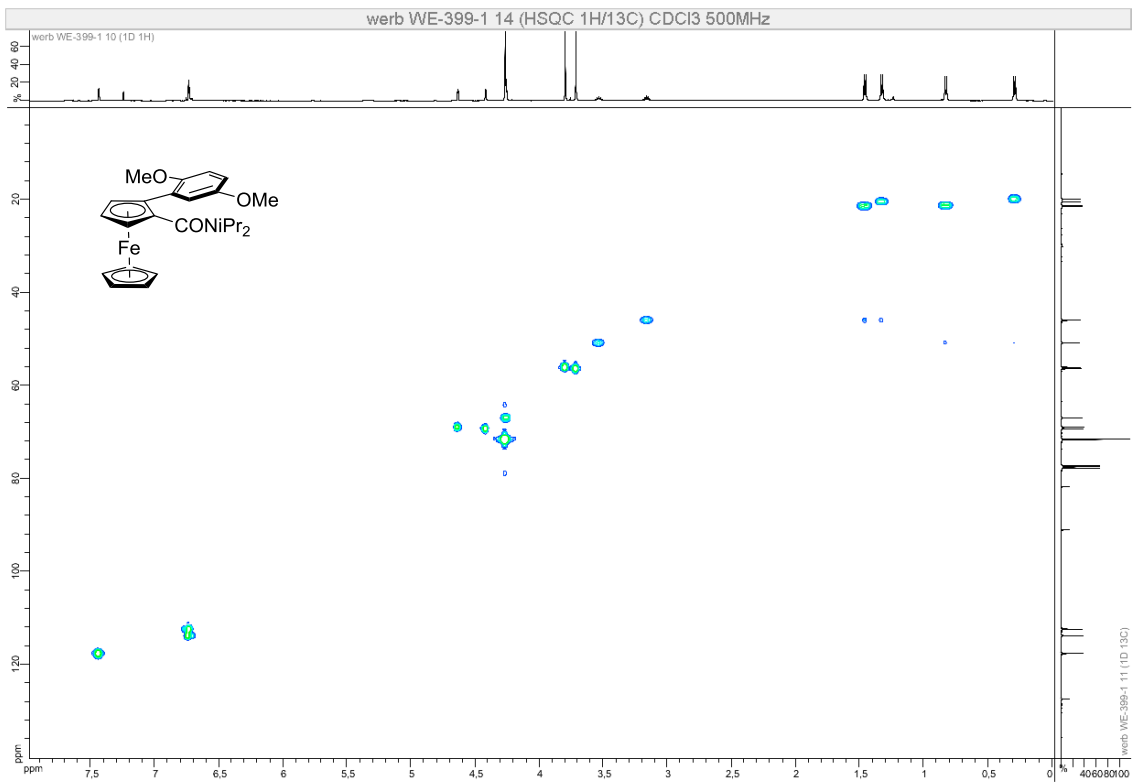
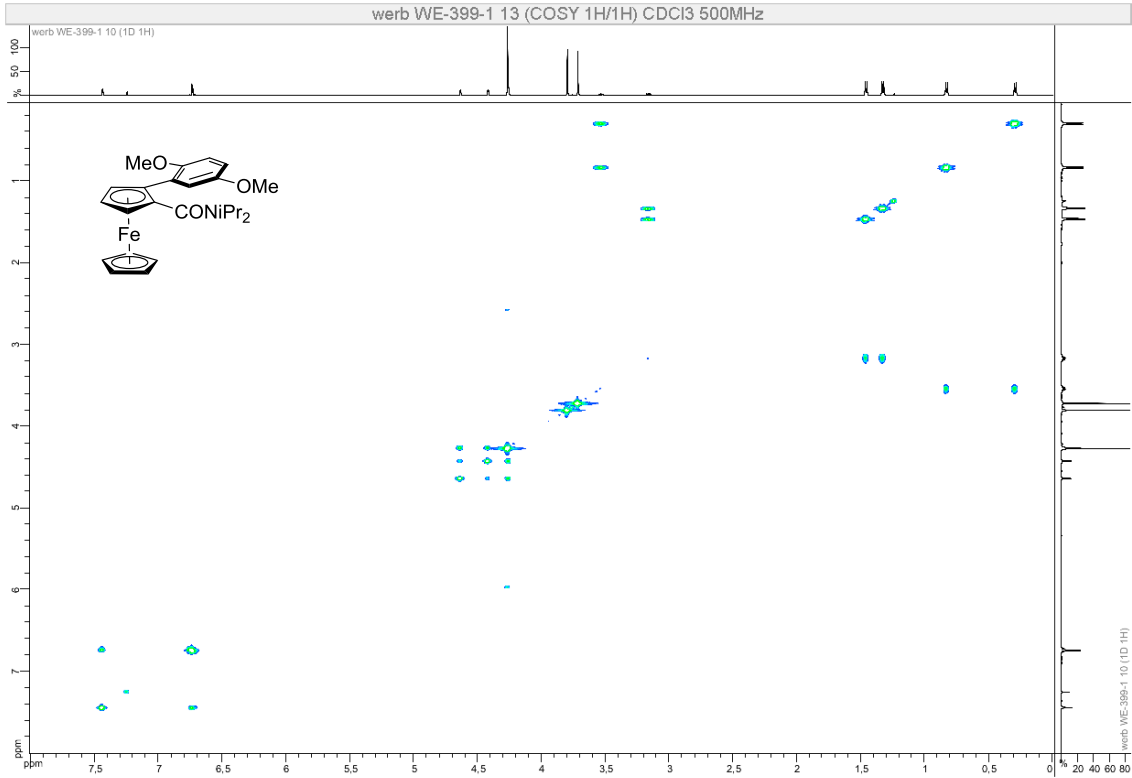


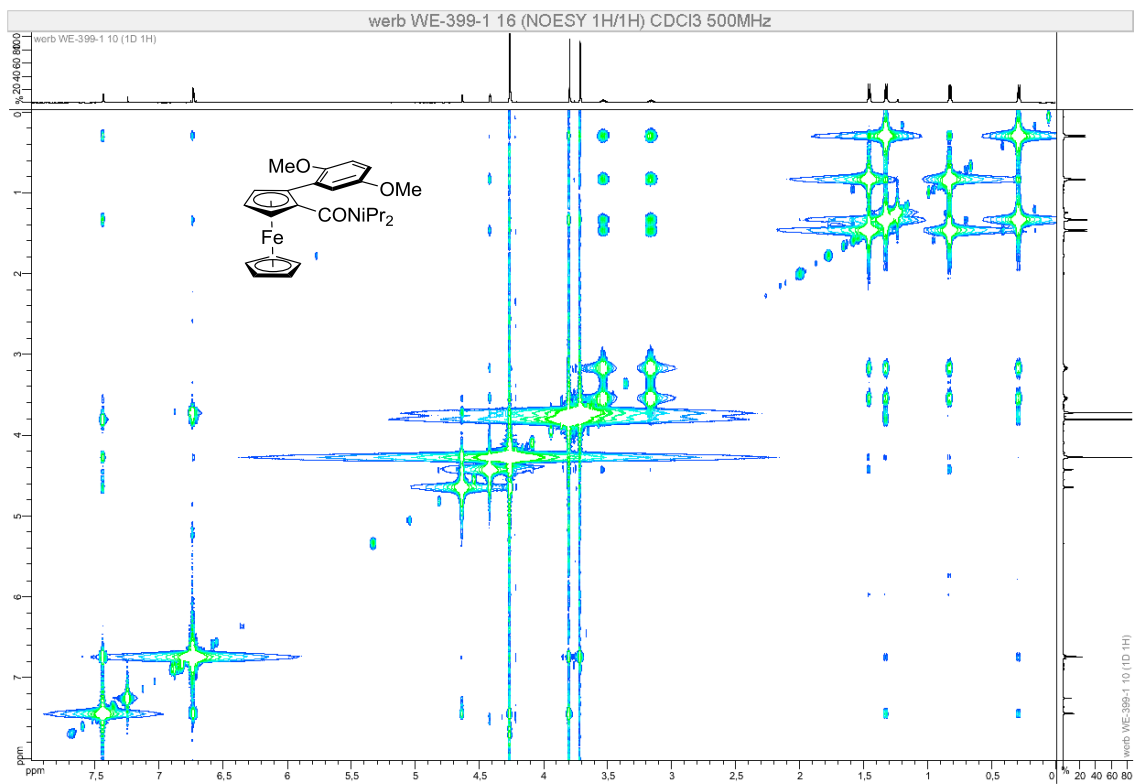
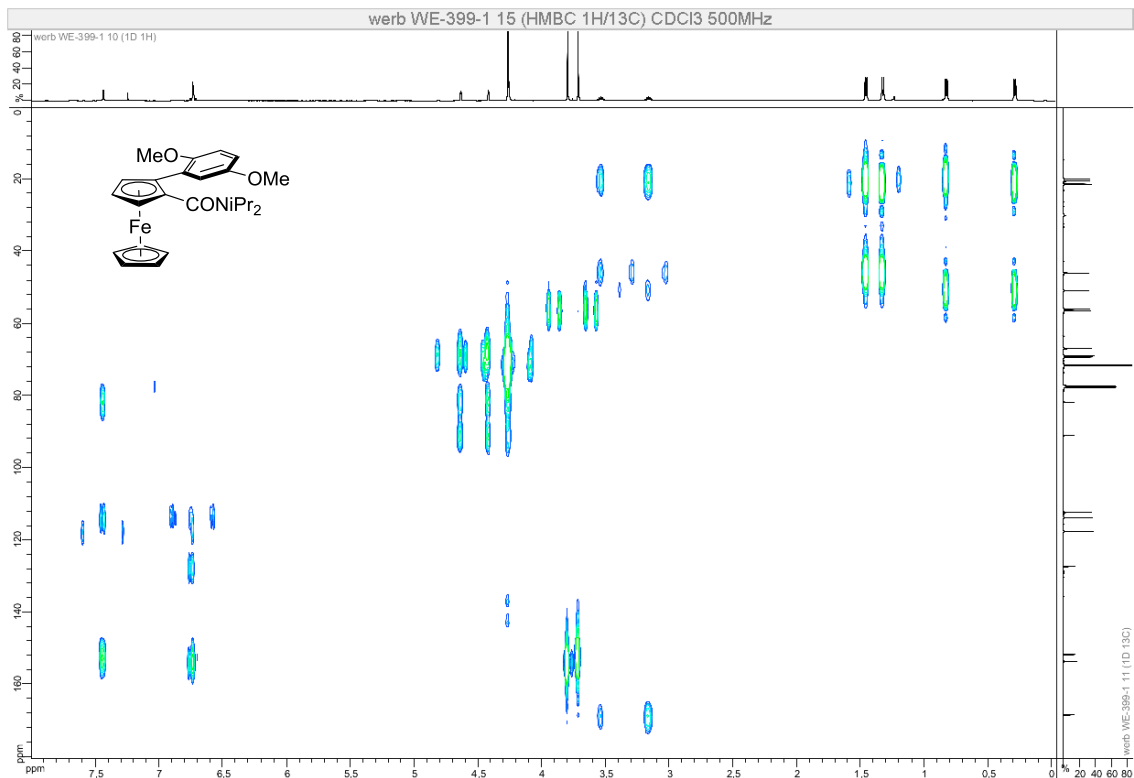




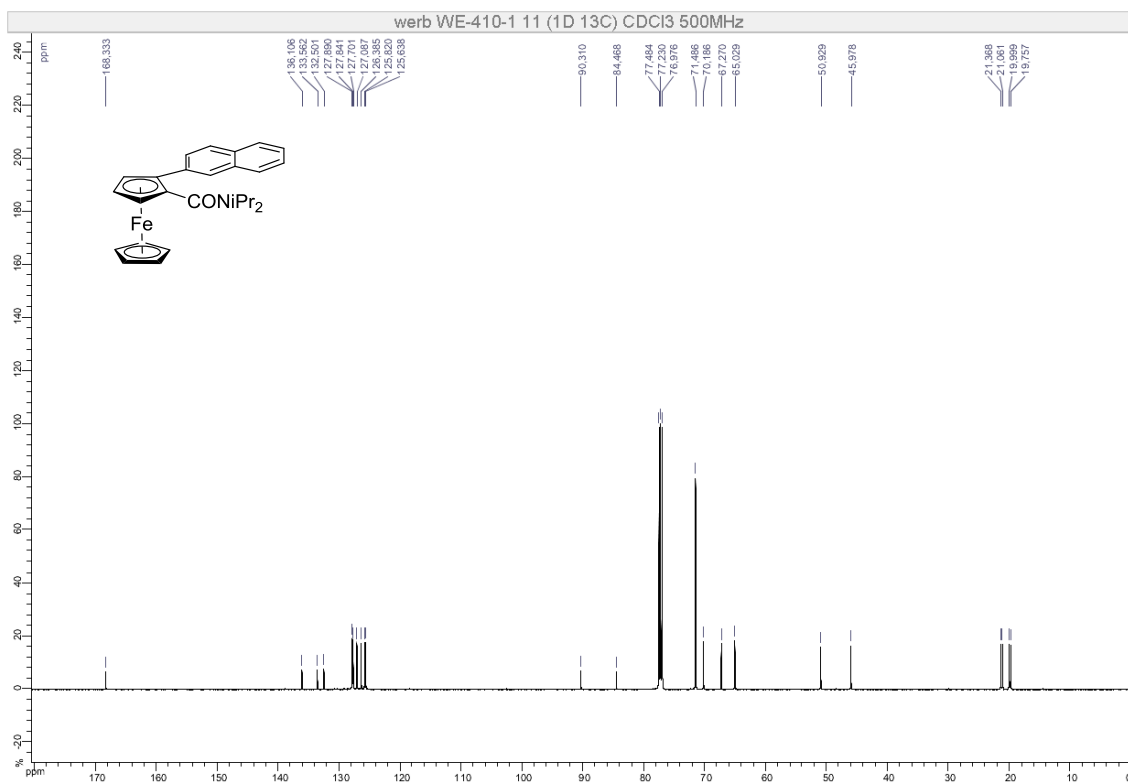
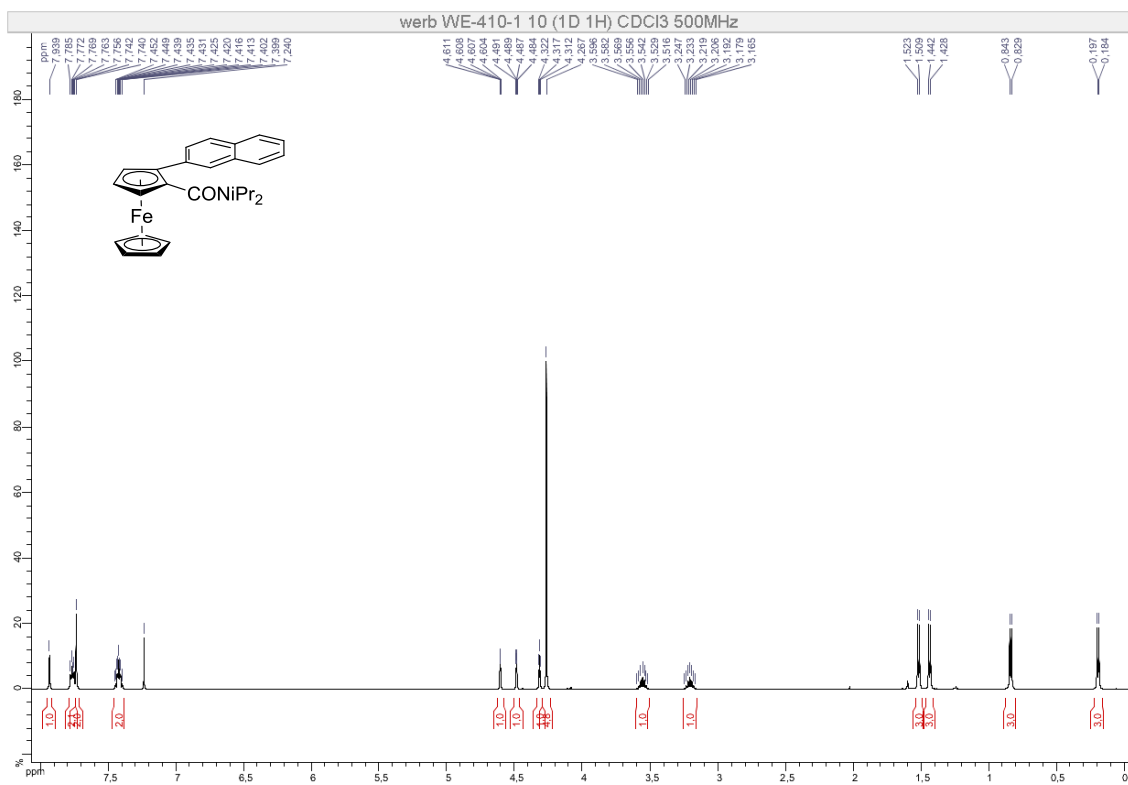
Compound (\pm)-6

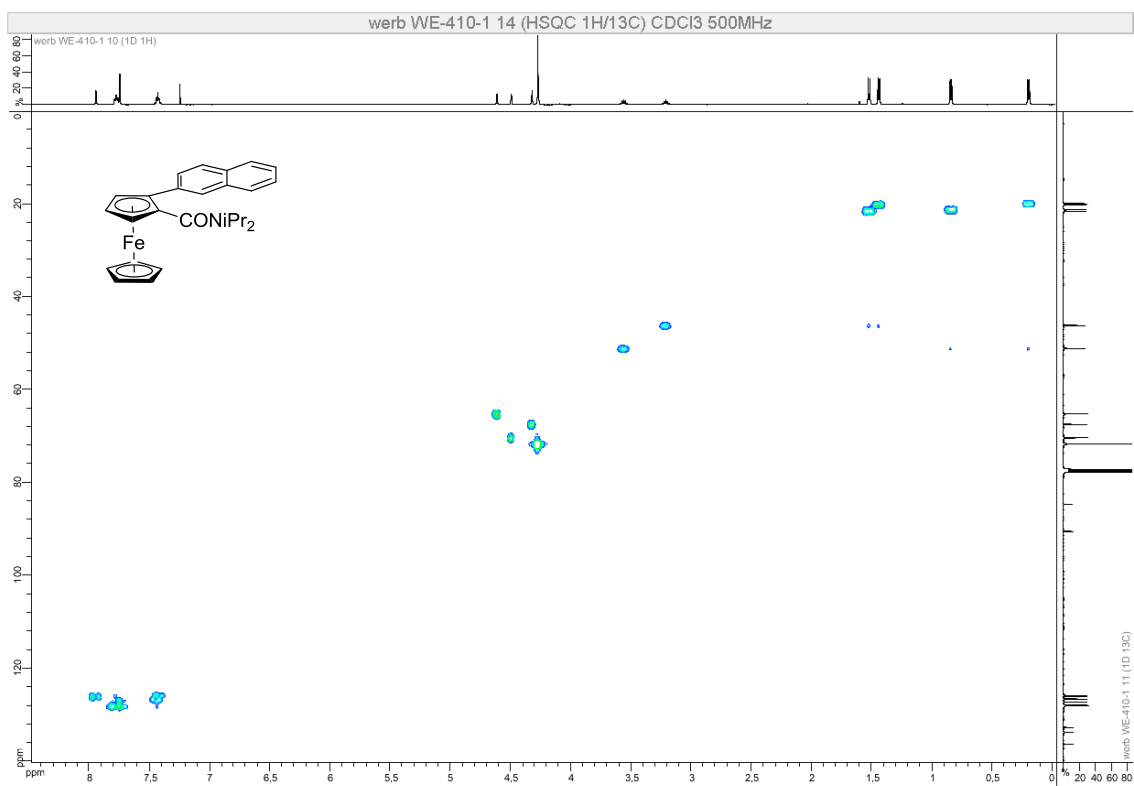
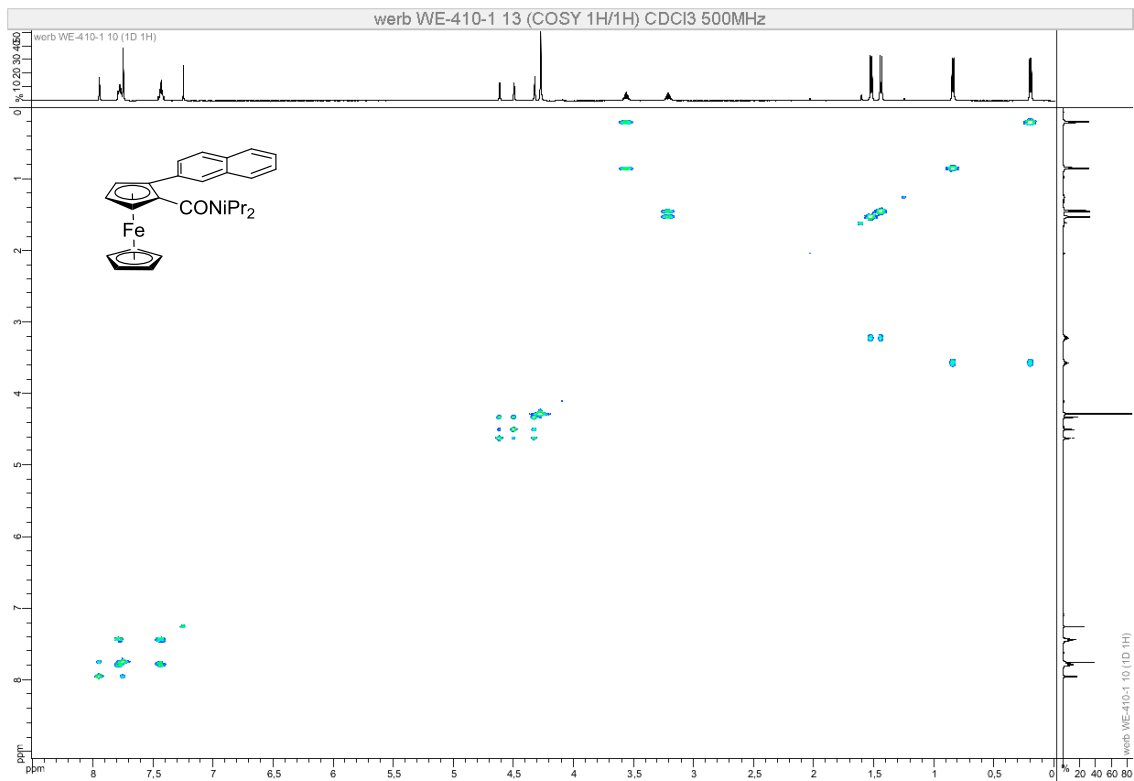


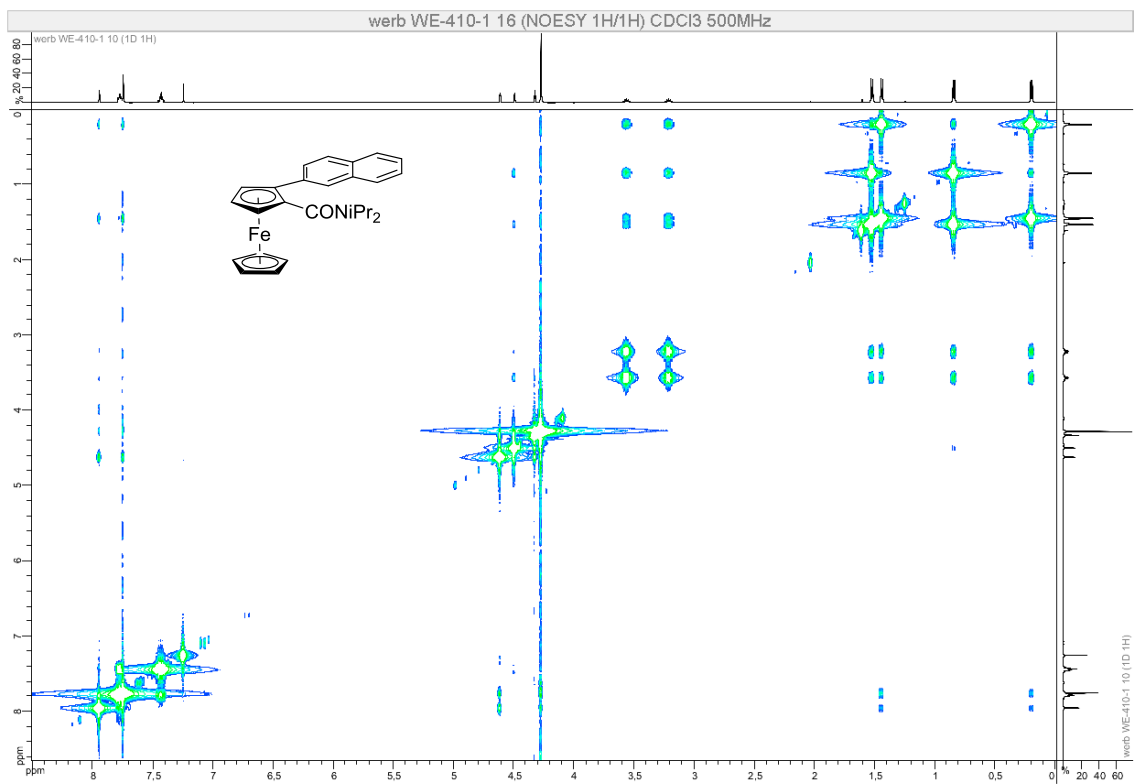
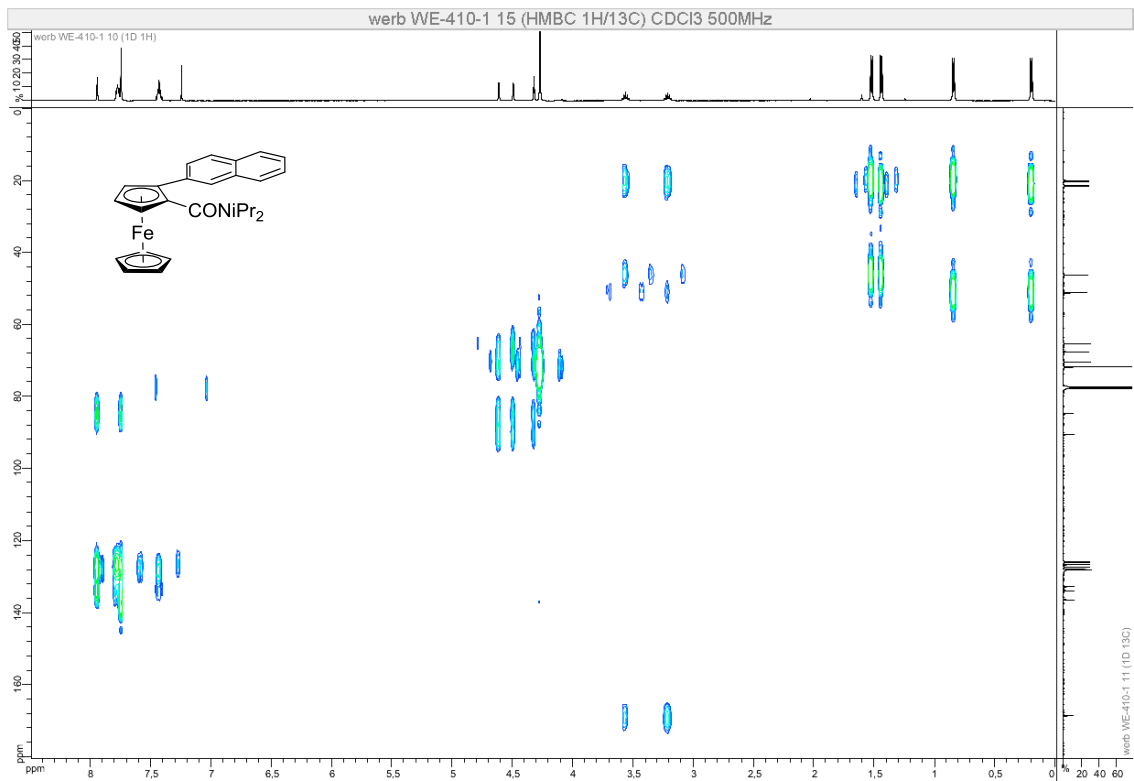




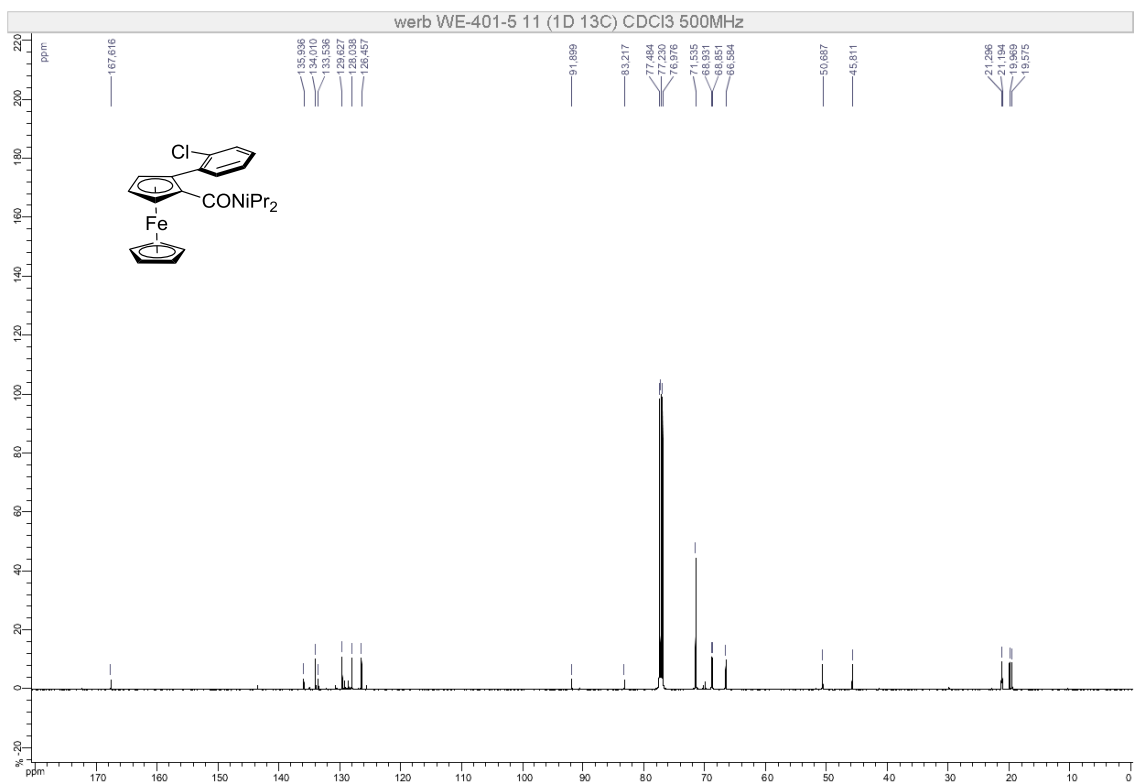
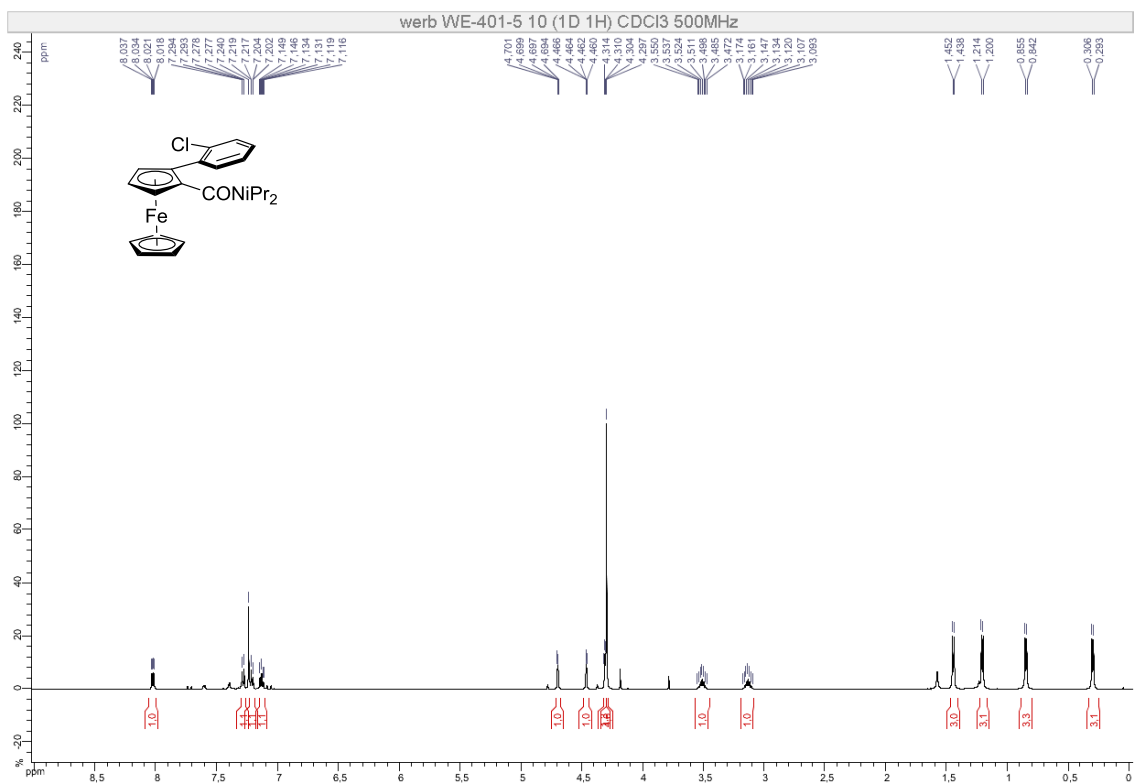
Compound (\pm)-7

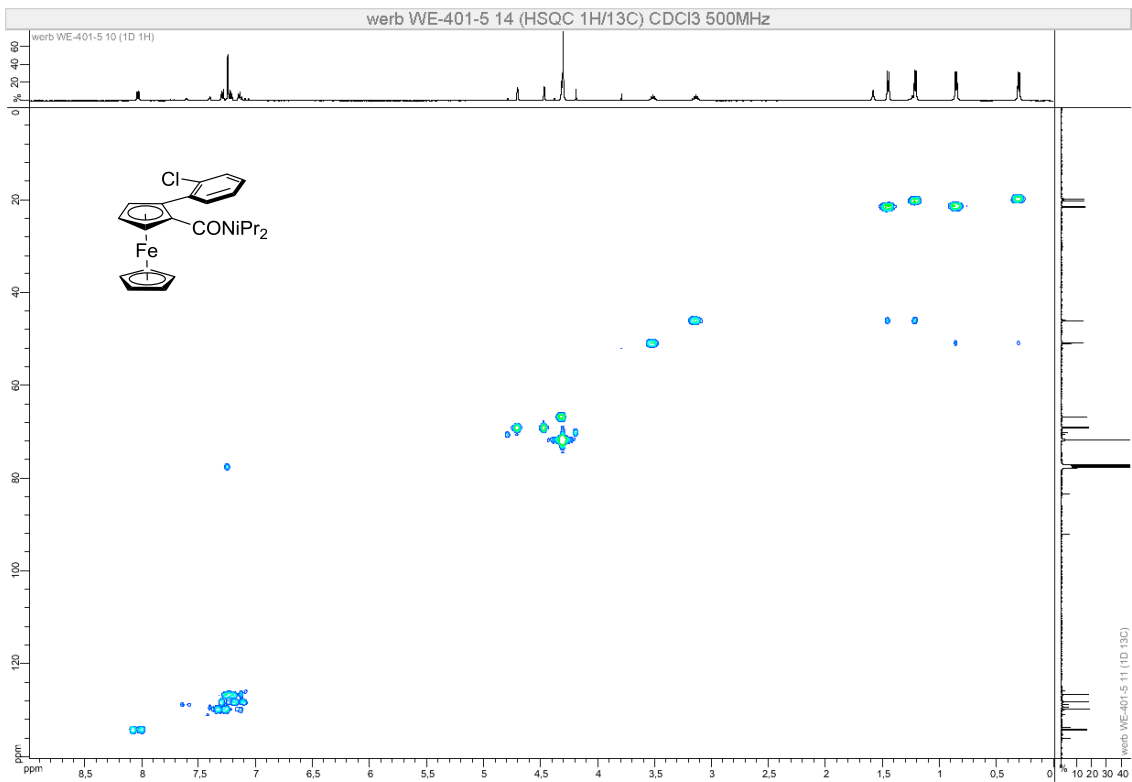
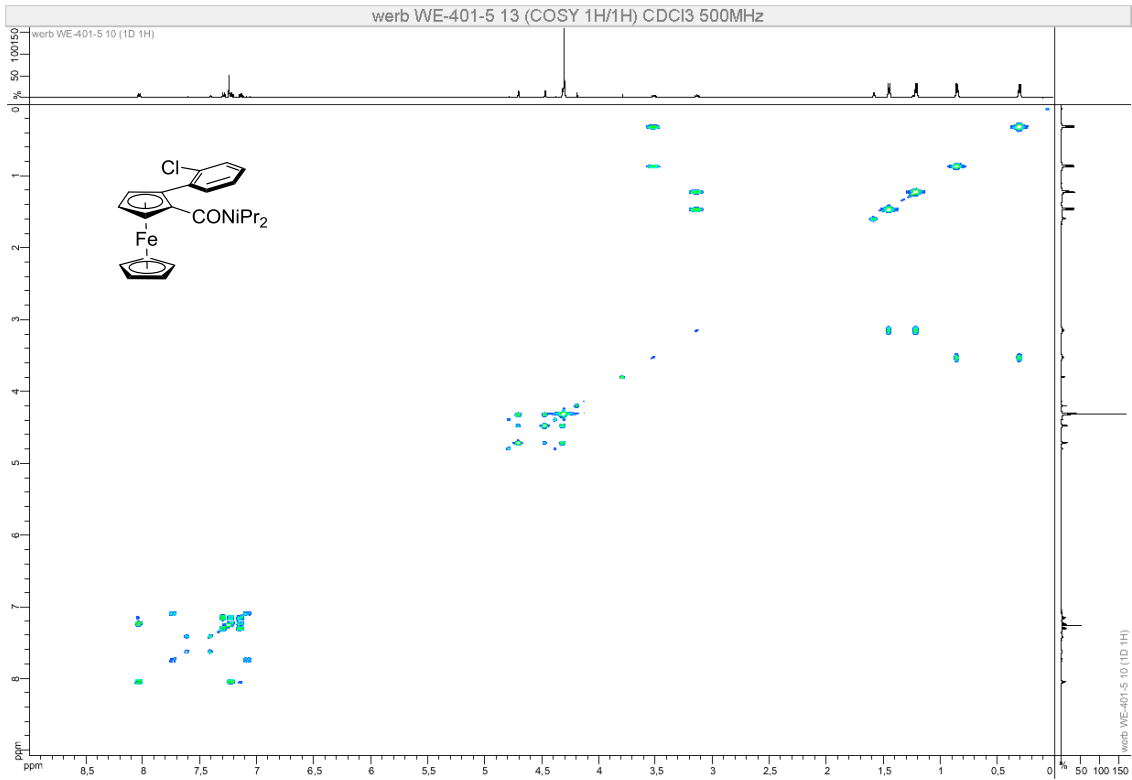


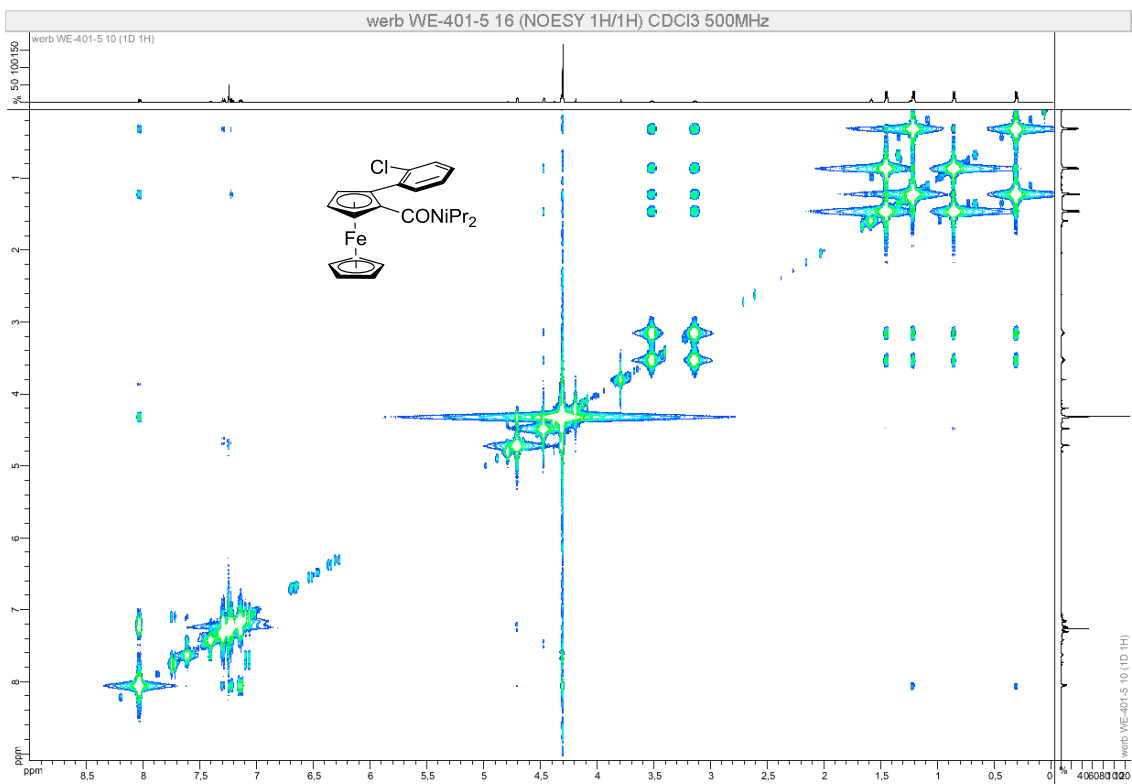
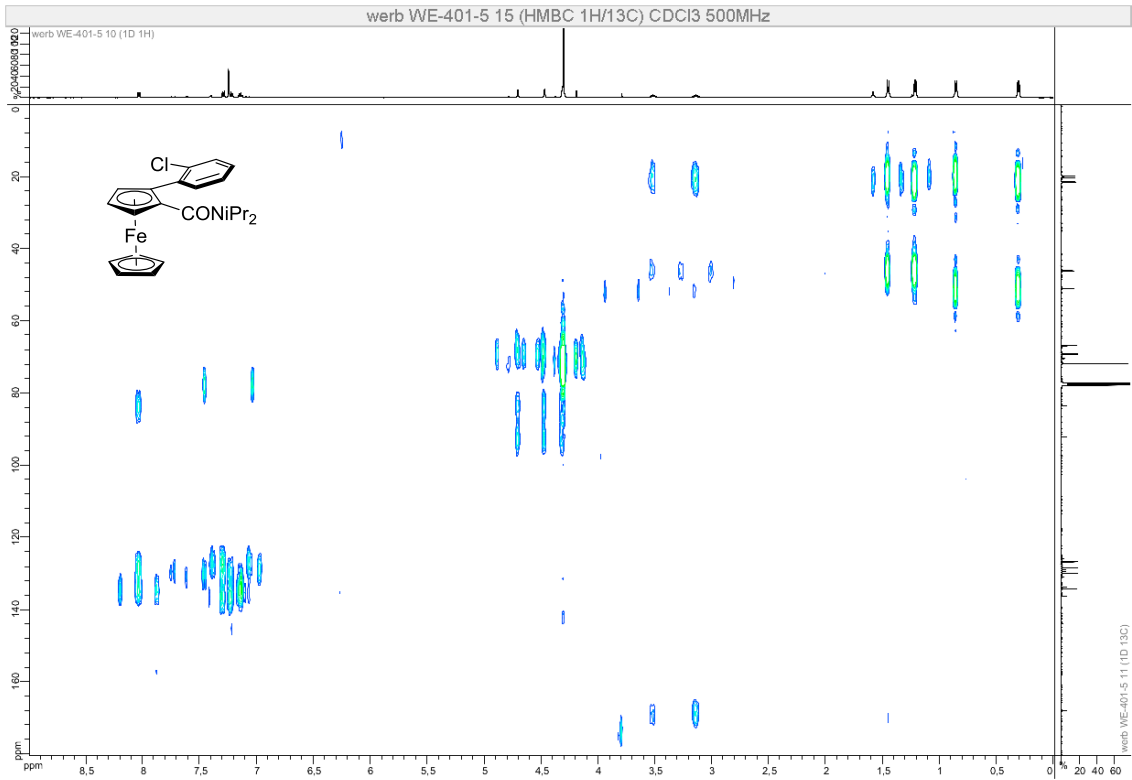




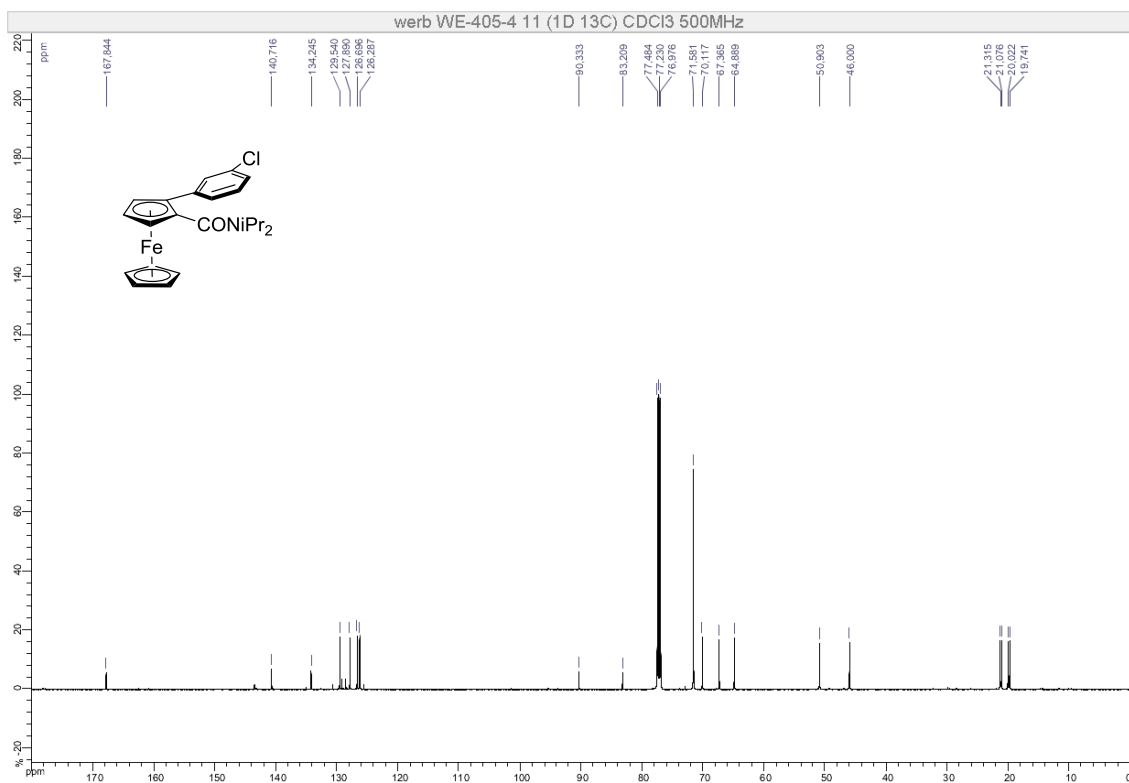
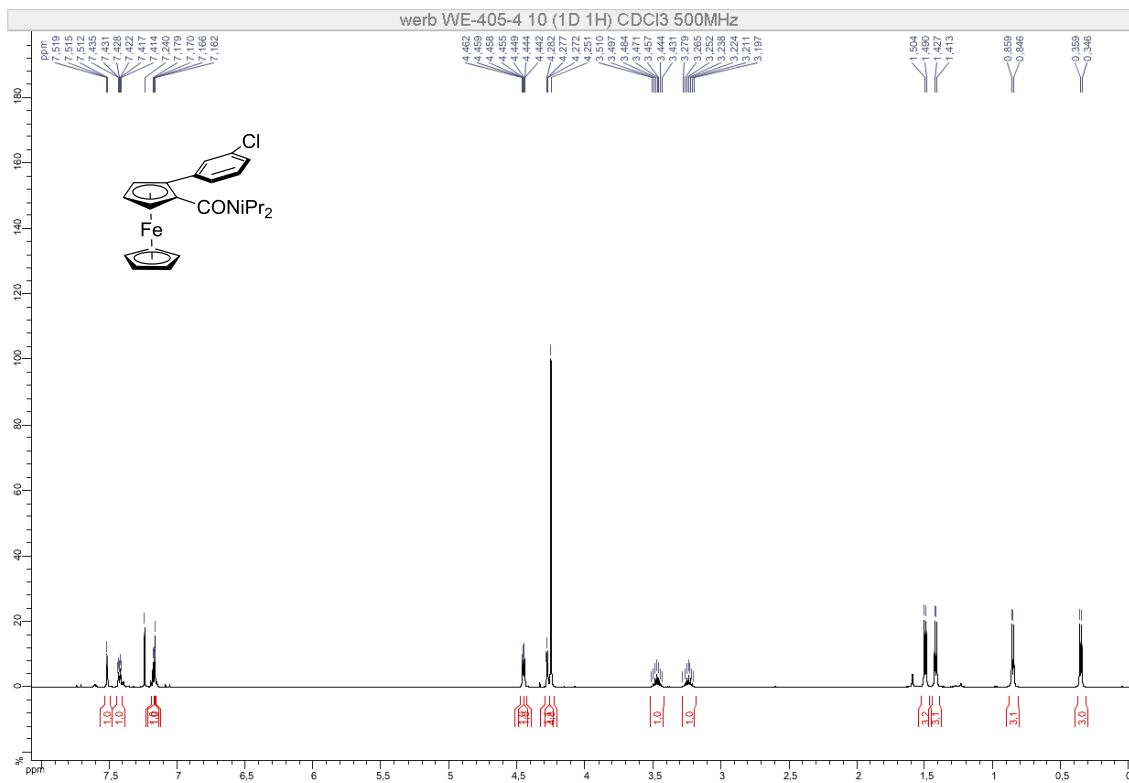
Compound (\pm)-8

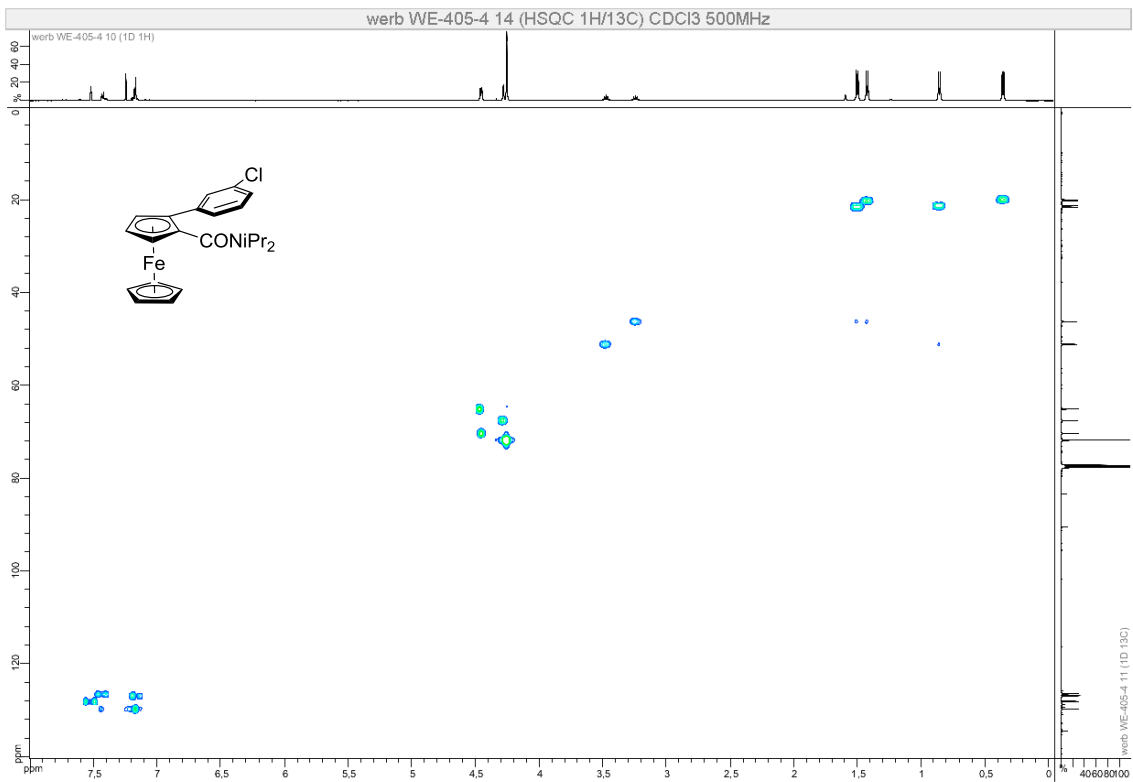
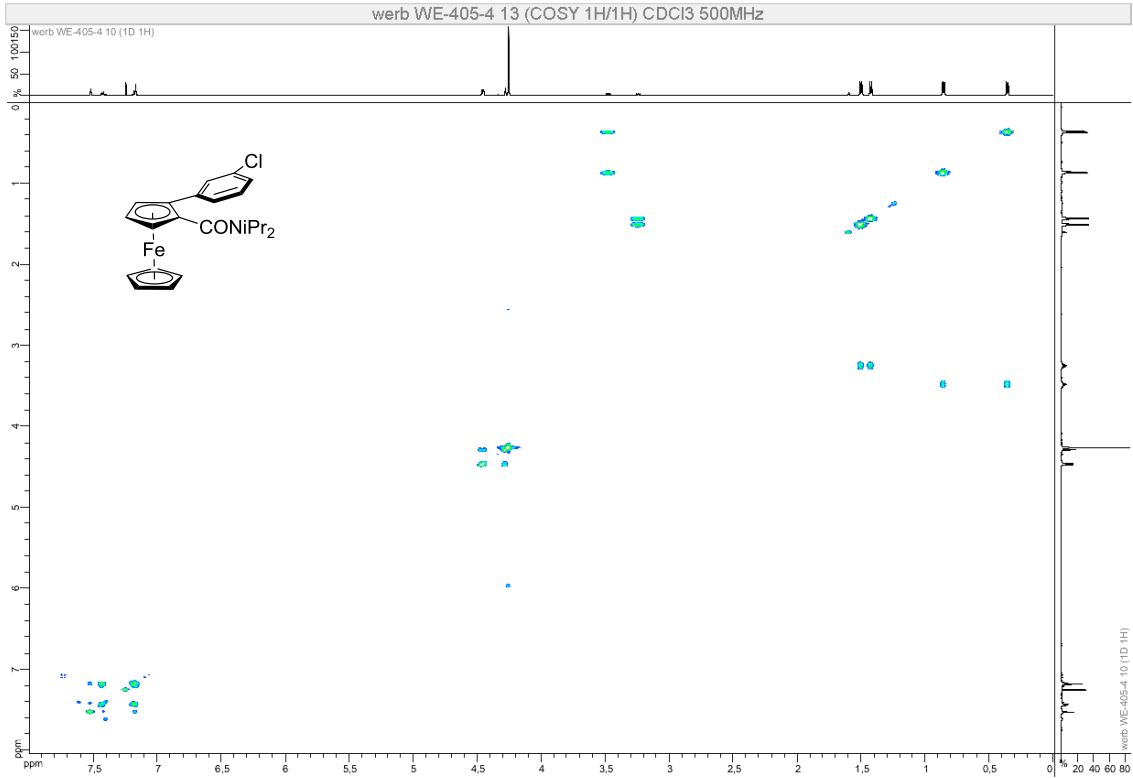


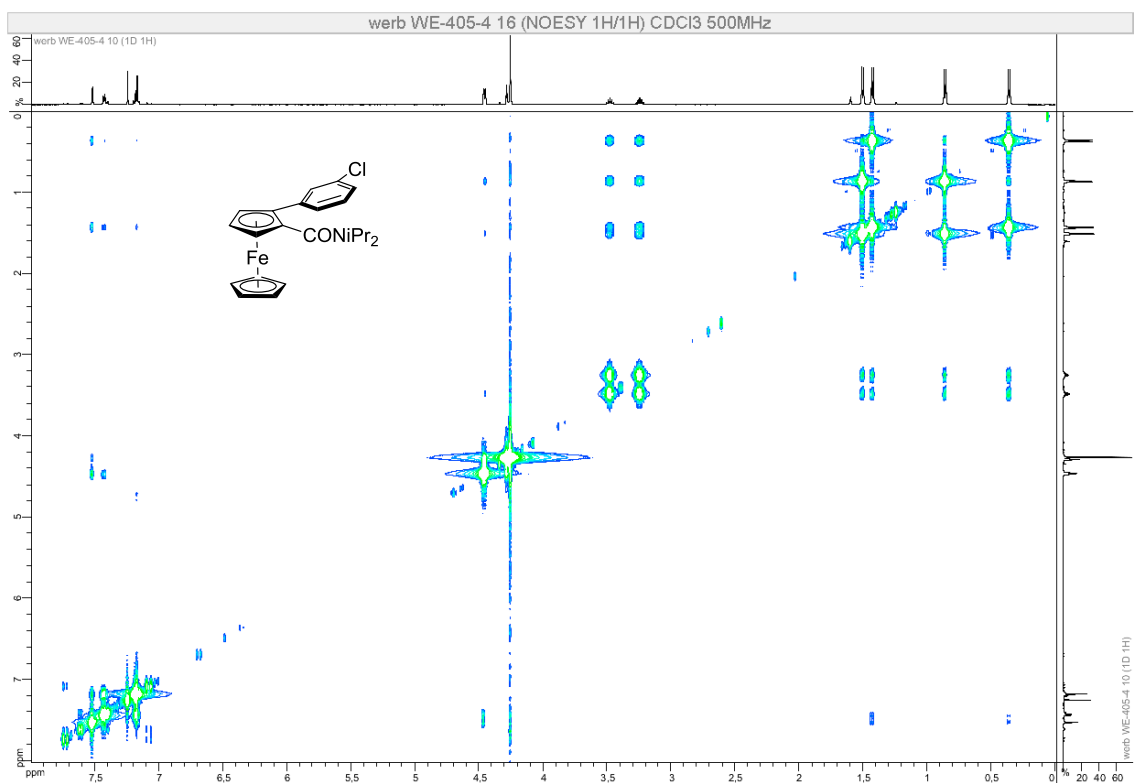
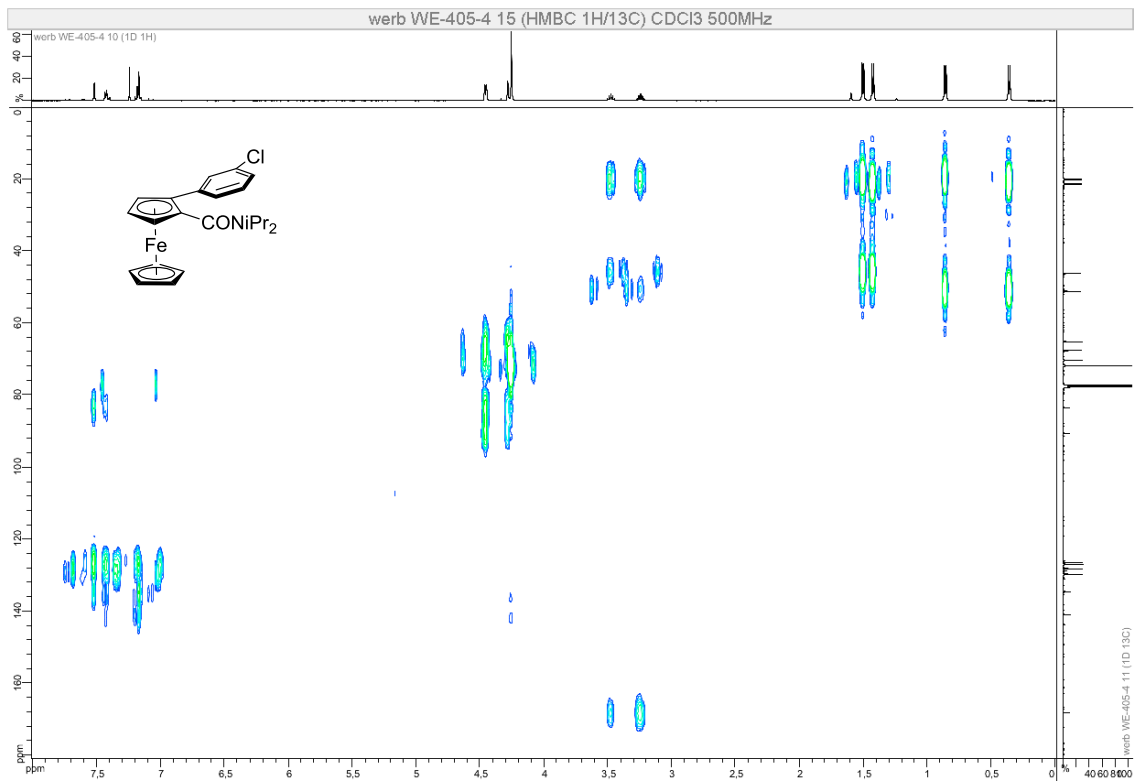




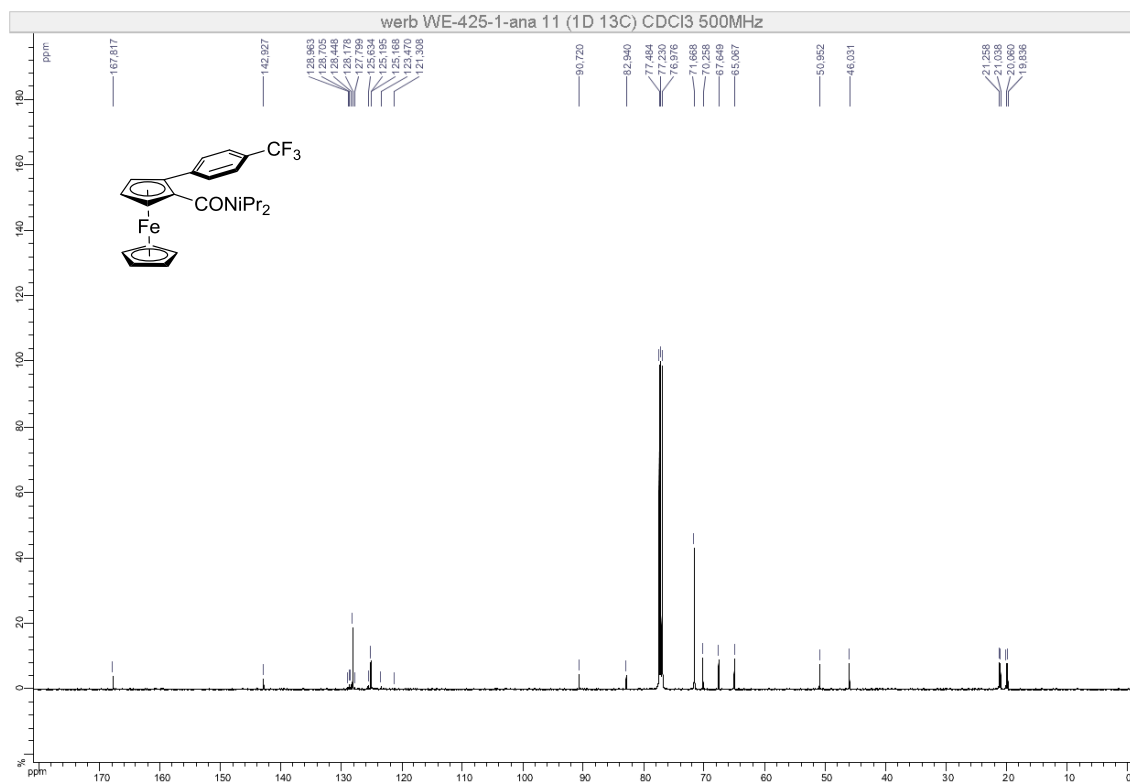
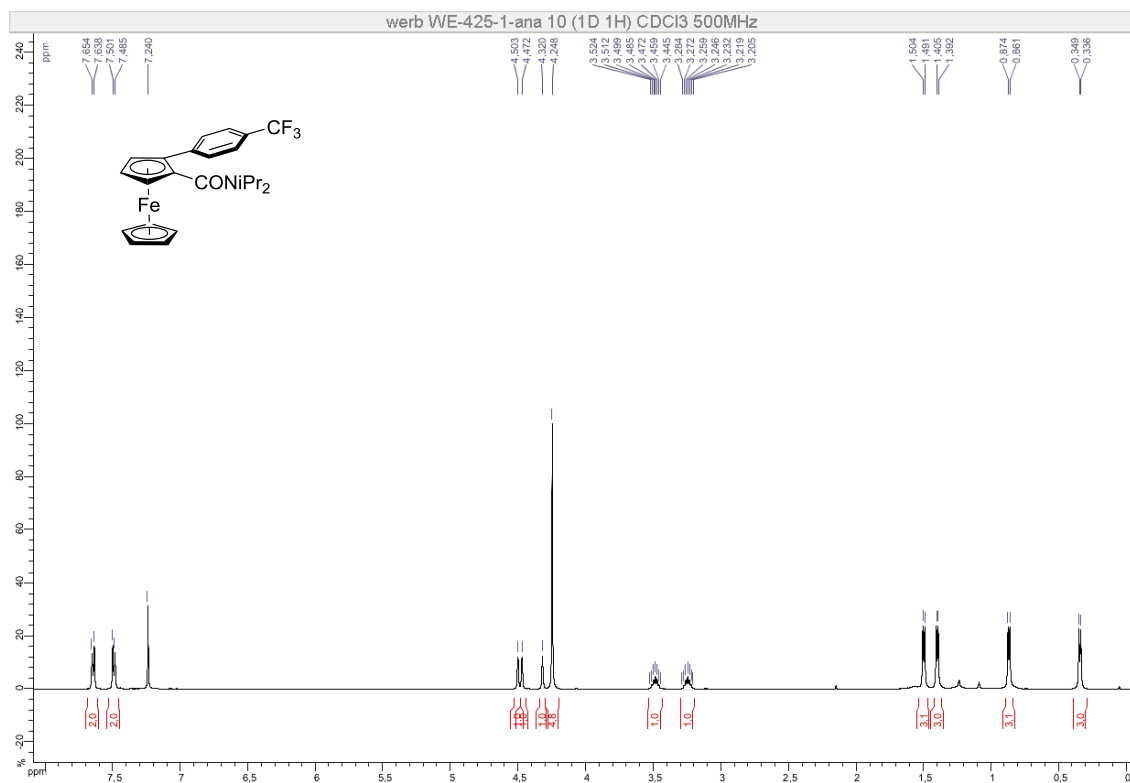
Compound (\pm)-9

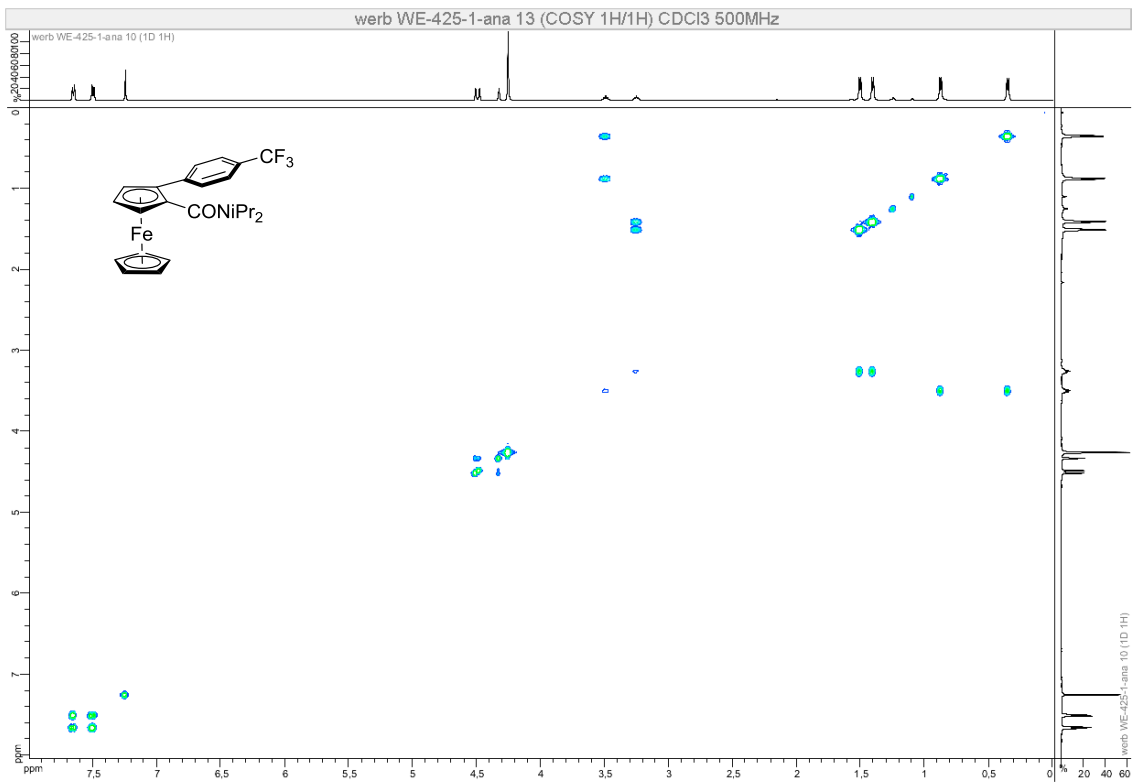
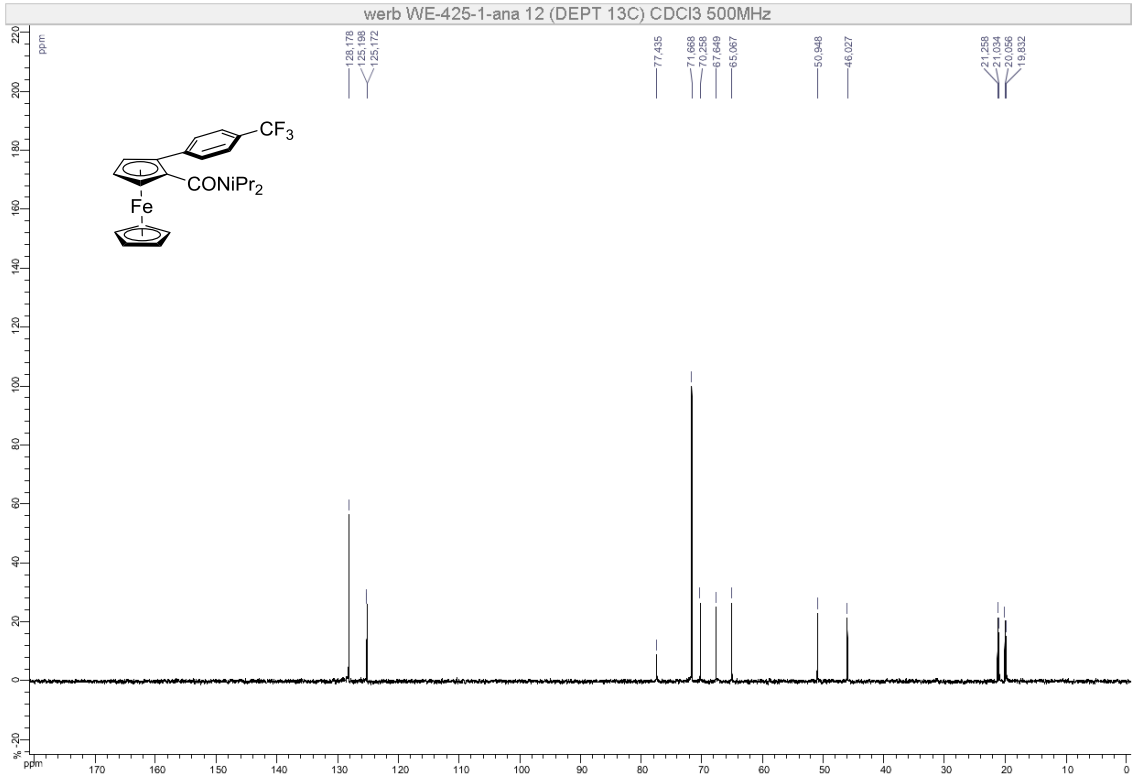


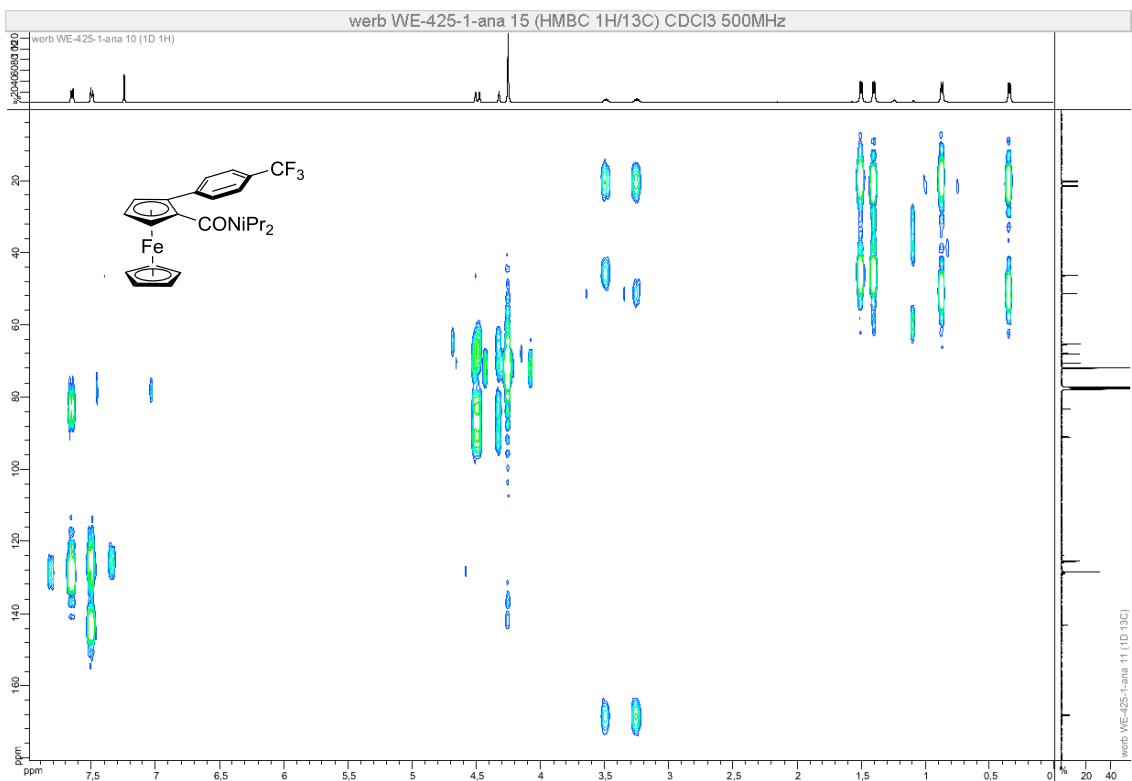
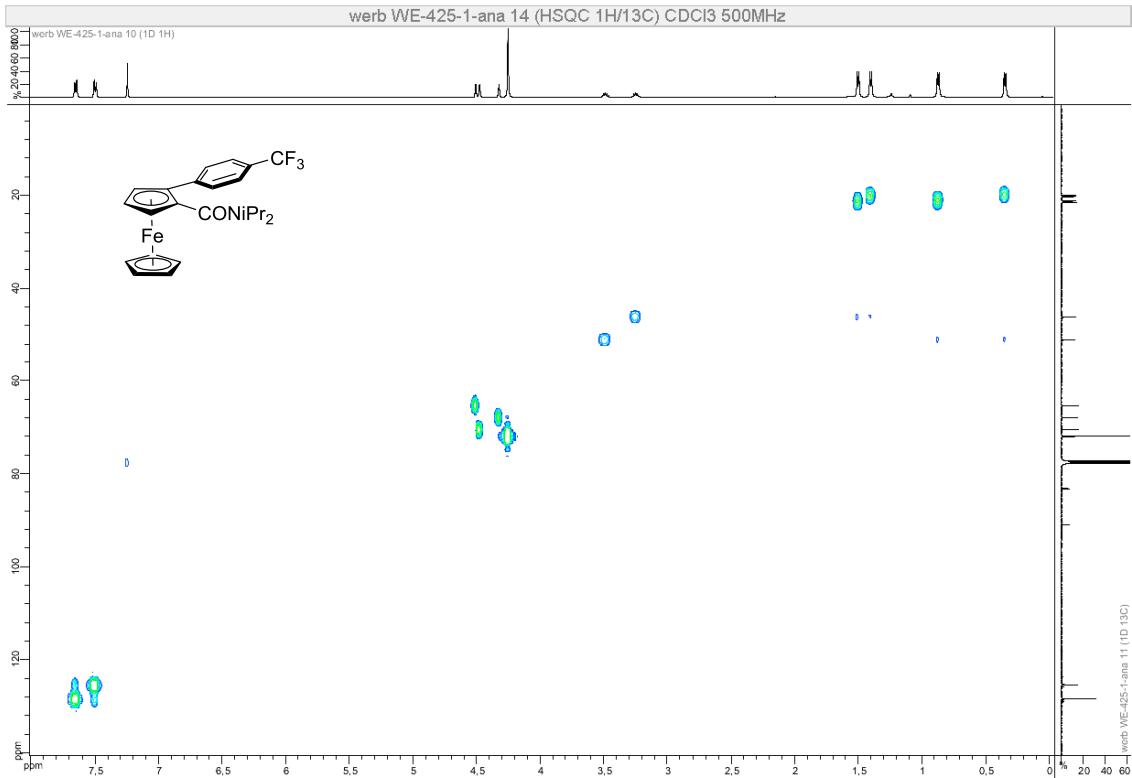


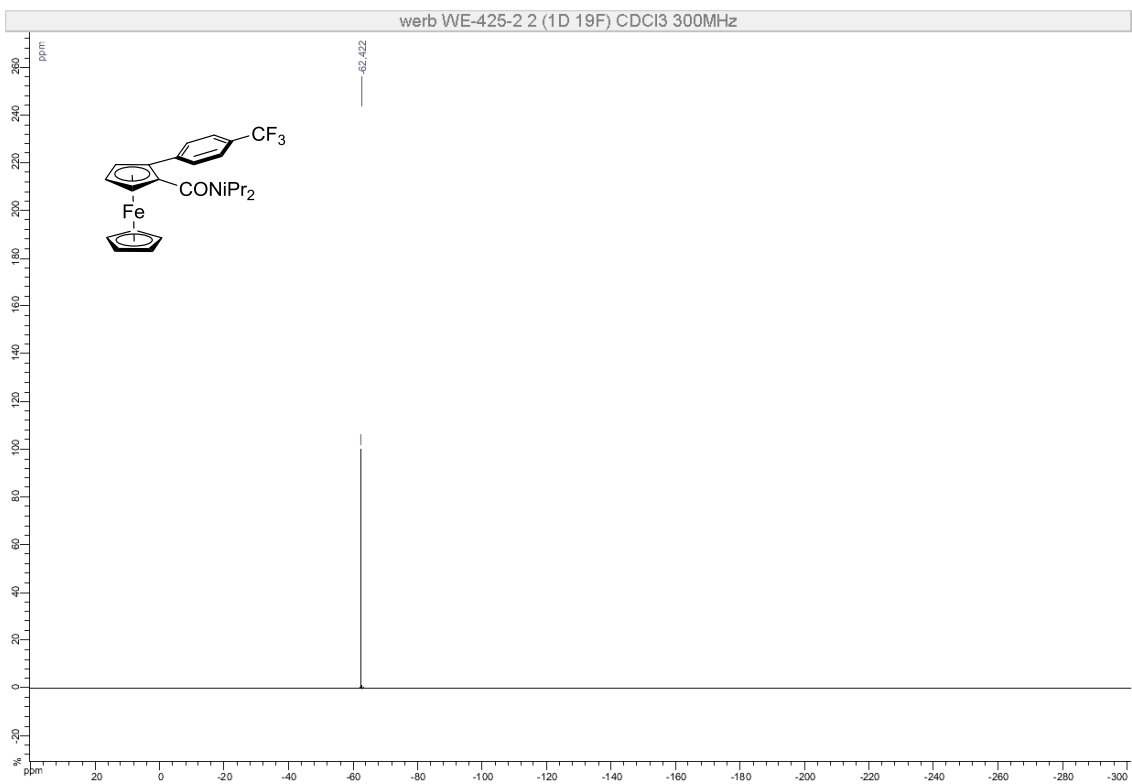
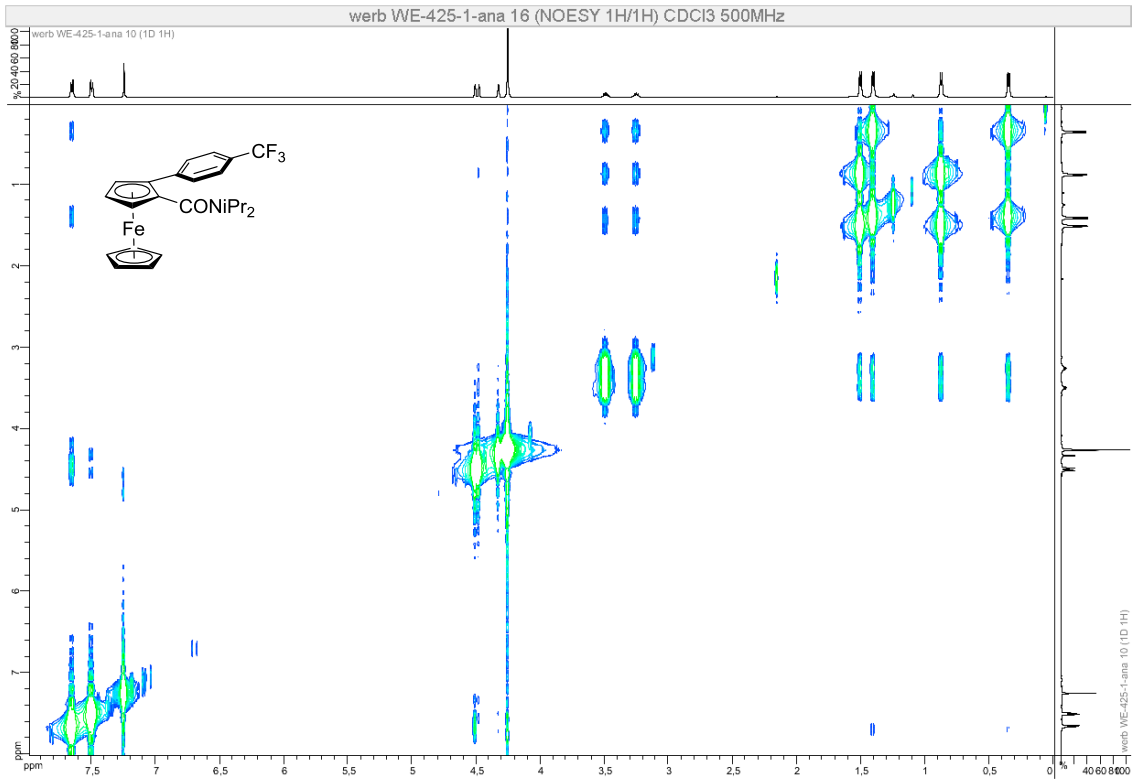


Compound (\pm)-10

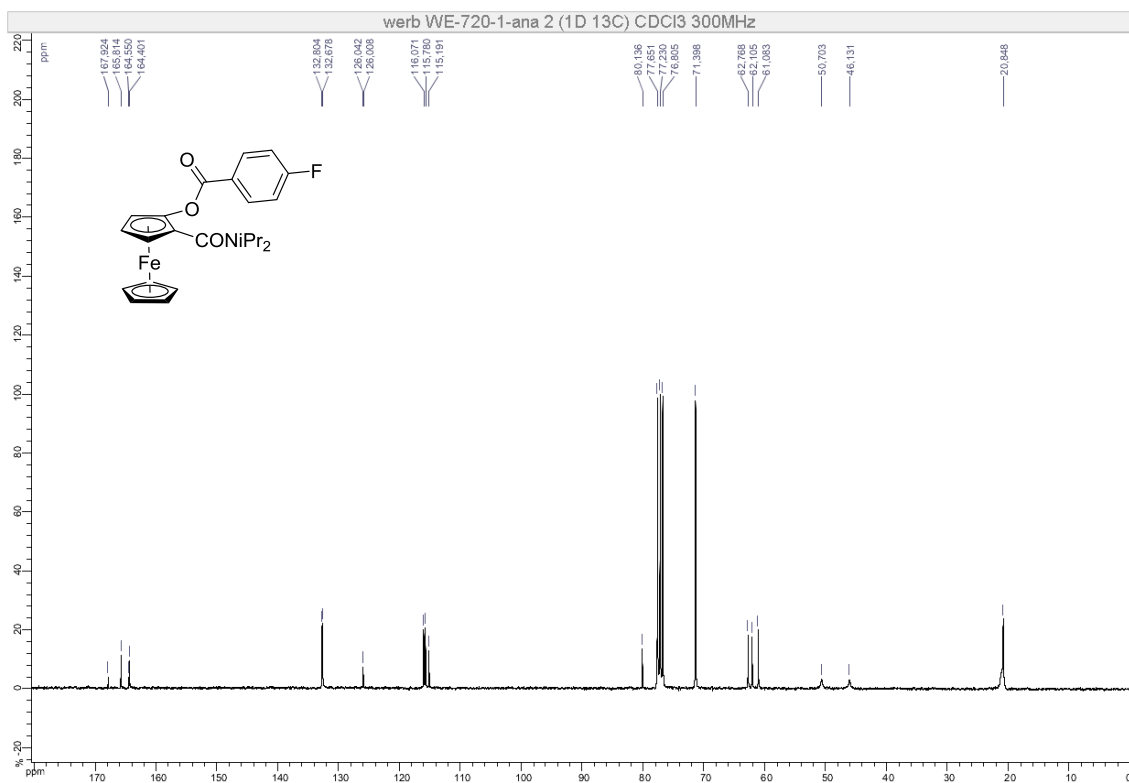
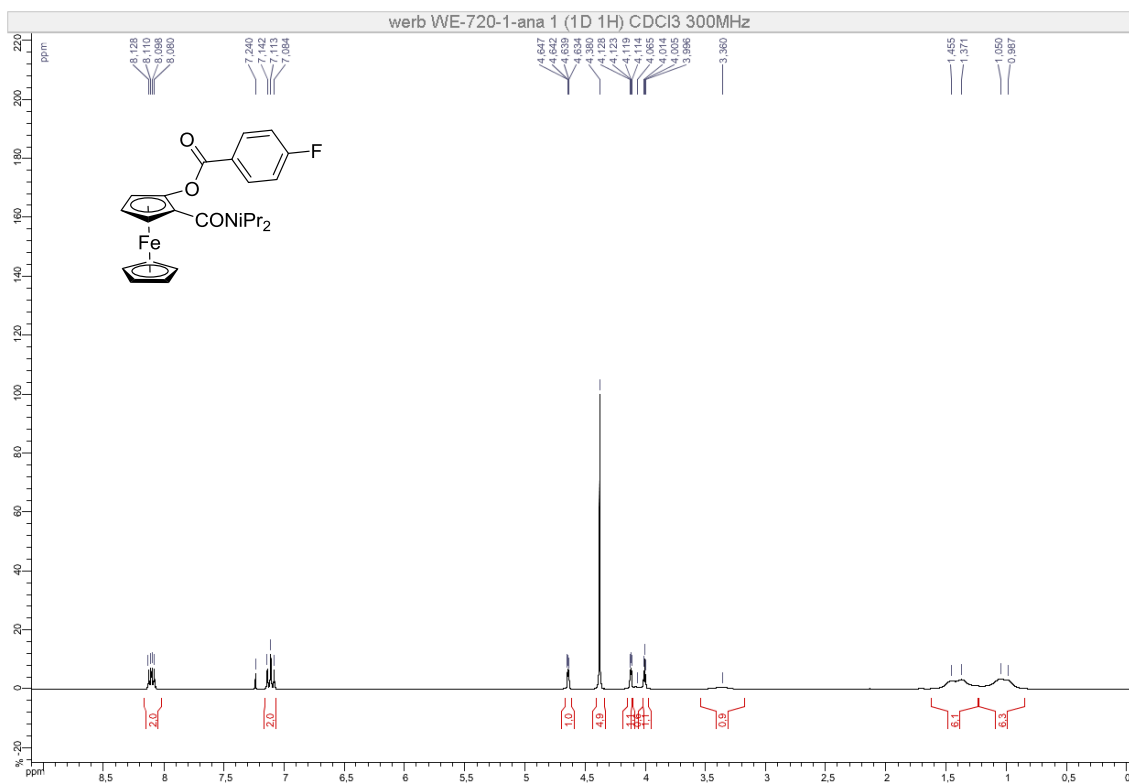


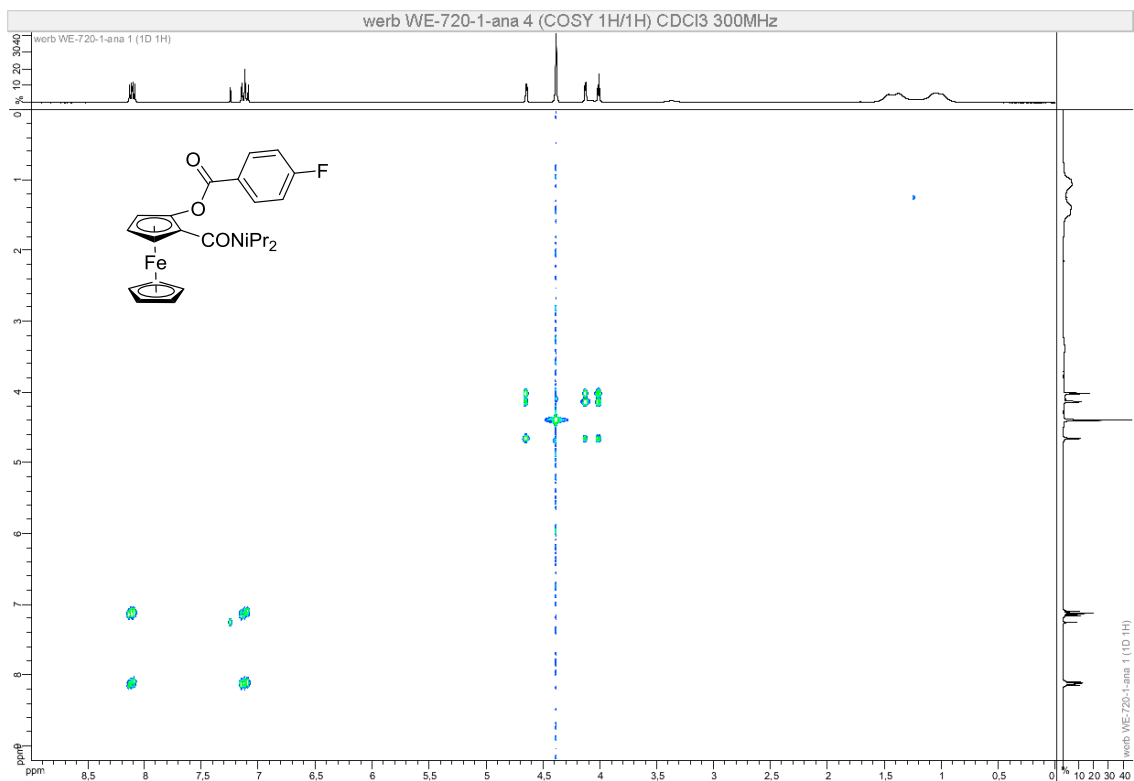
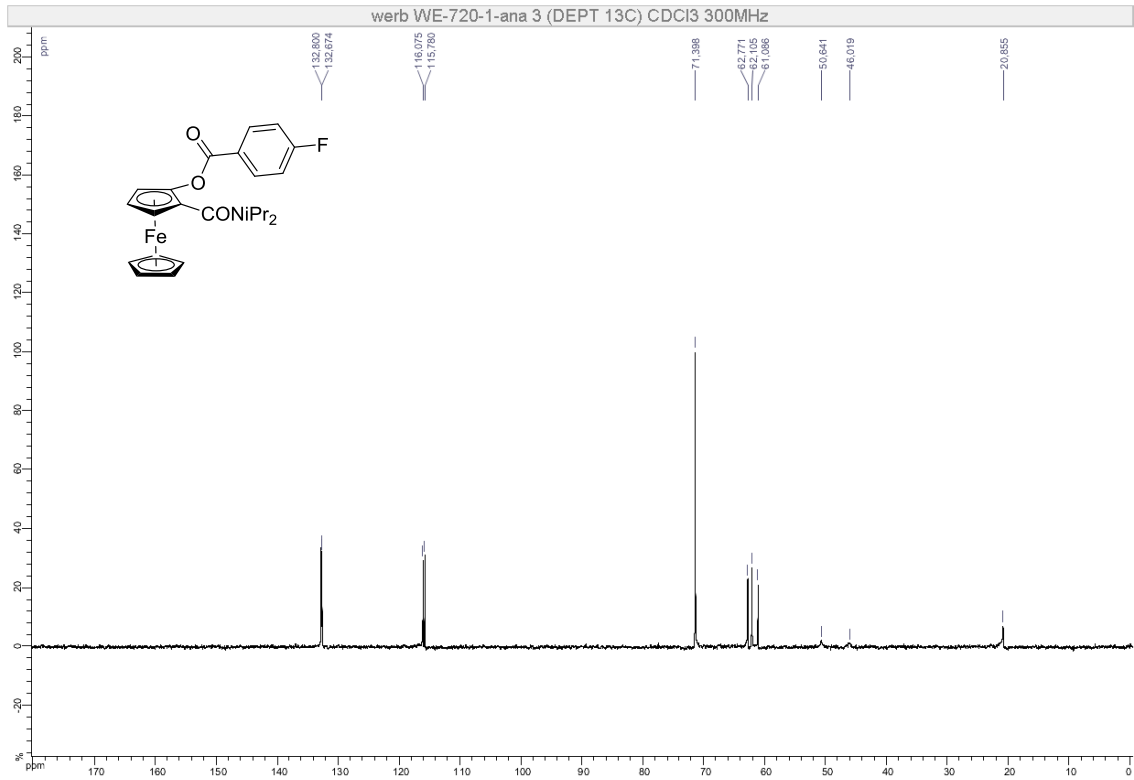


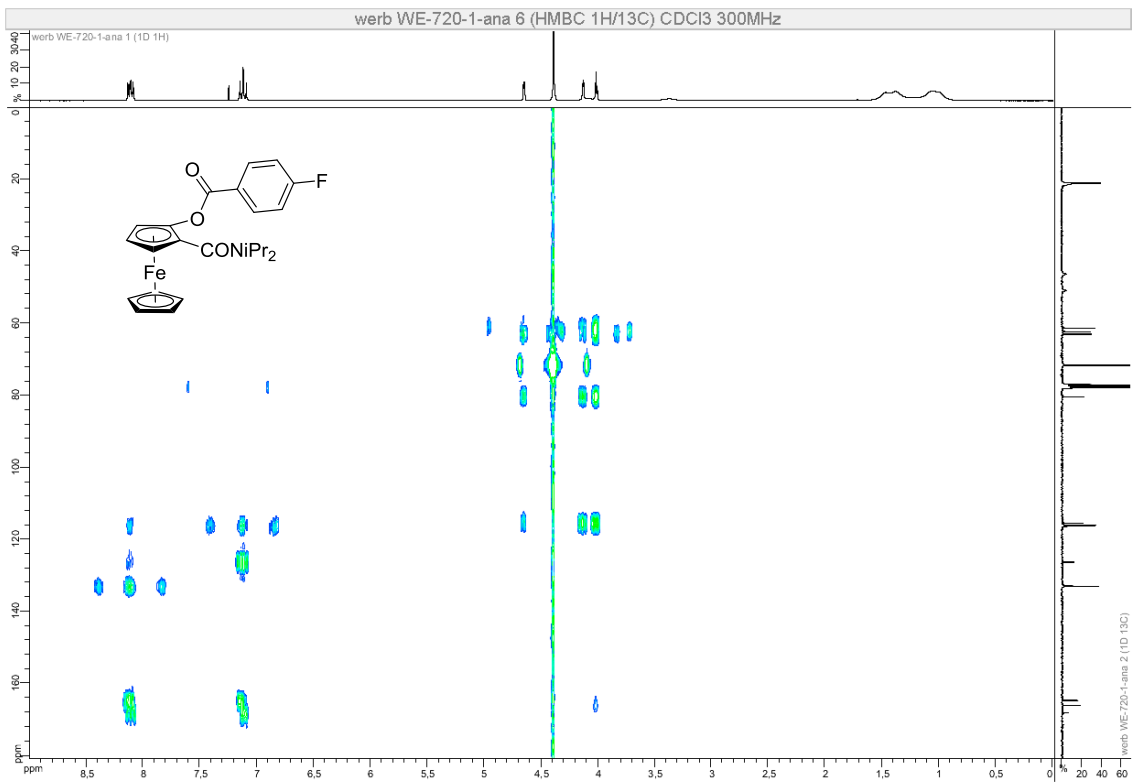
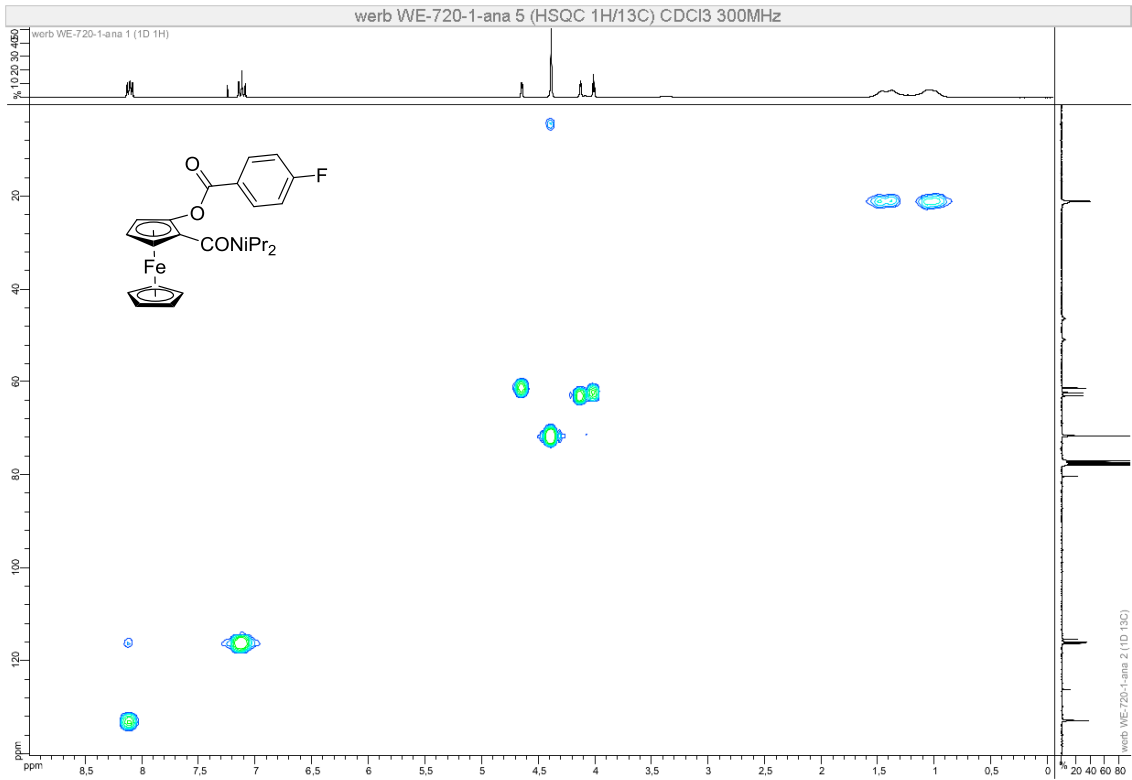


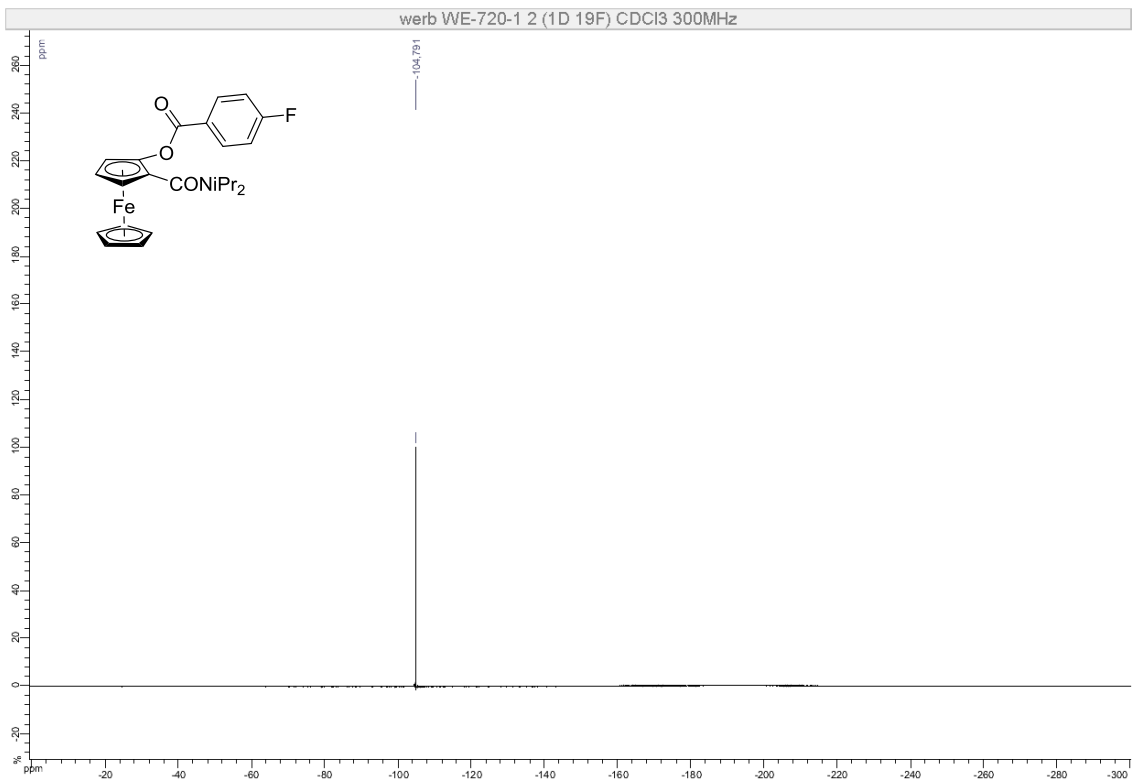


Compound (\pm)-11

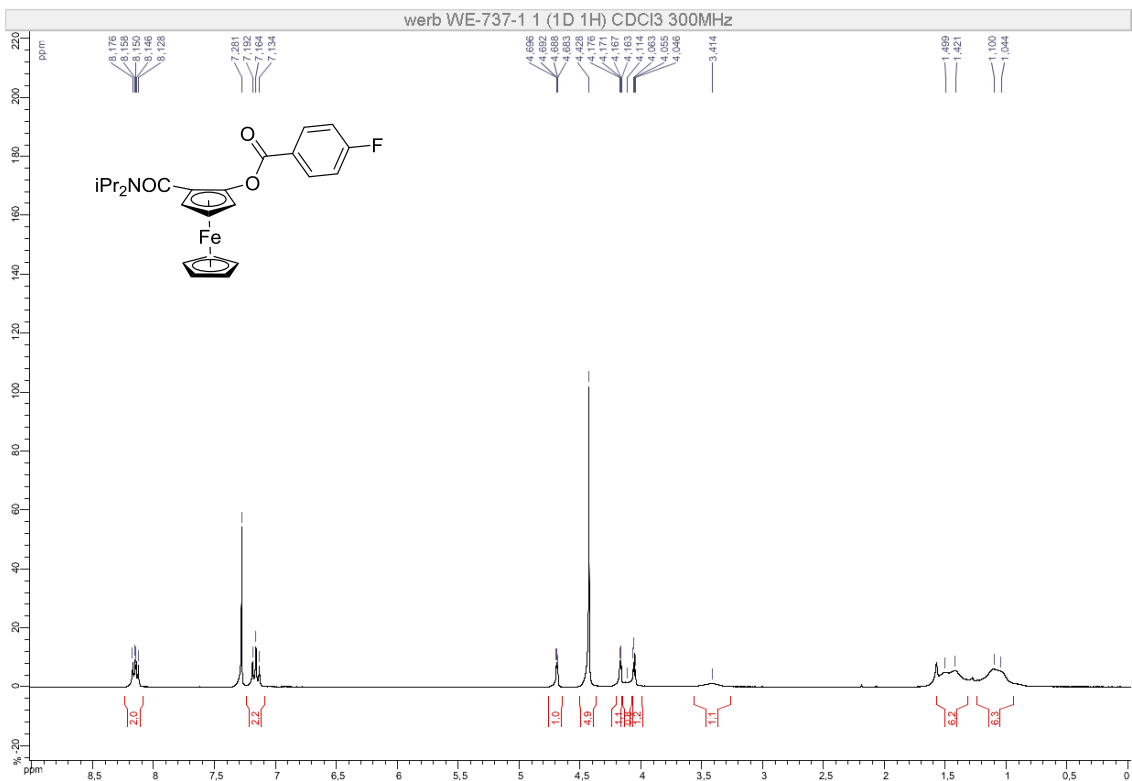




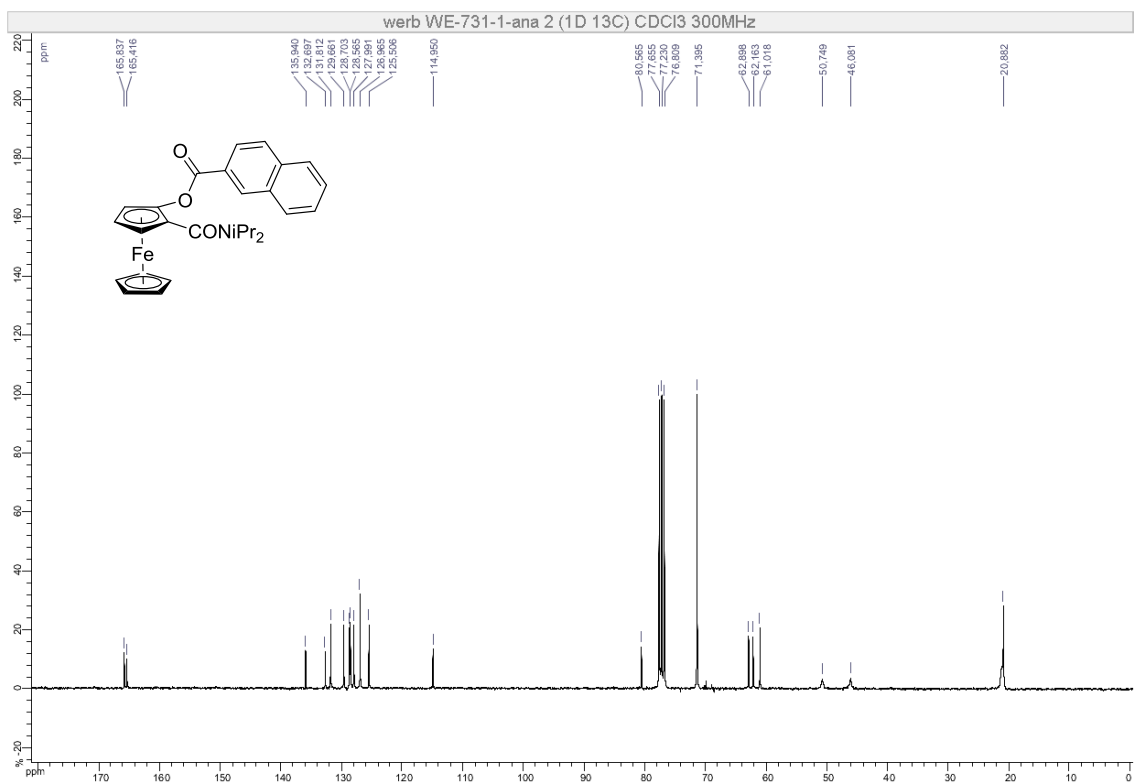
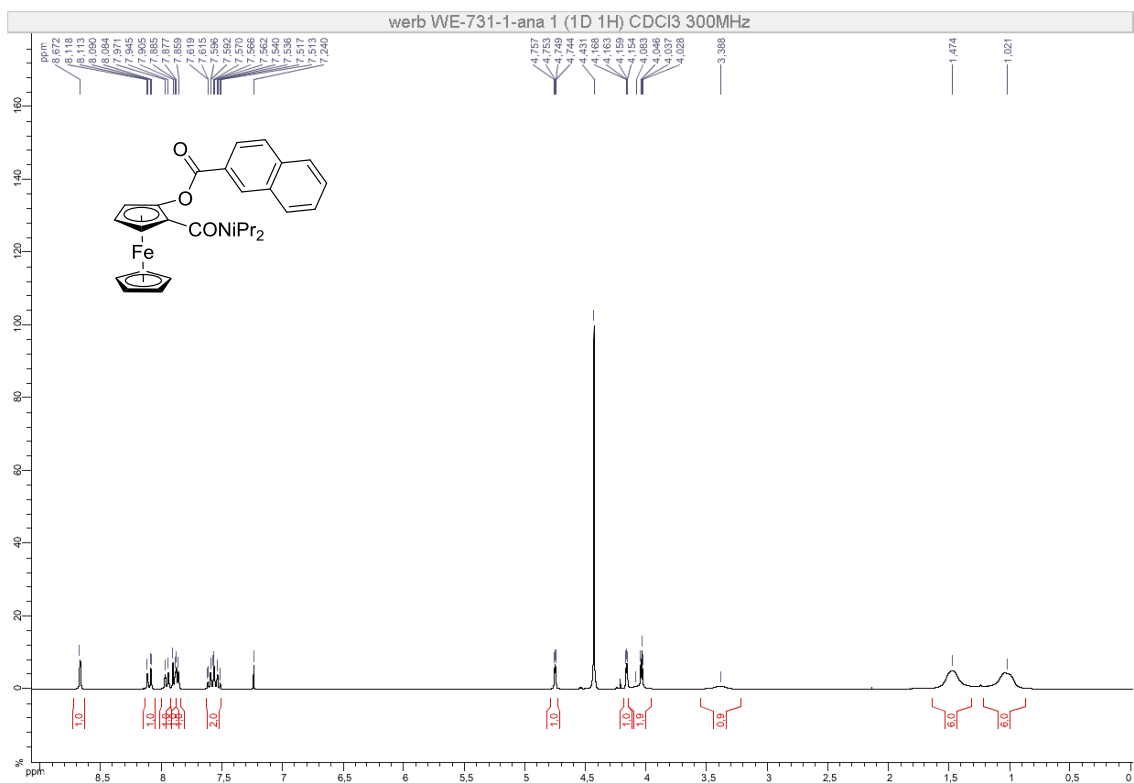


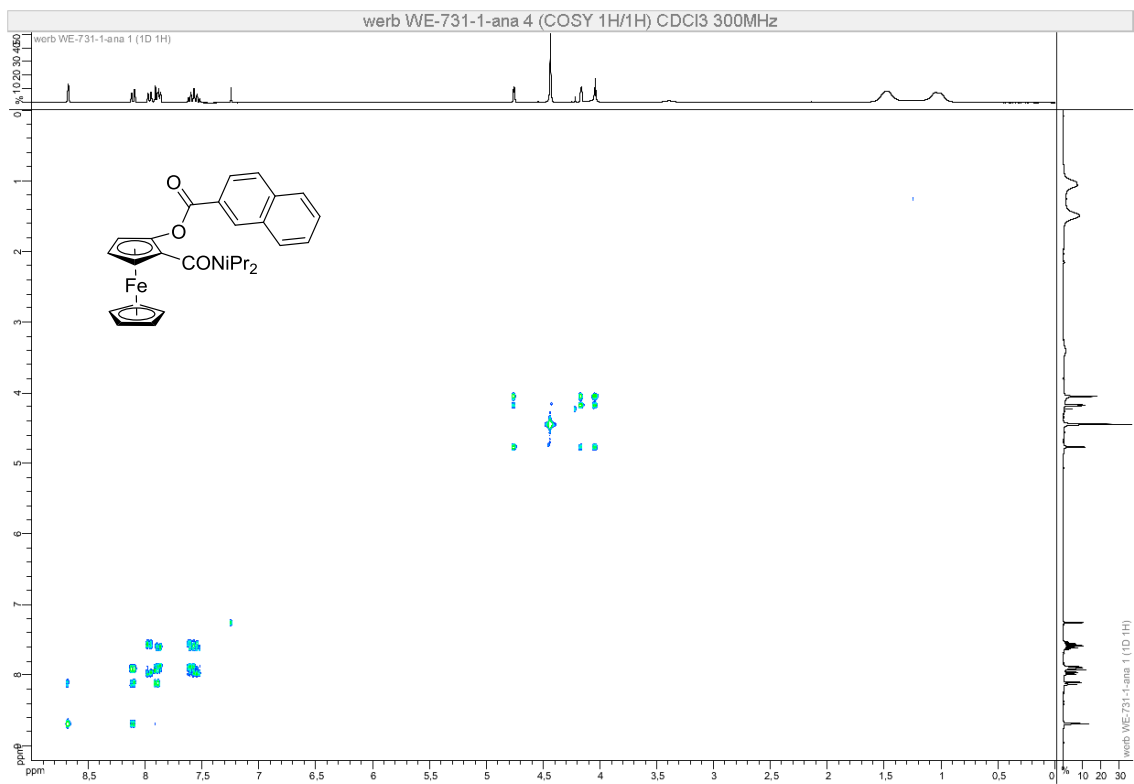
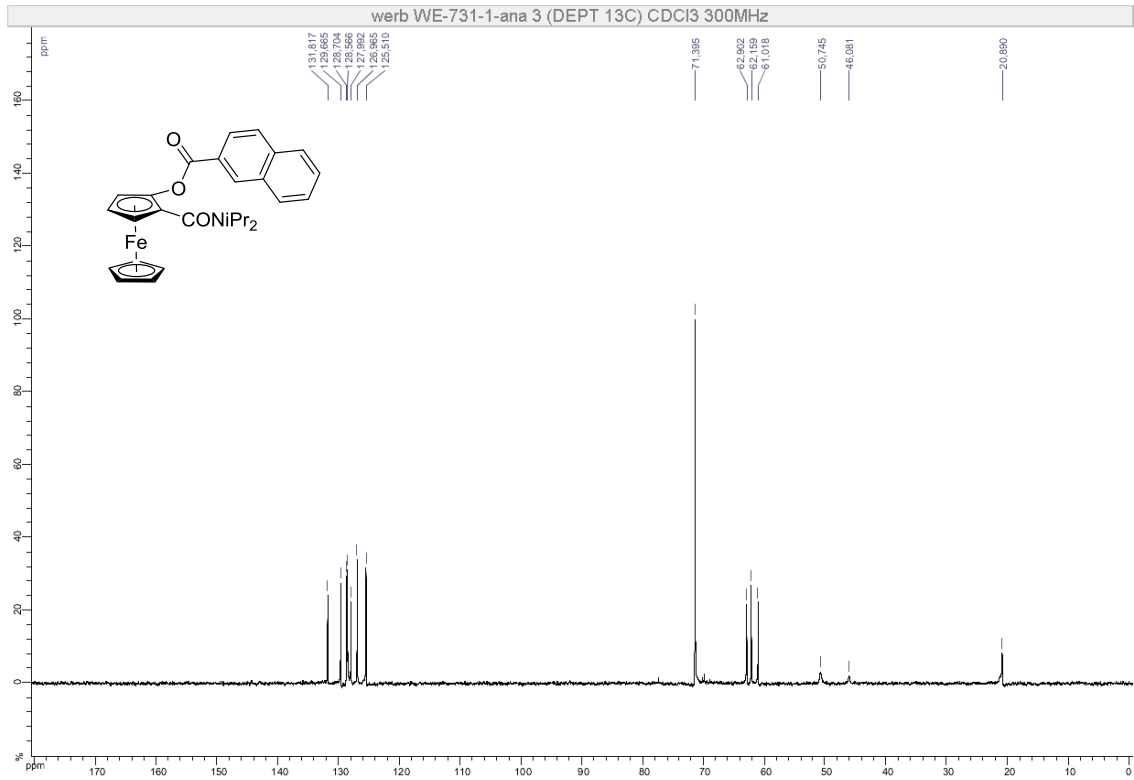


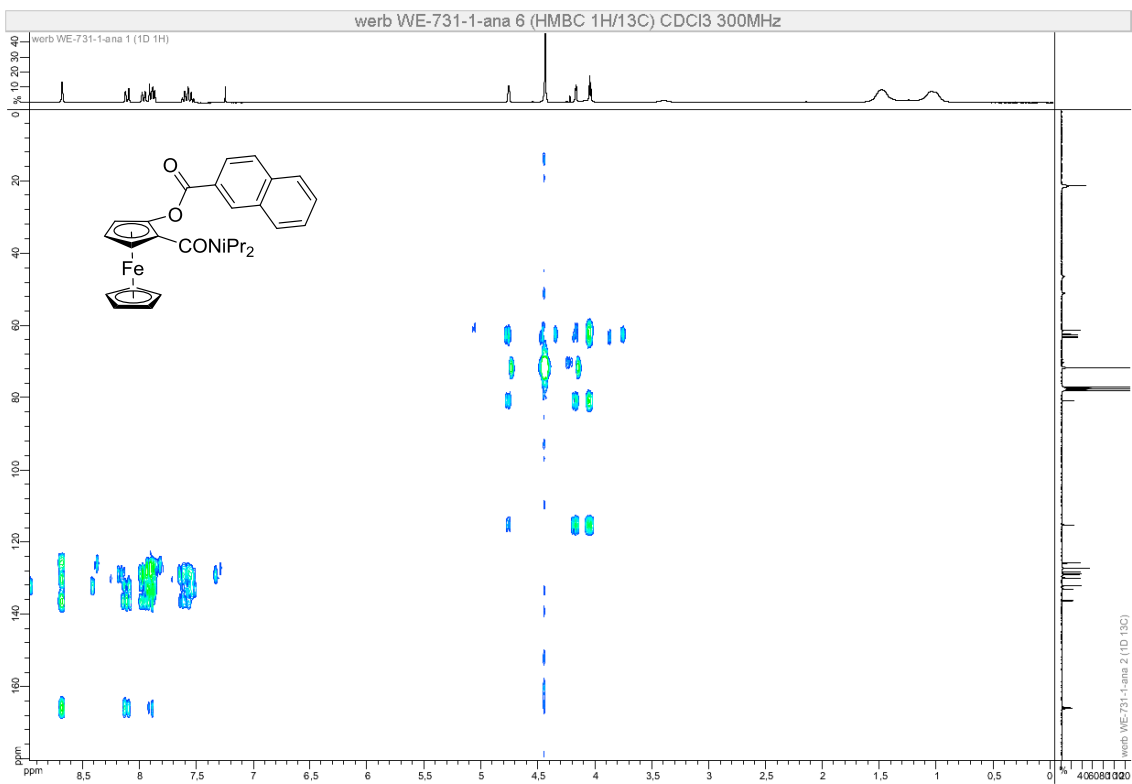
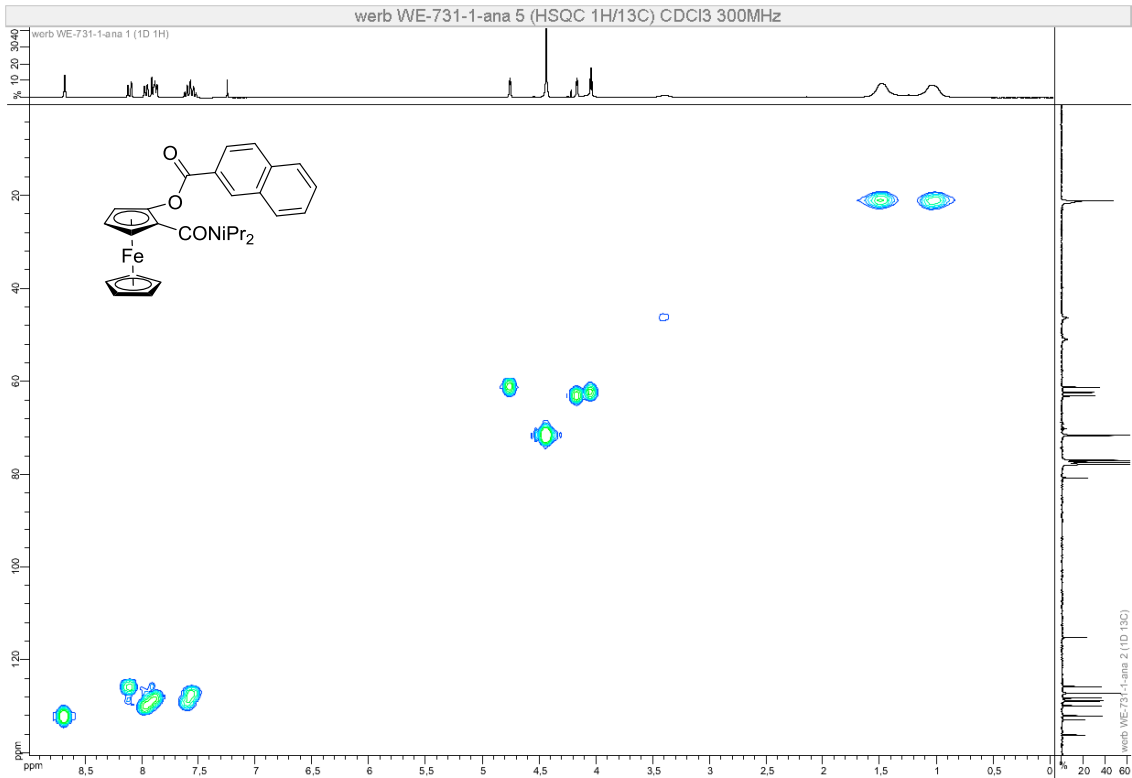
Compound (Sp)-11



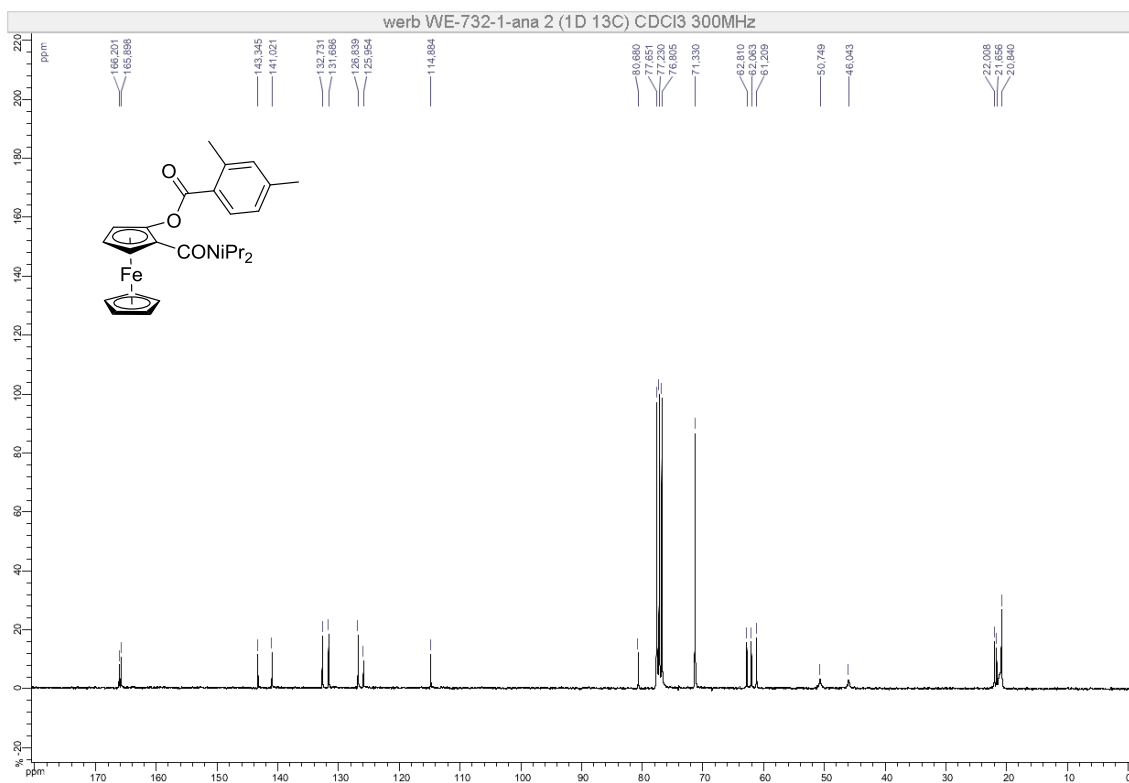
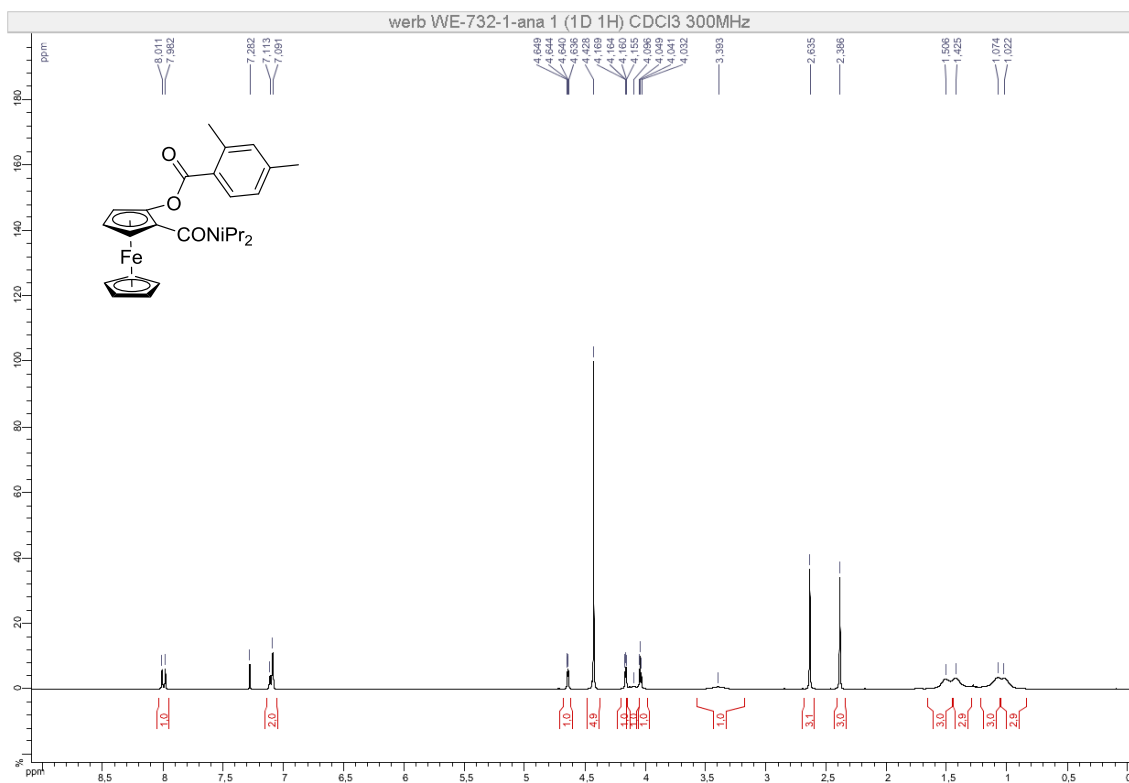
Compound (\pm)-12

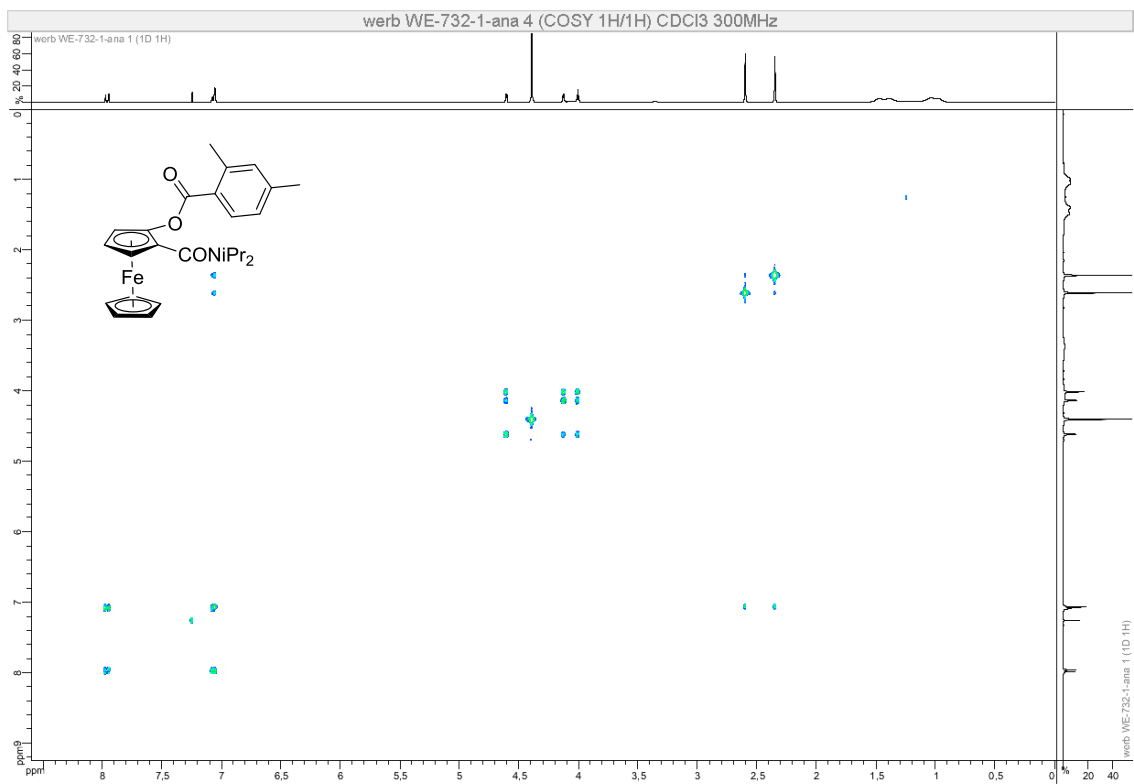
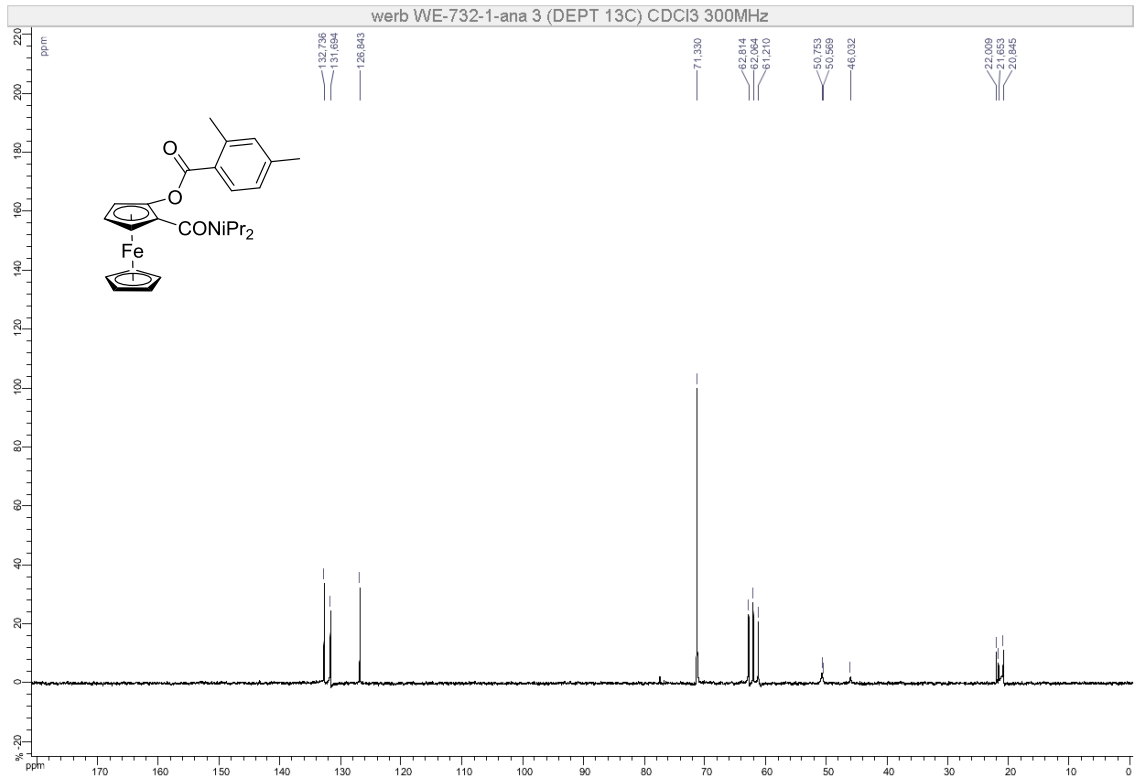


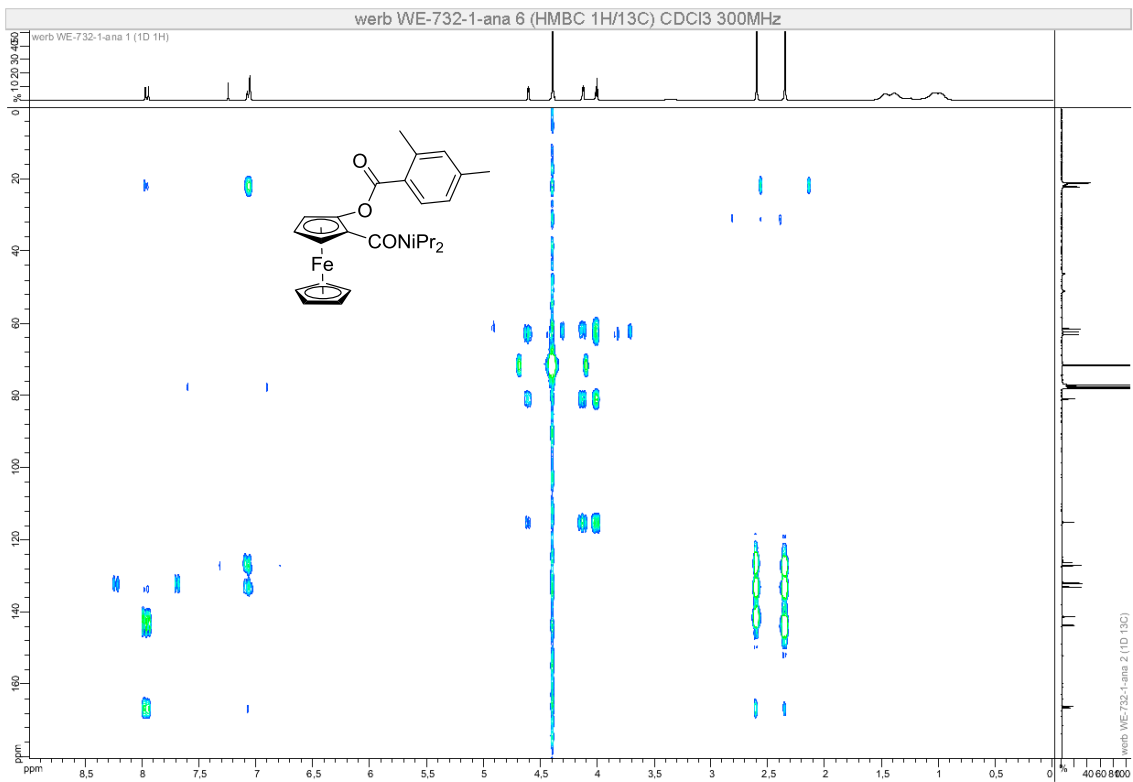
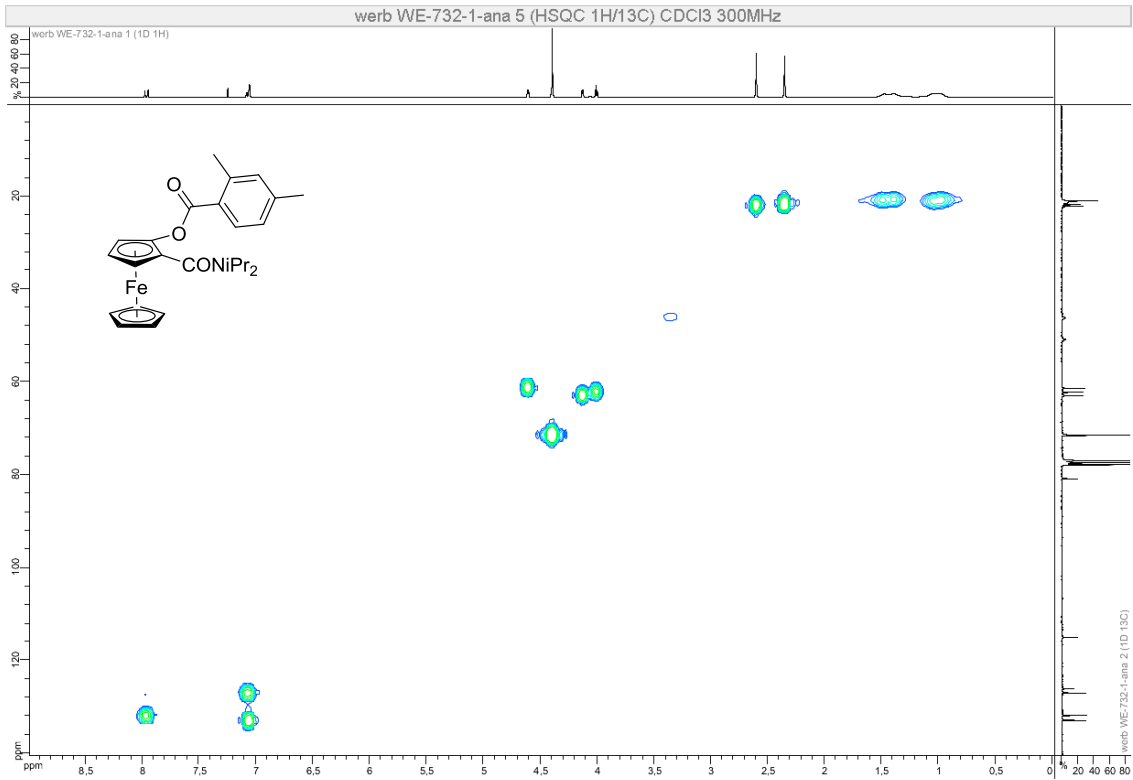




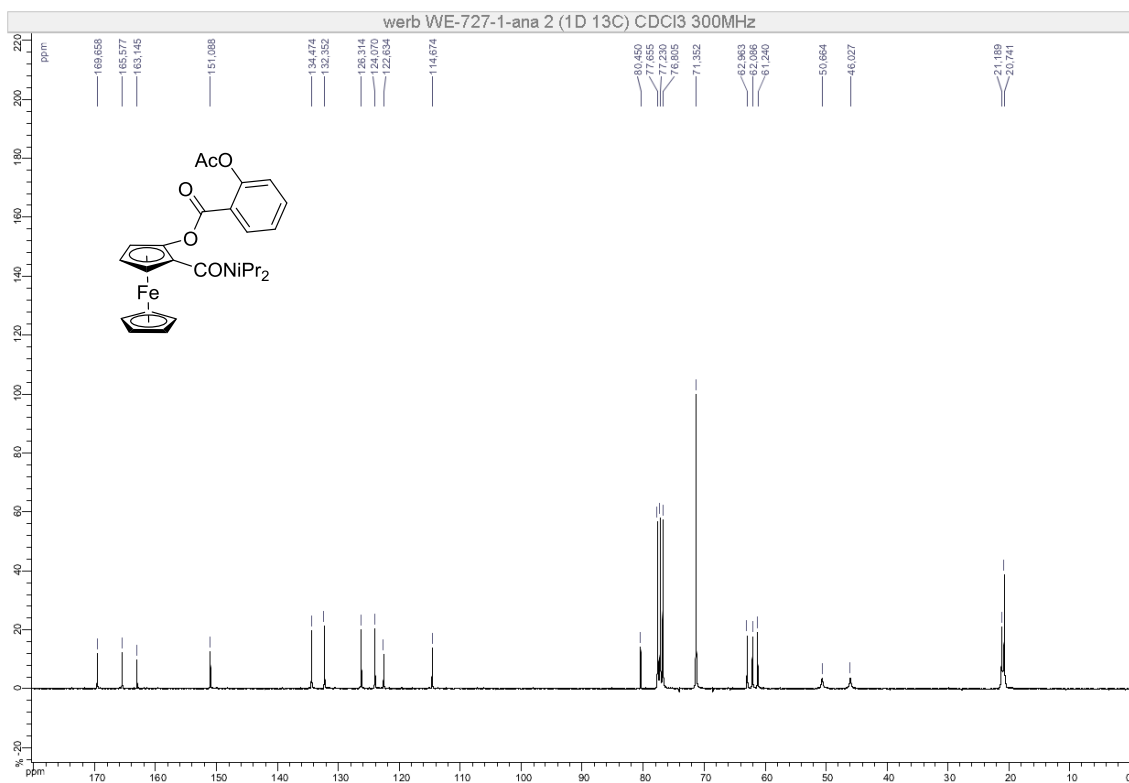
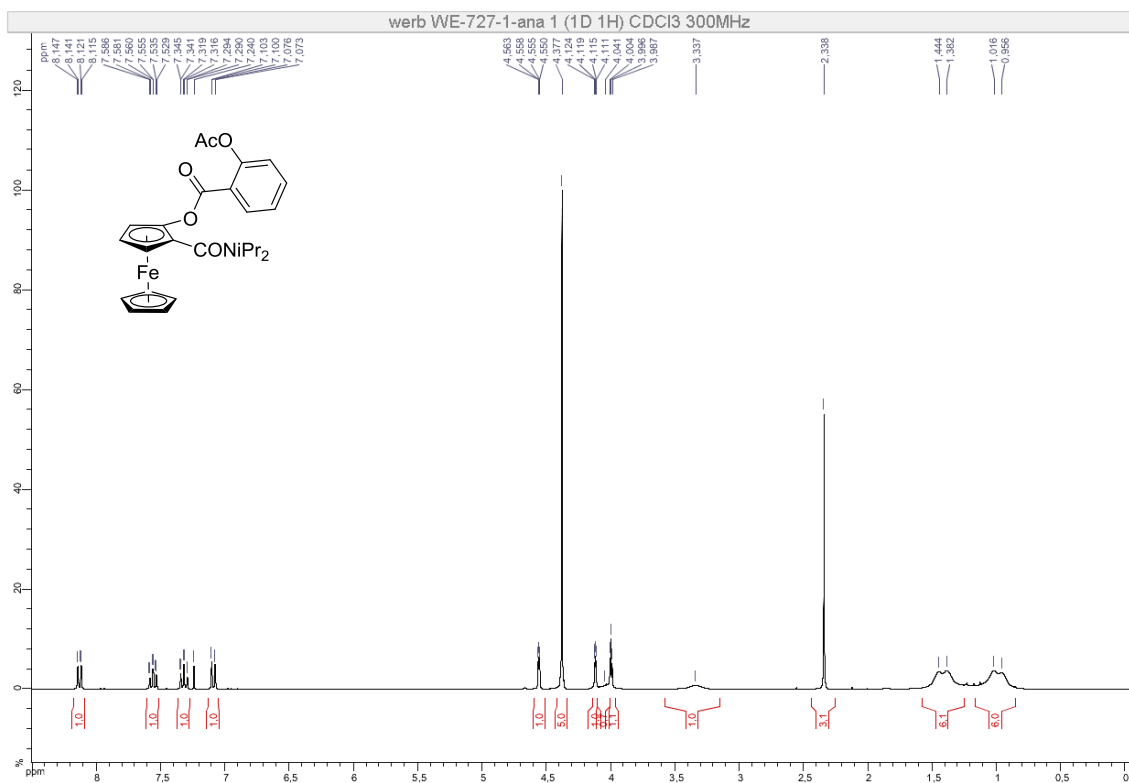
Compound (\pm)-13

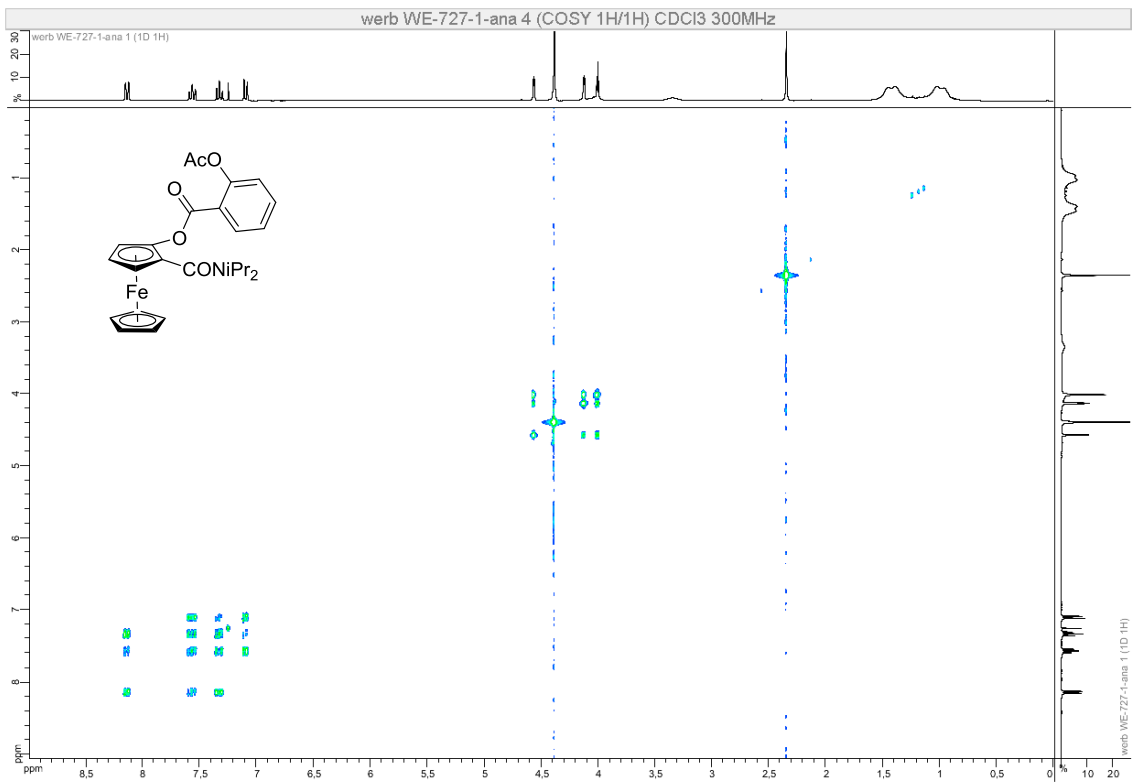
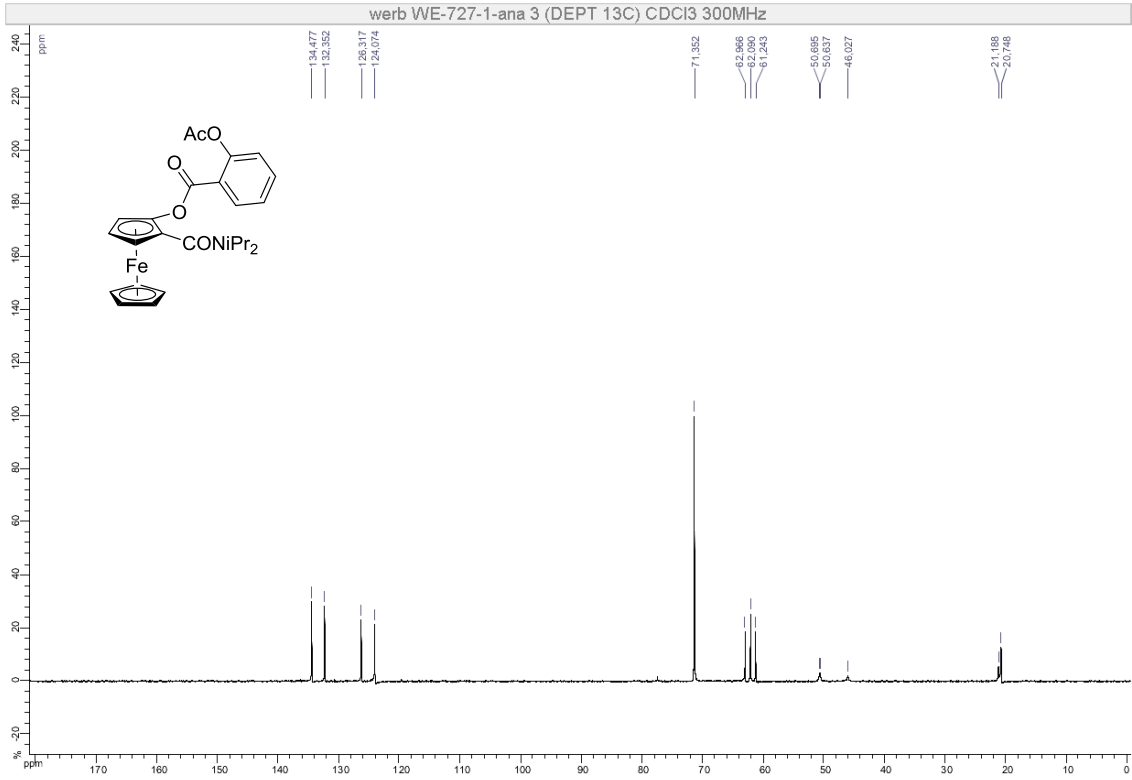


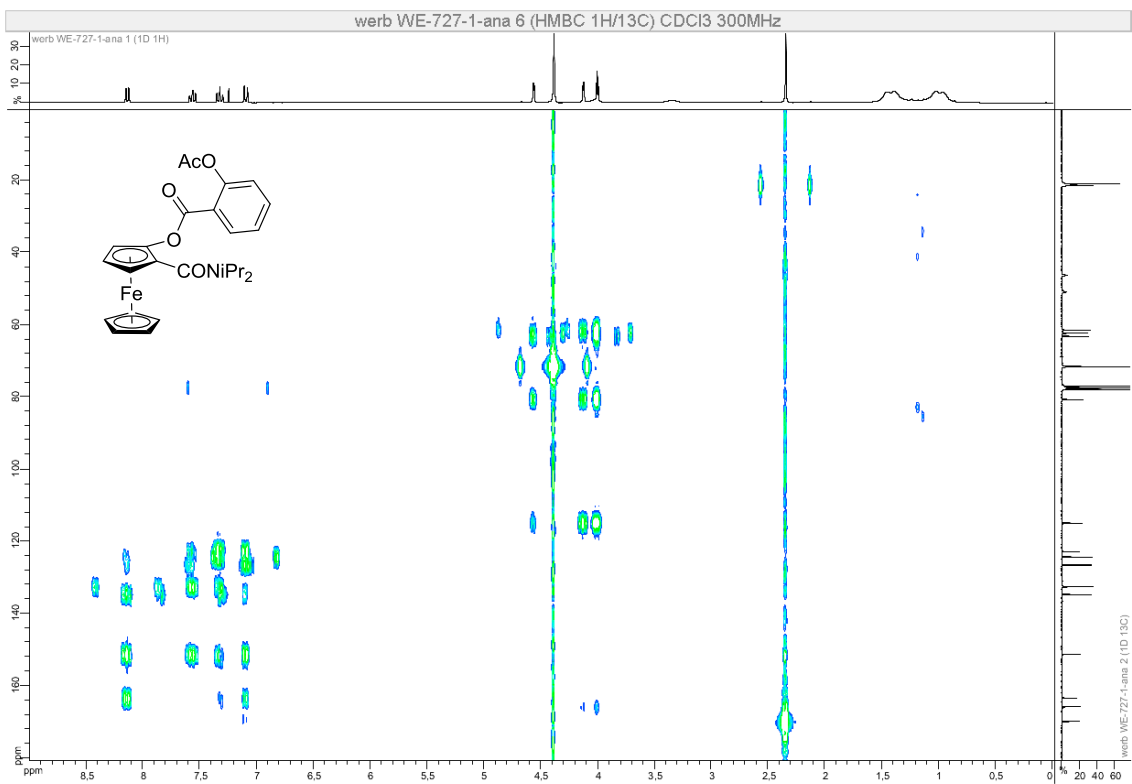
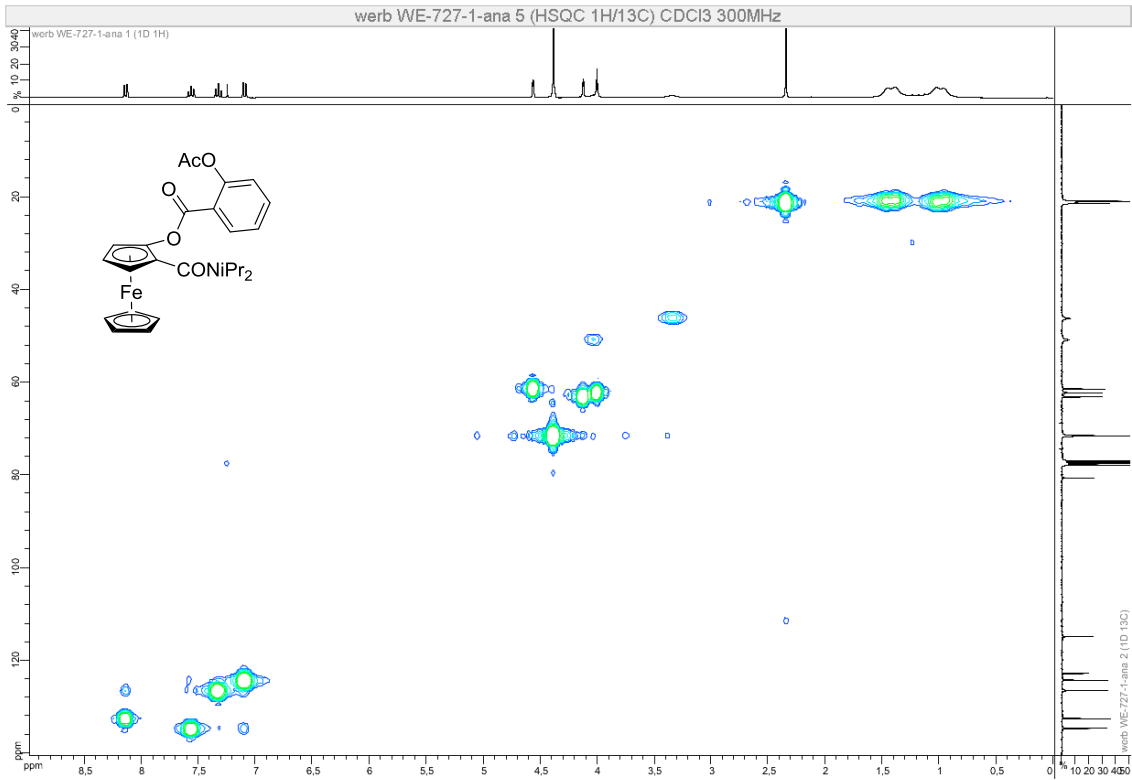




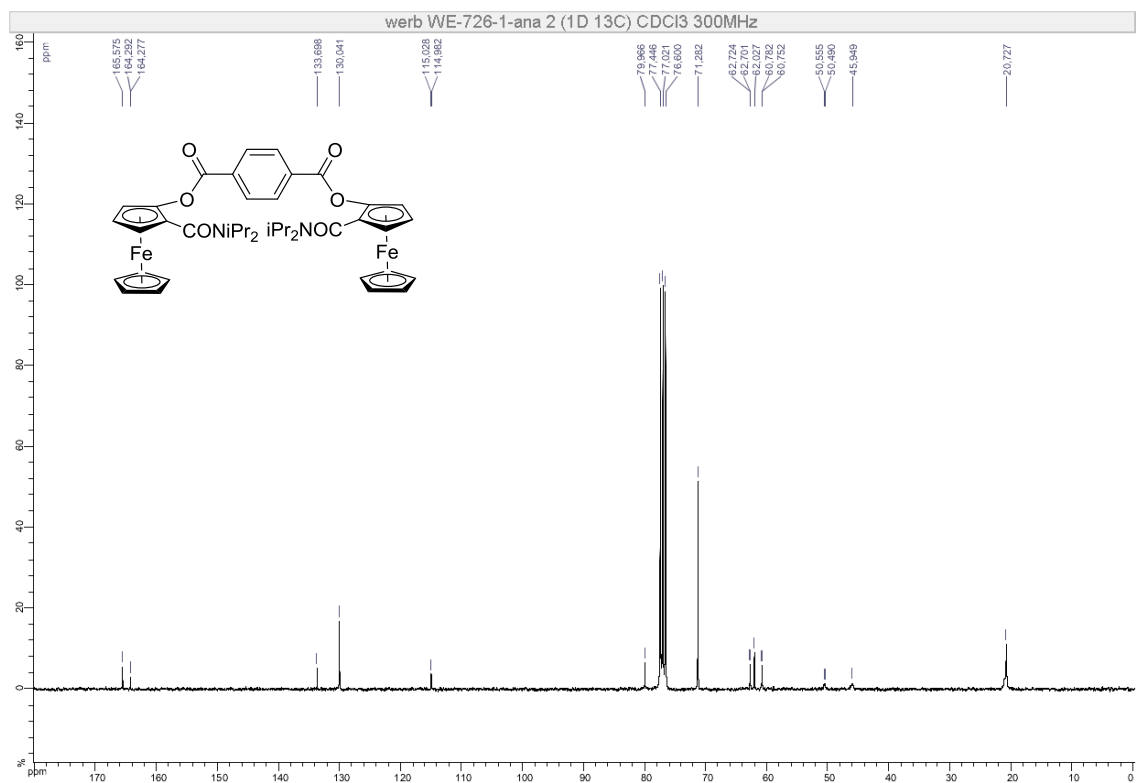
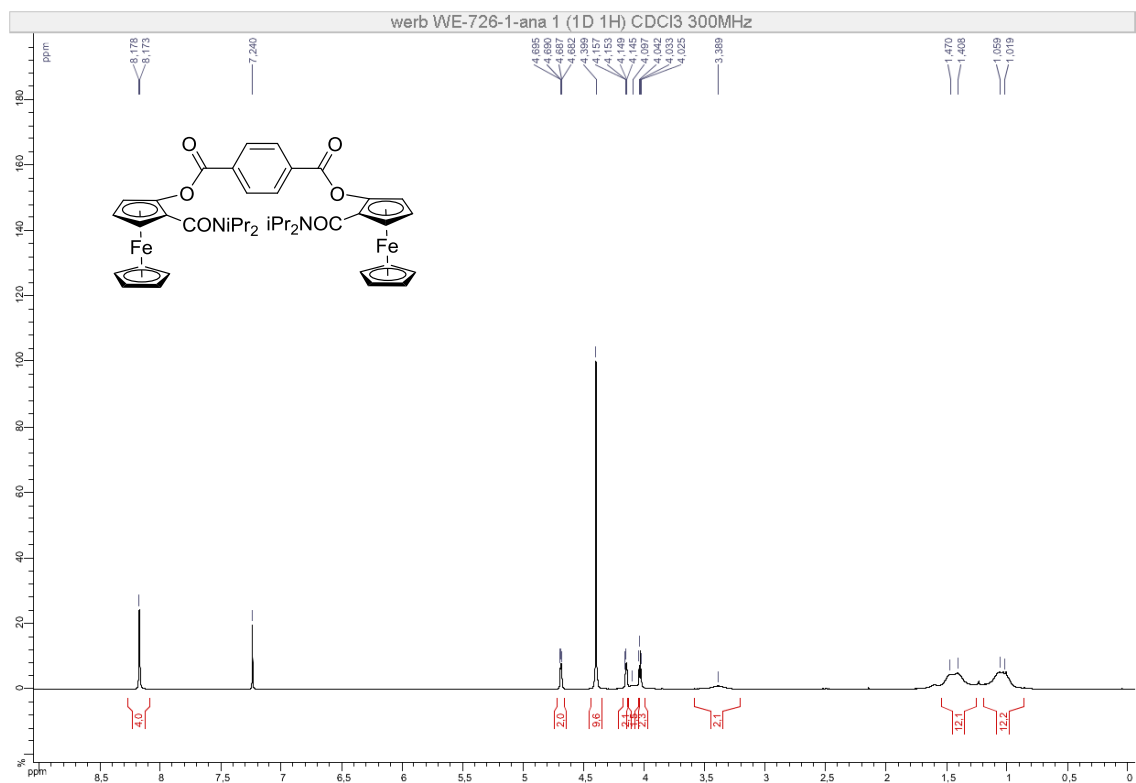
Compound (\pm)-14

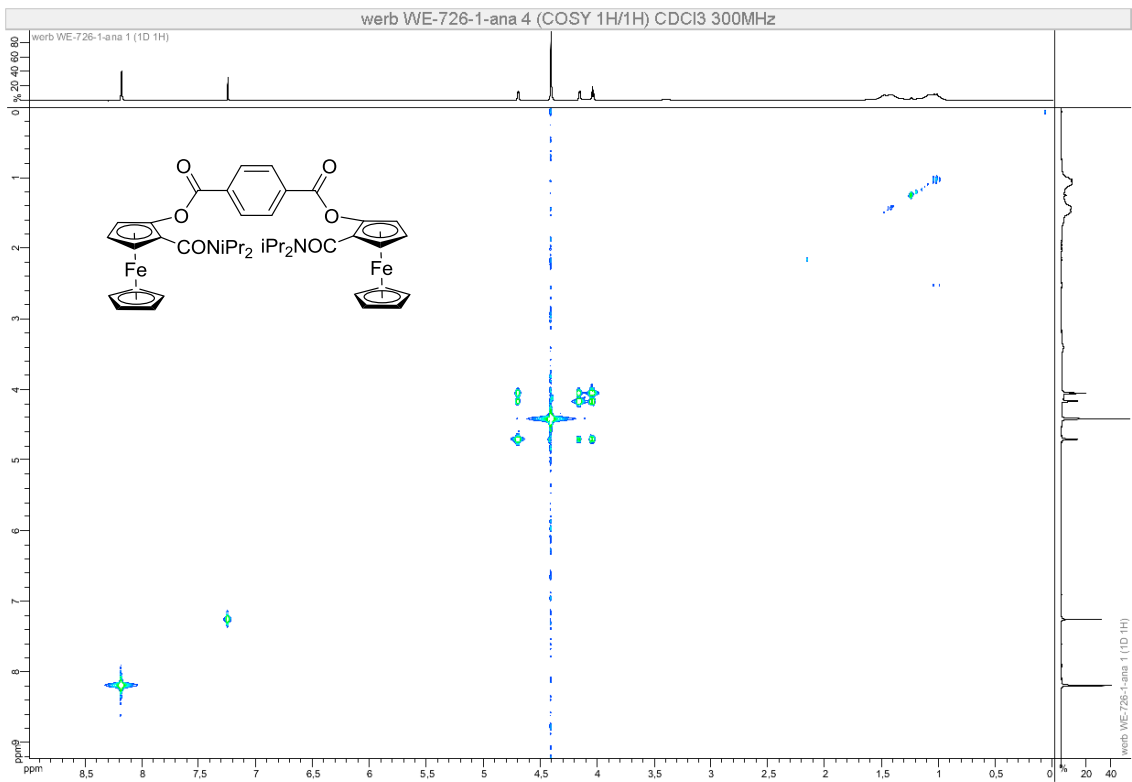
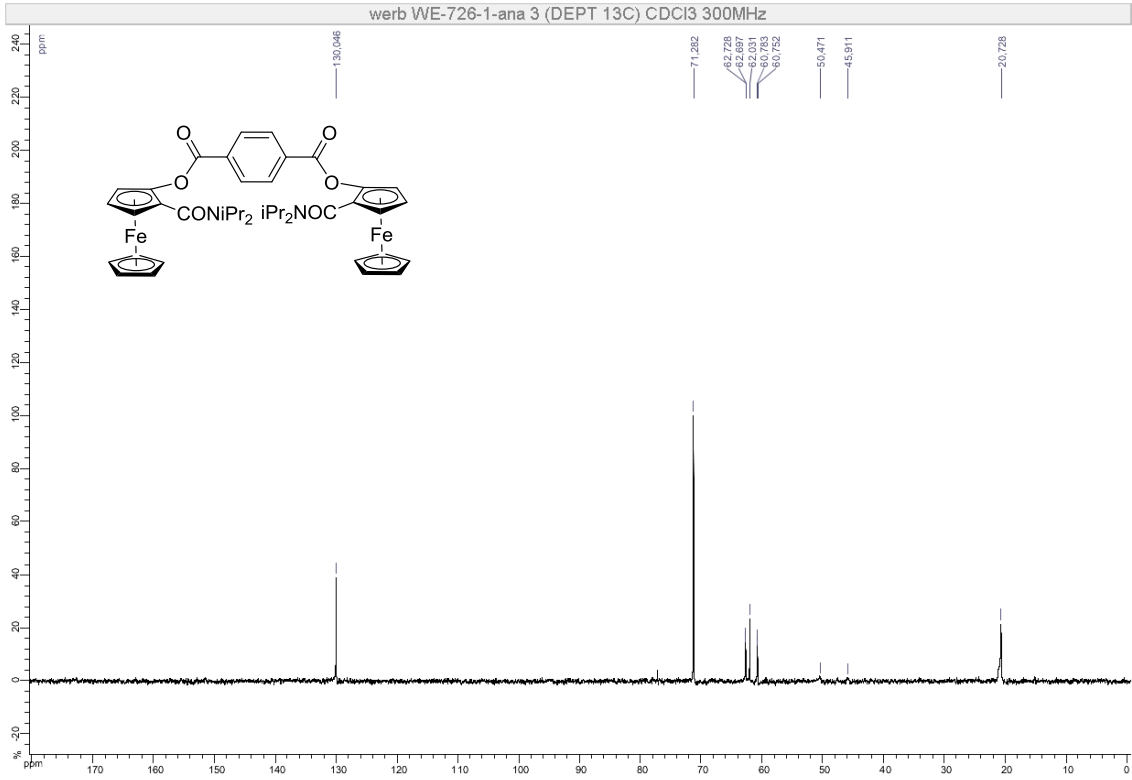


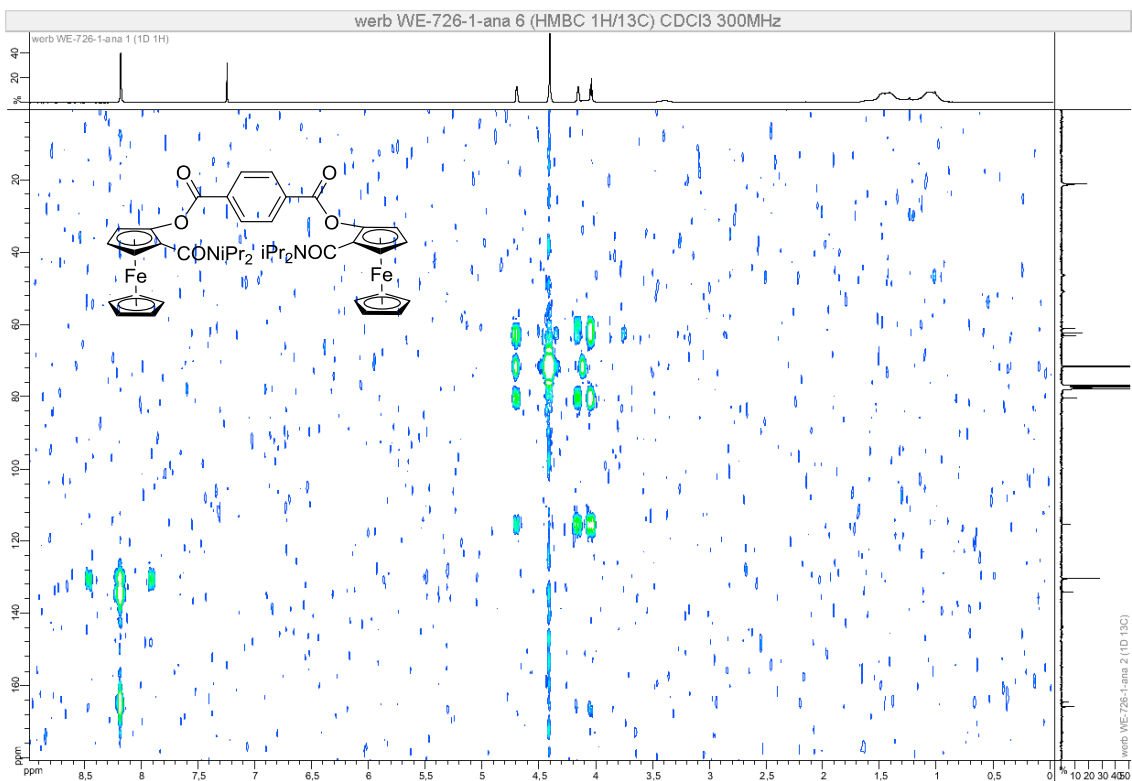
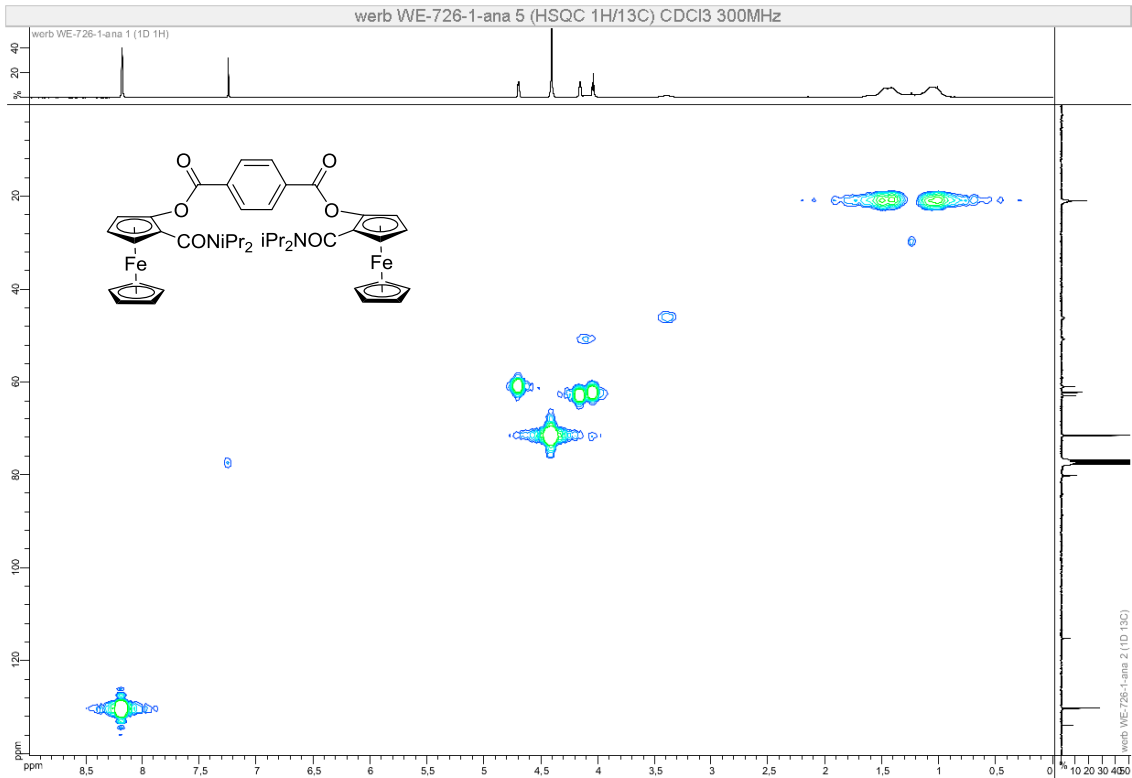




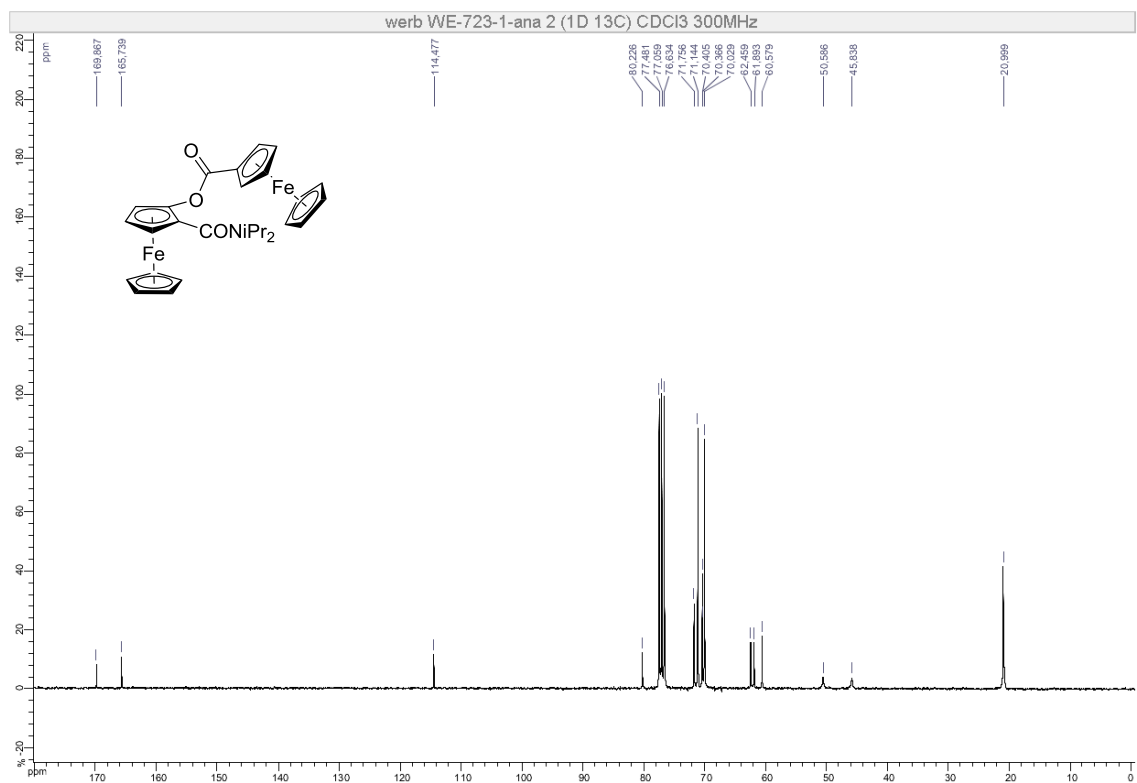
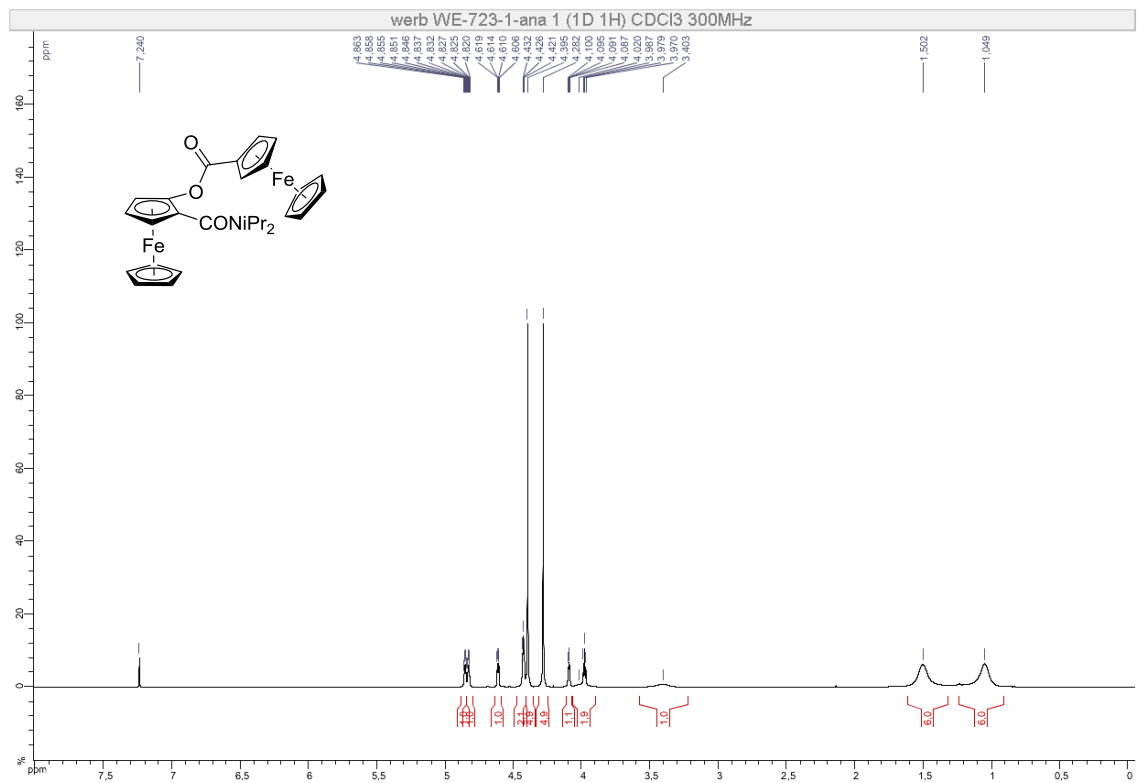
Compound (\pm)-15

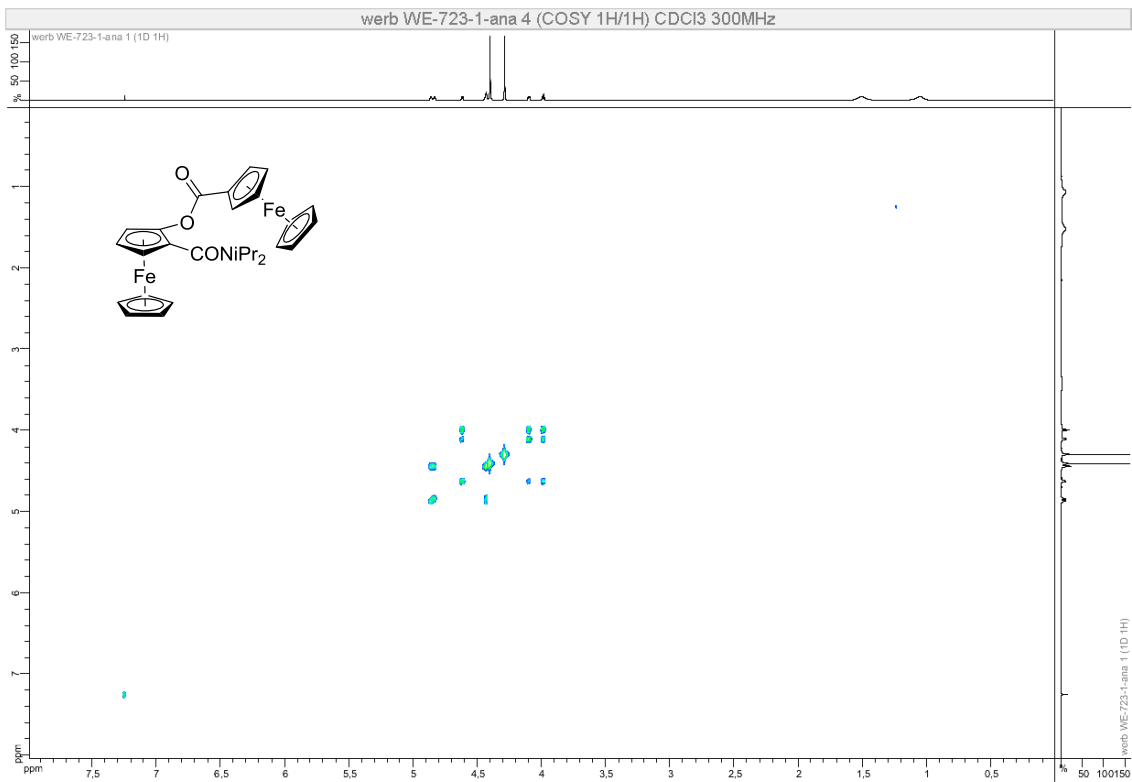
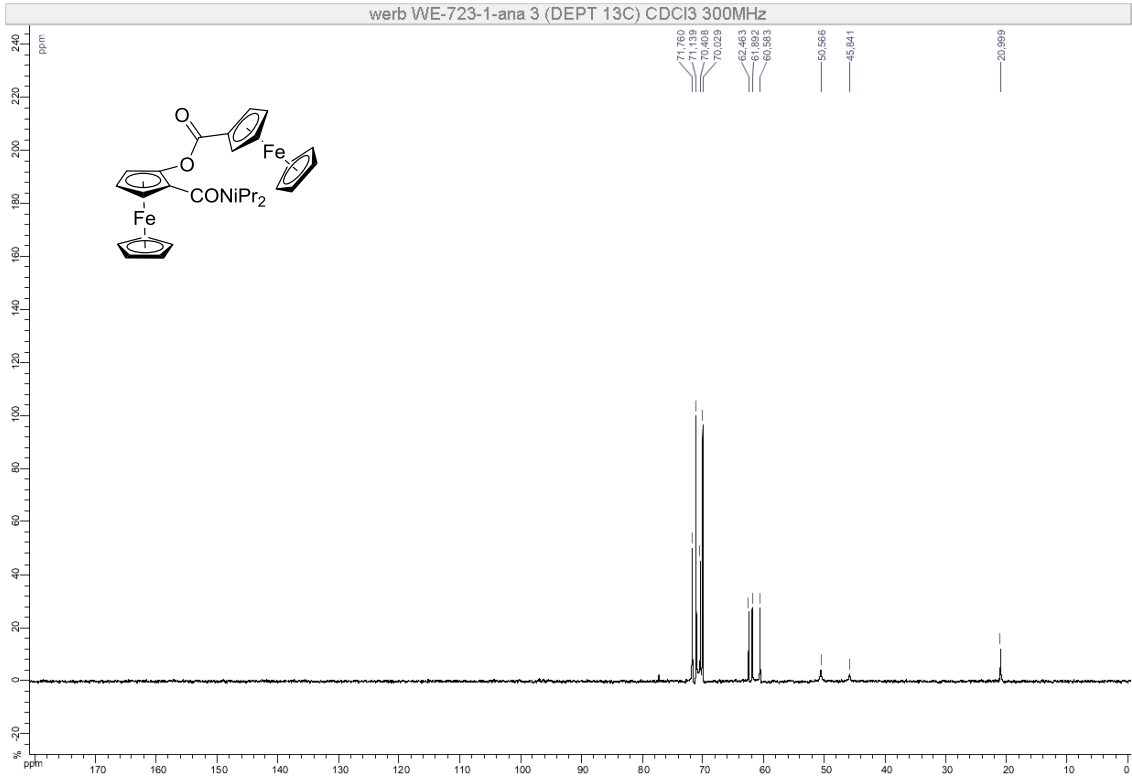


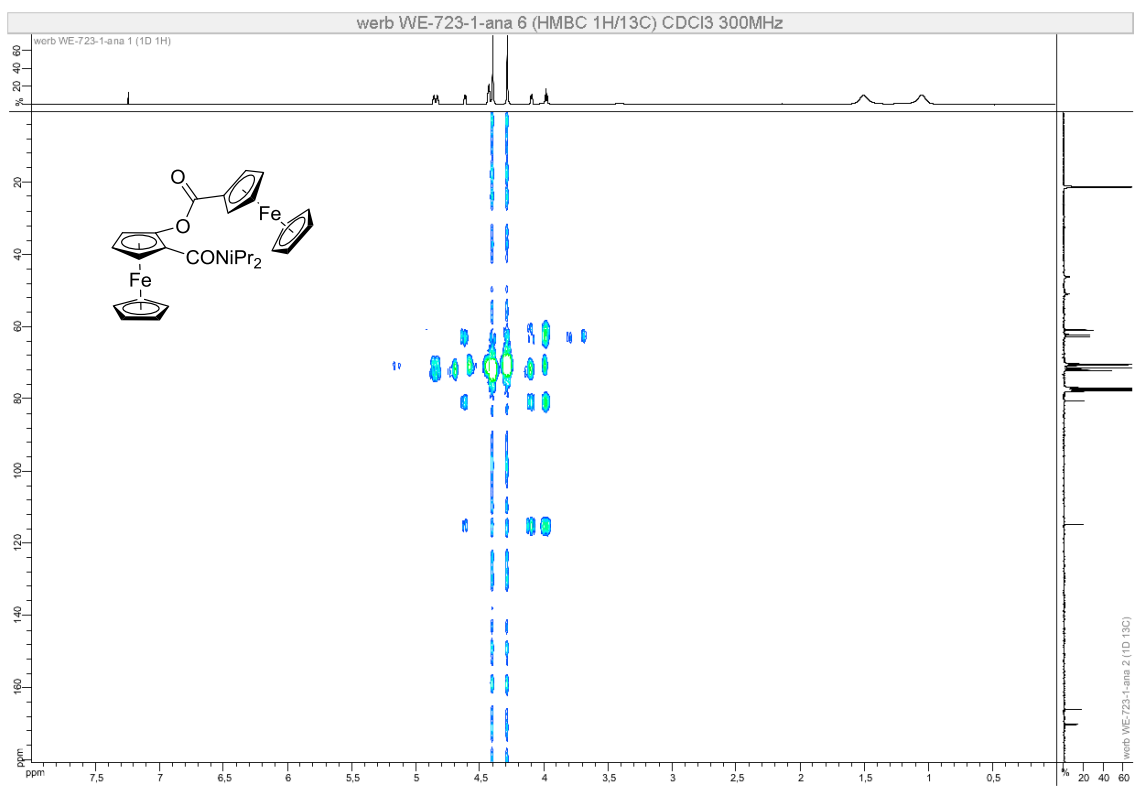
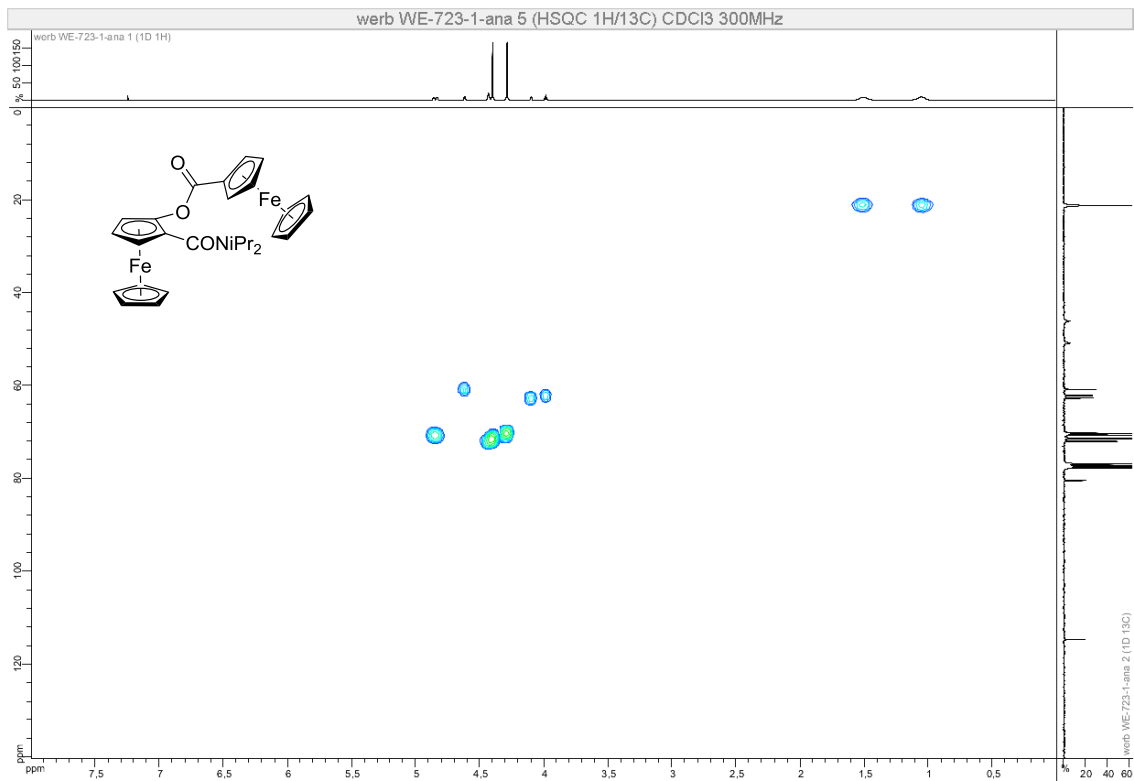




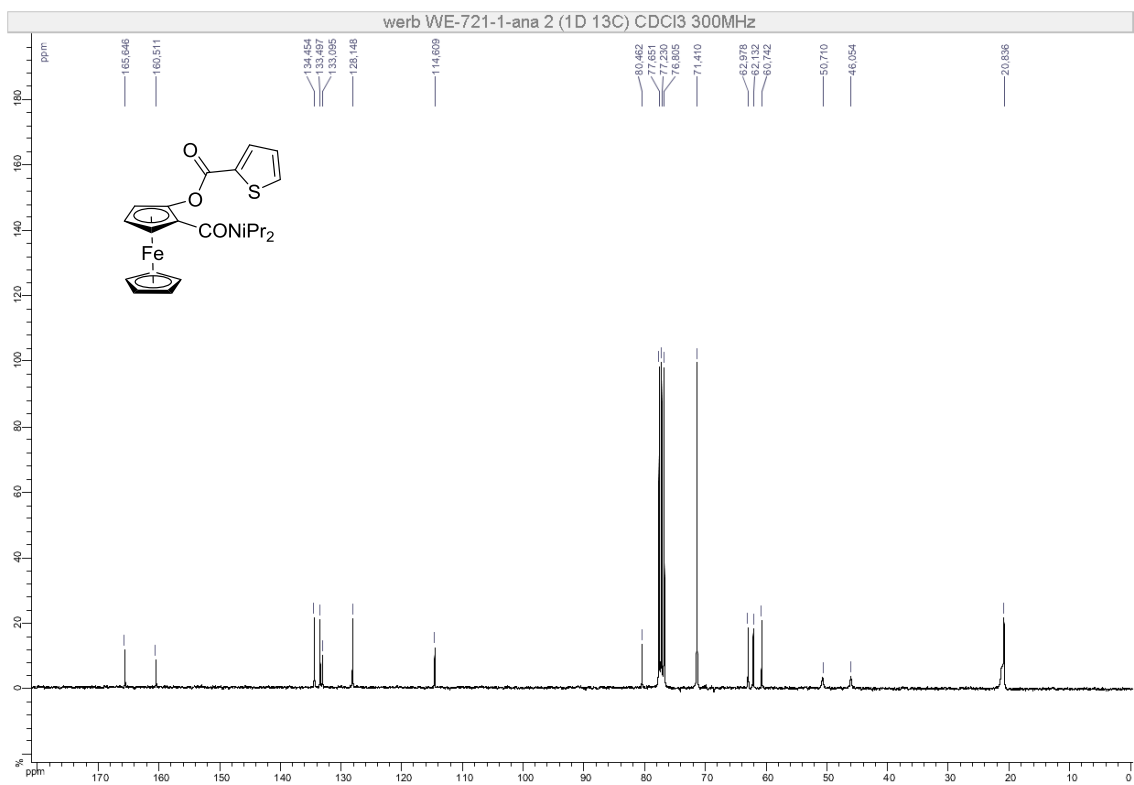
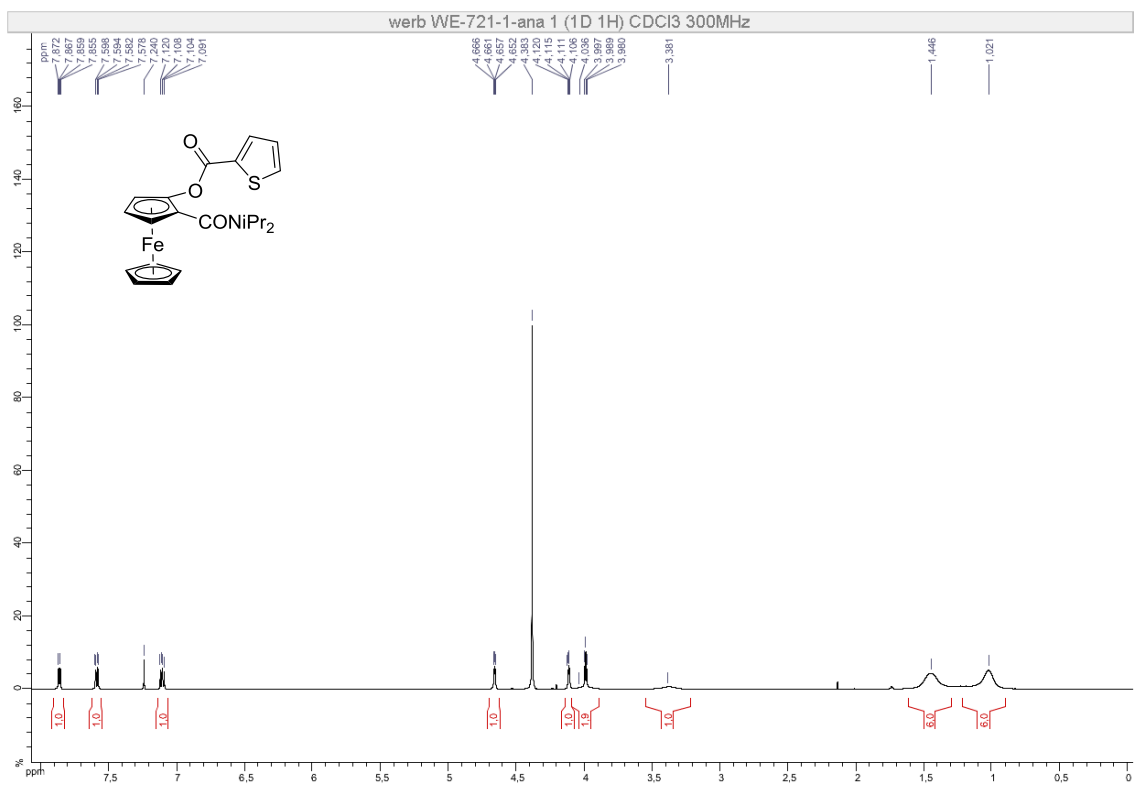
Compound (±)-16

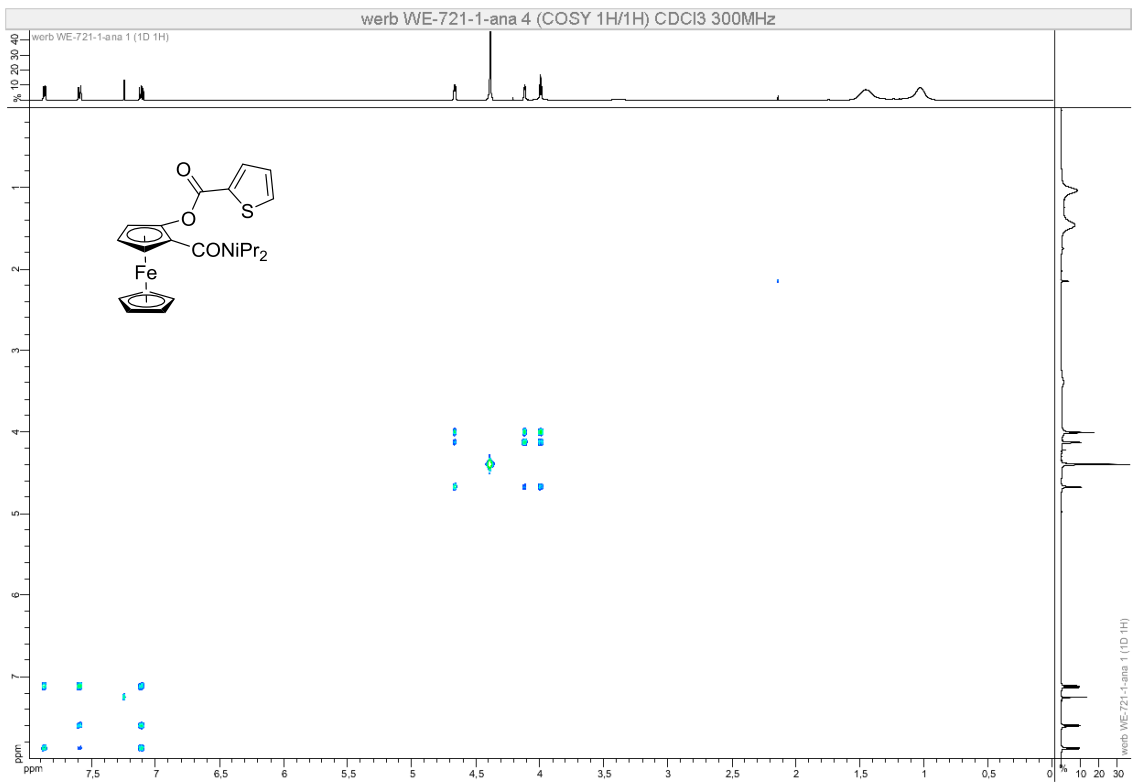
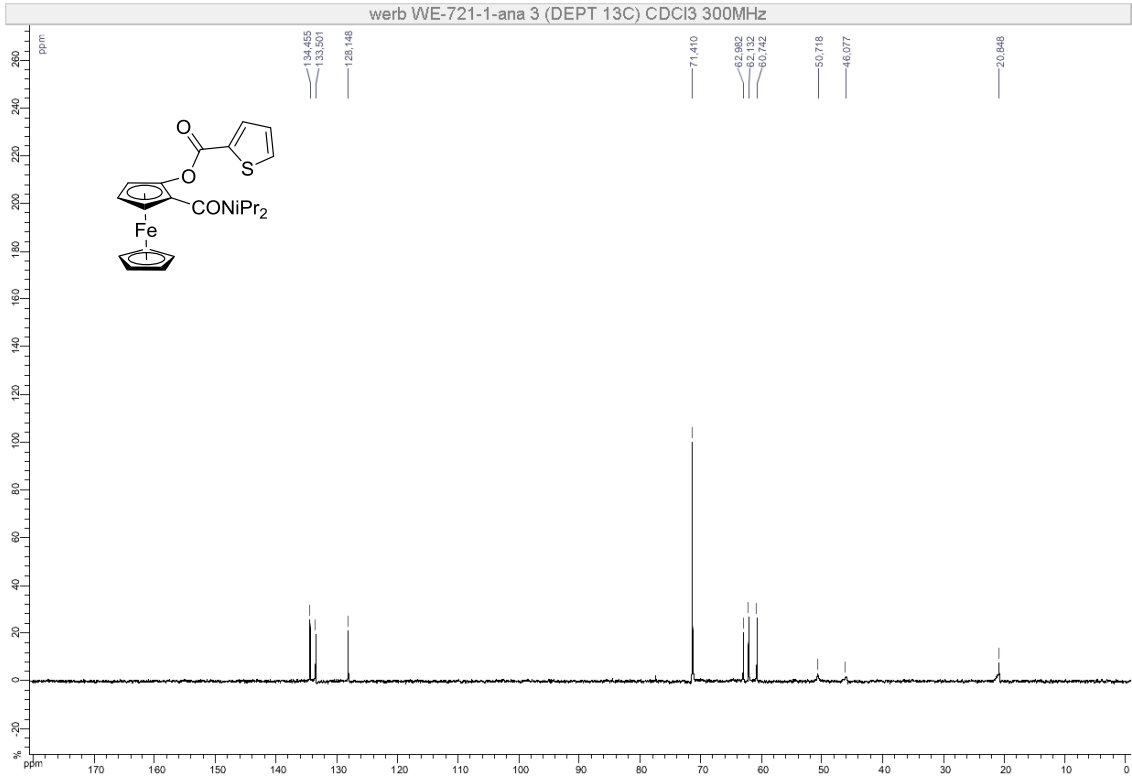


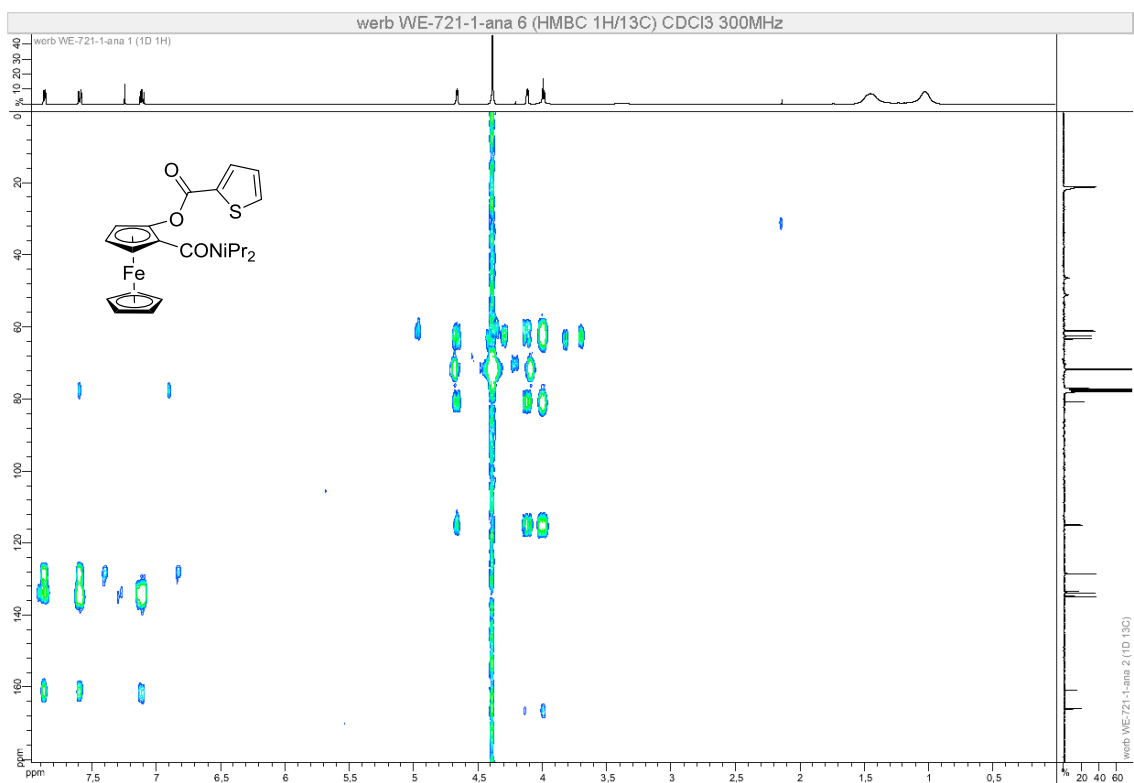
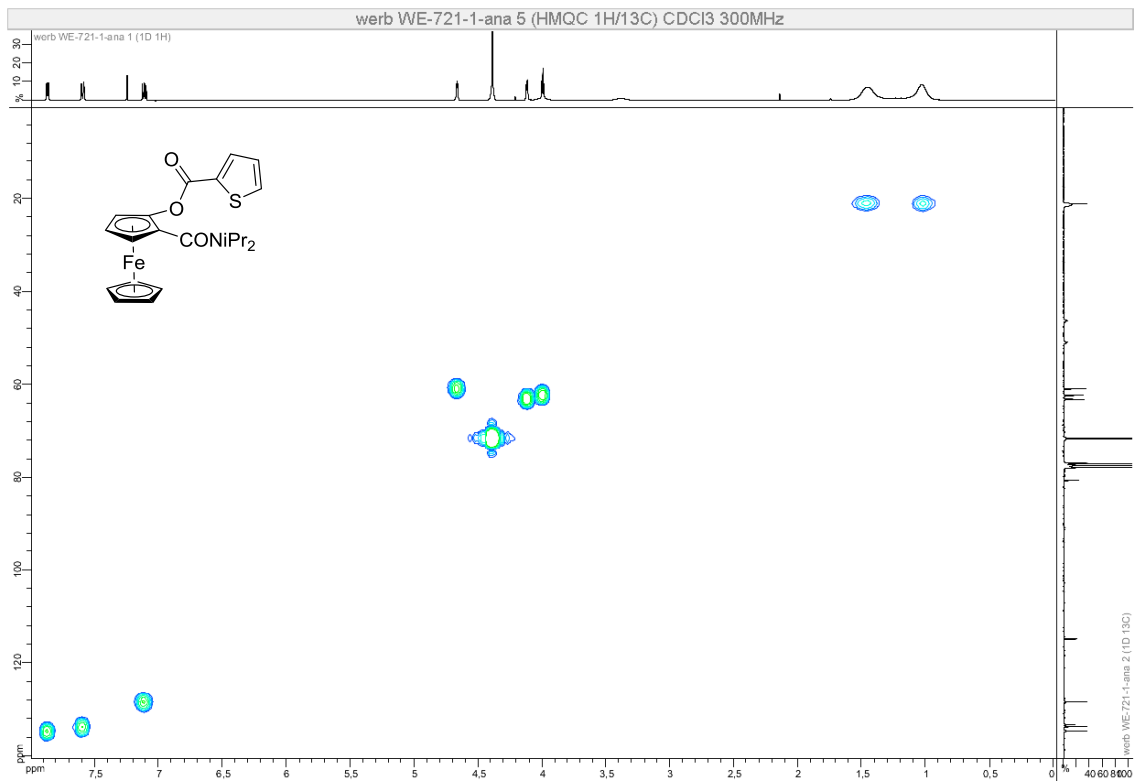




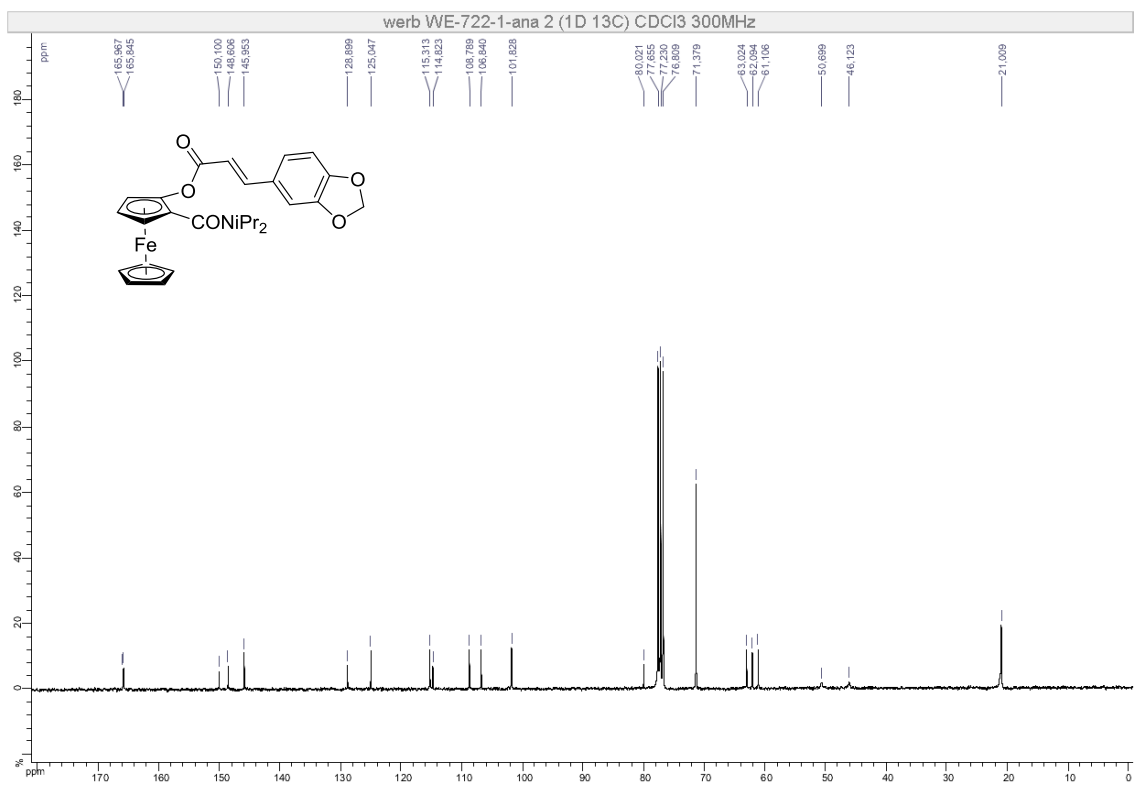
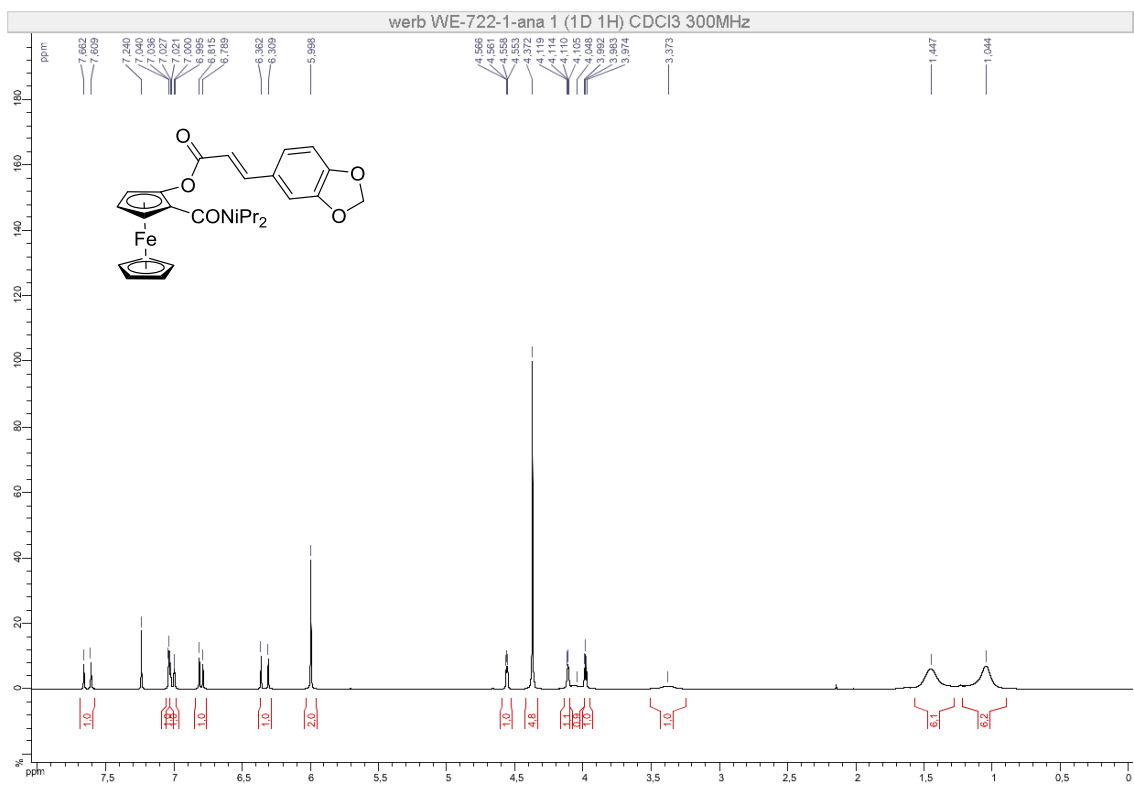
Compound (\pm)-17

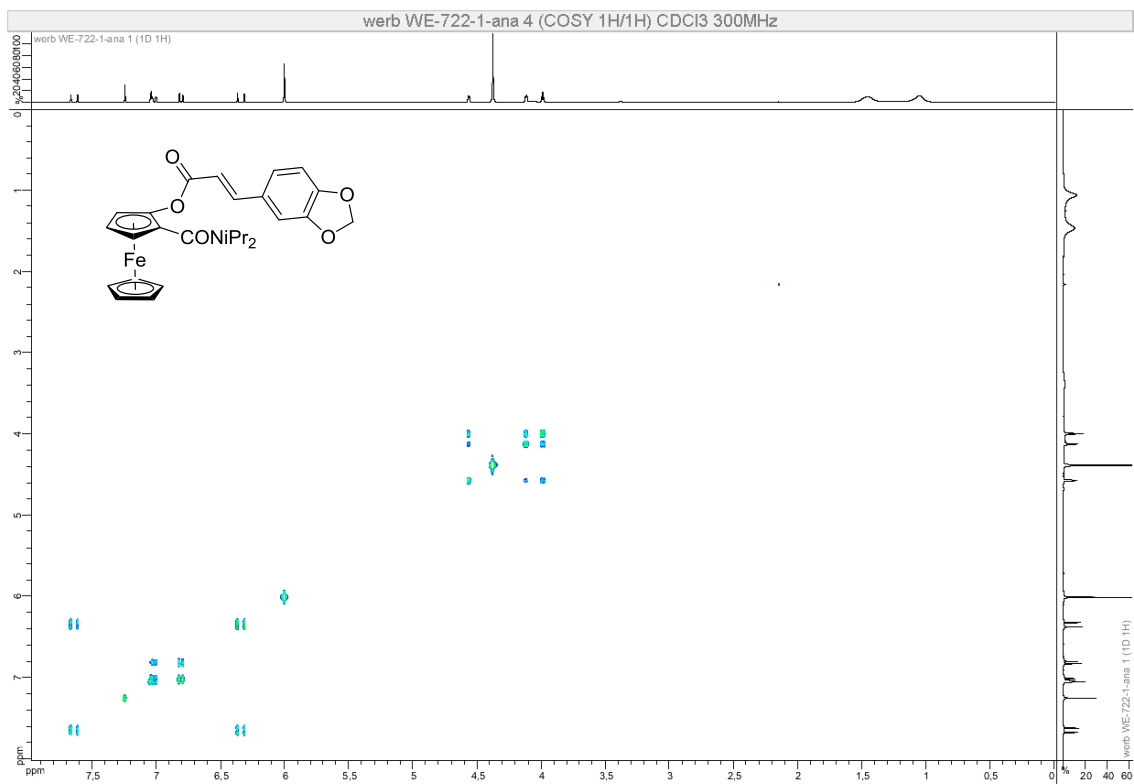
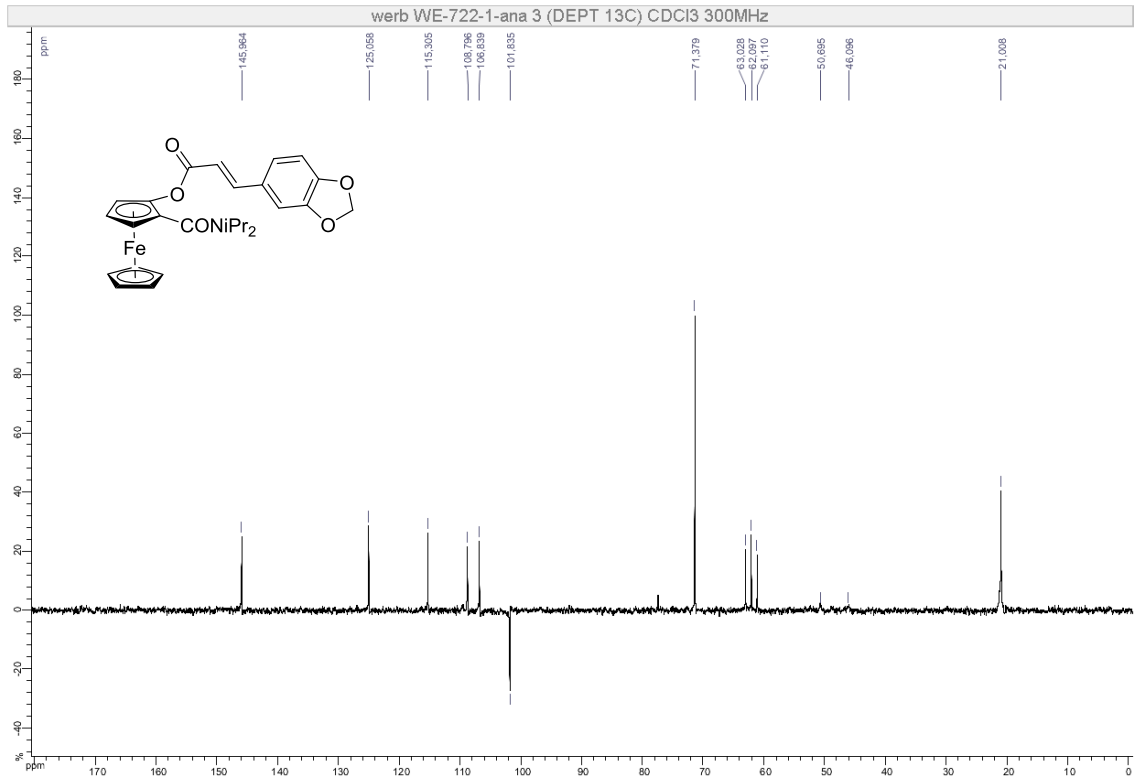


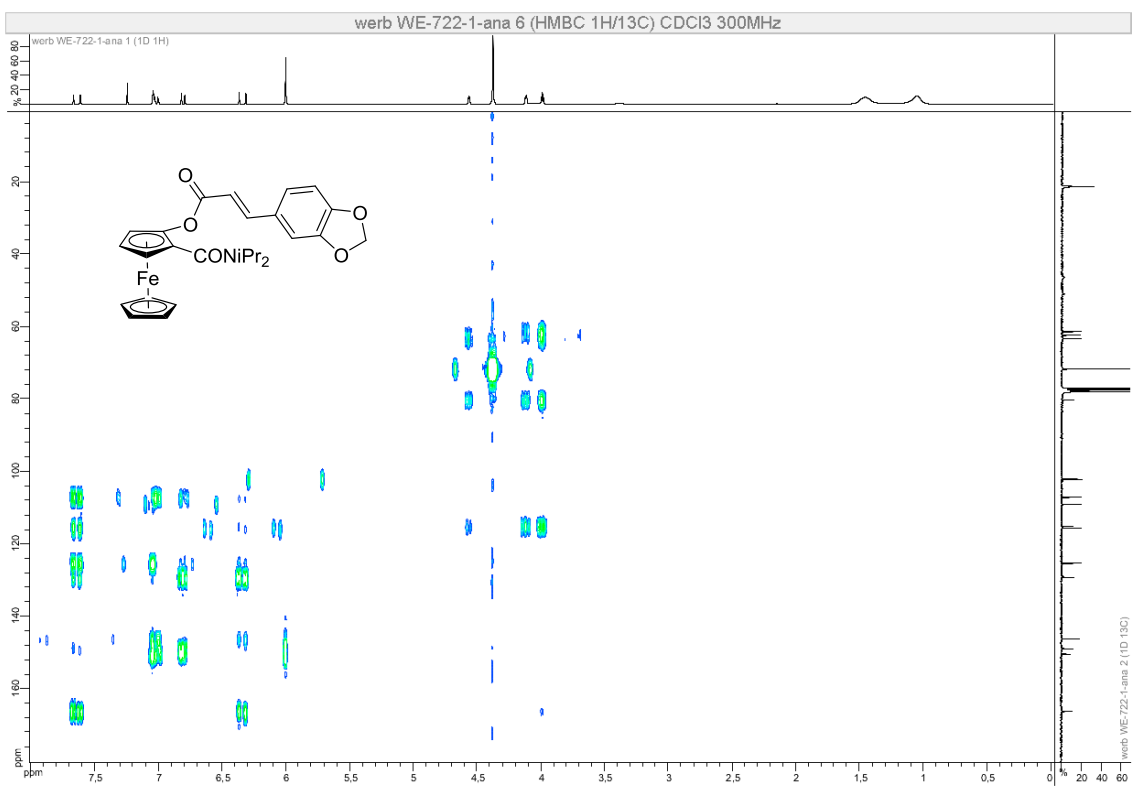
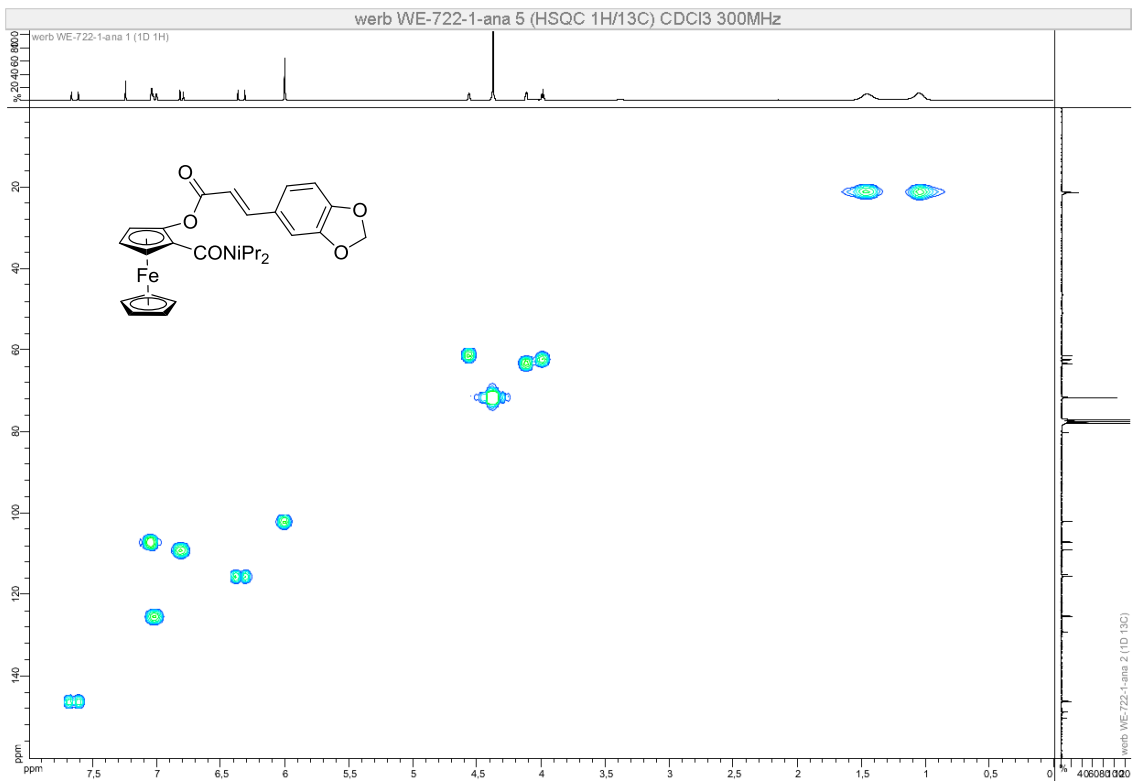




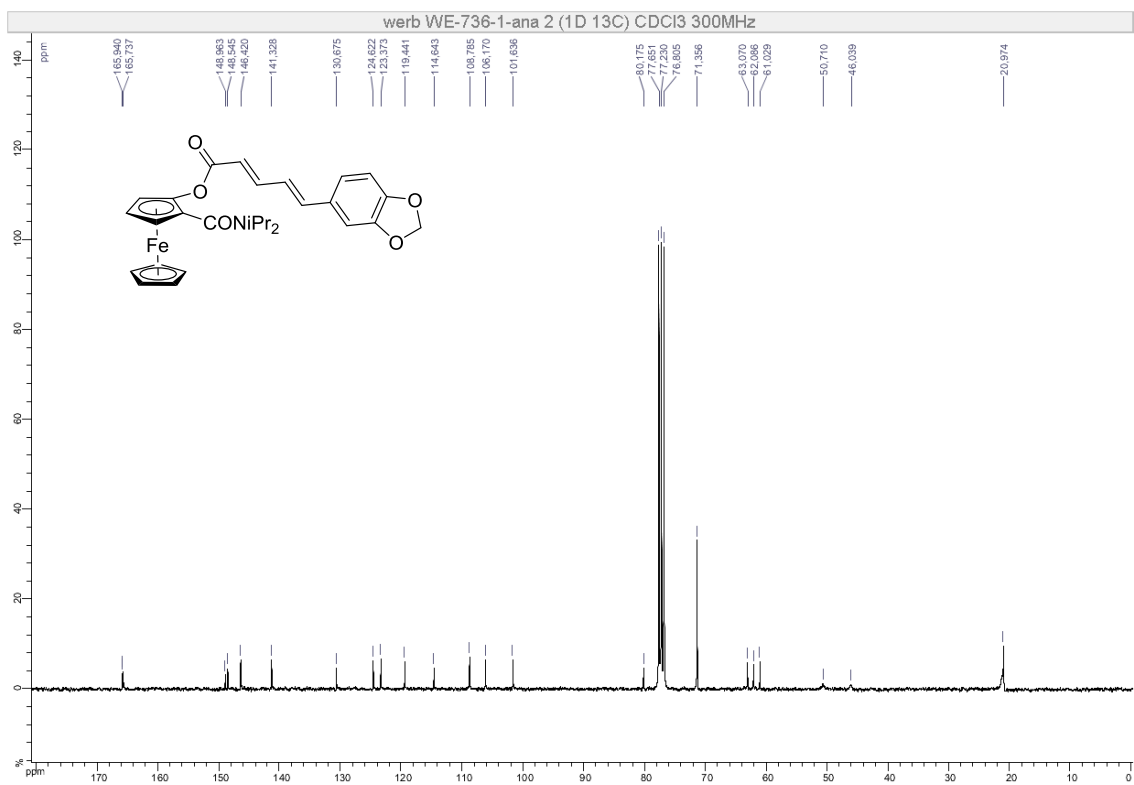
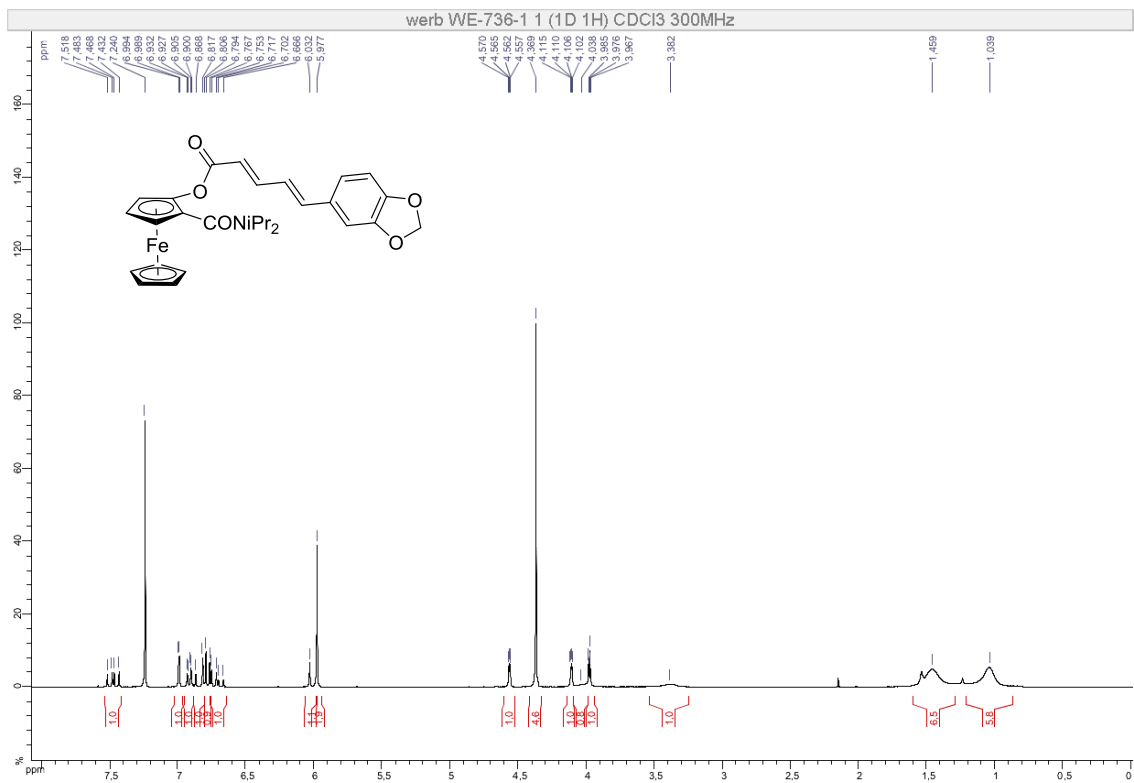
Compound (\pm)-18

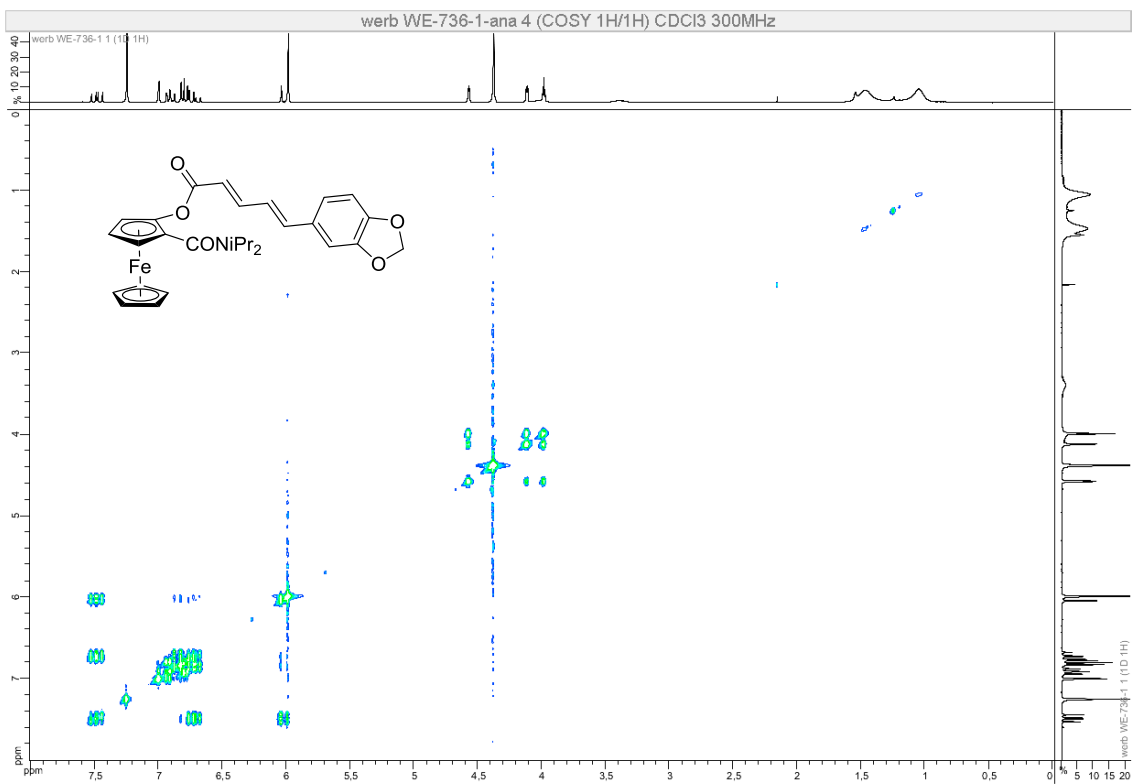
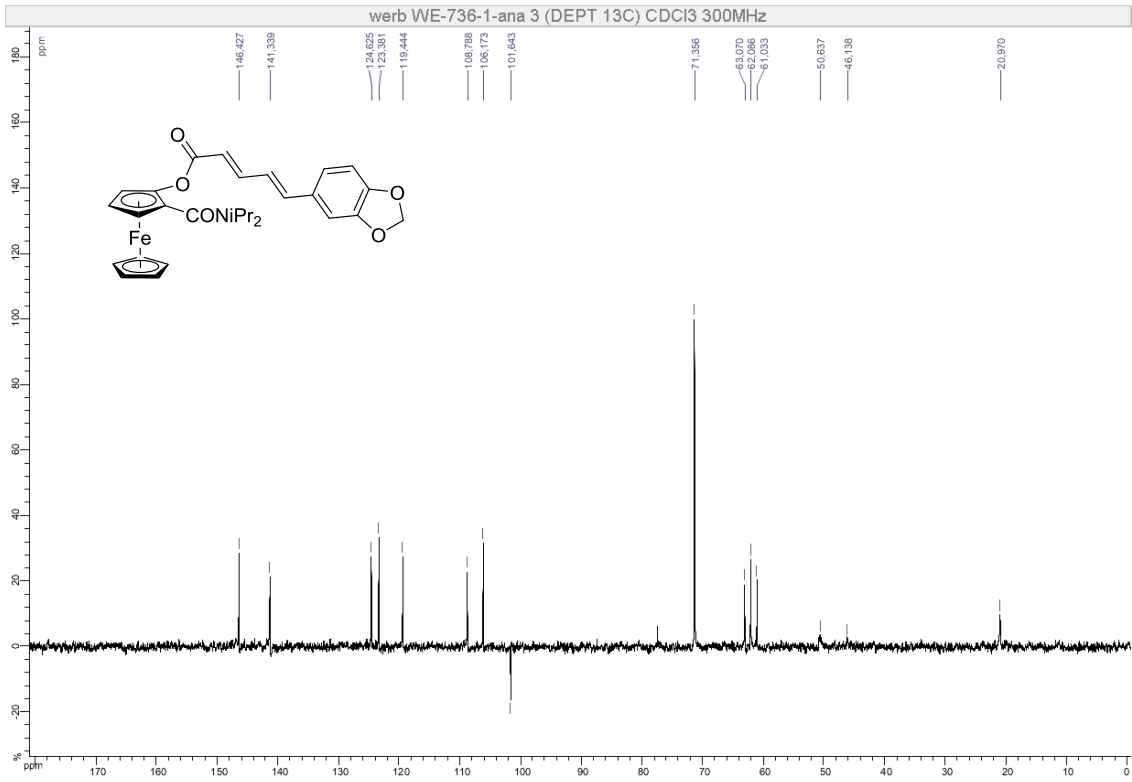


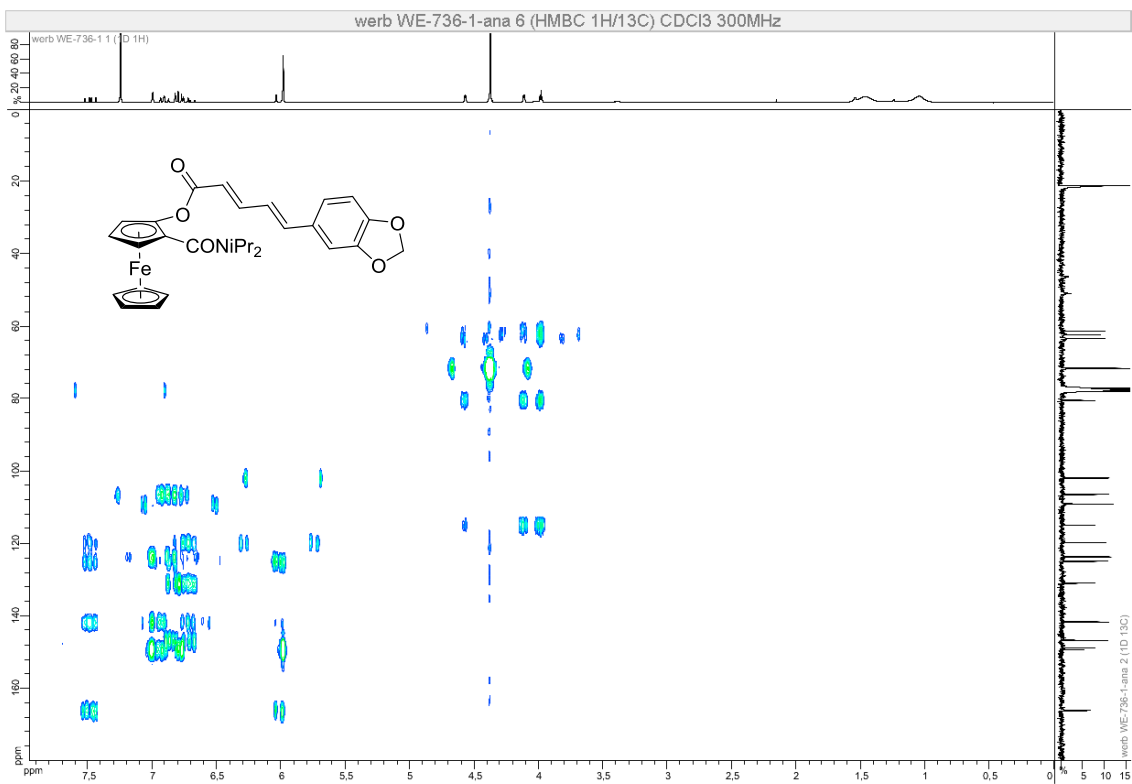
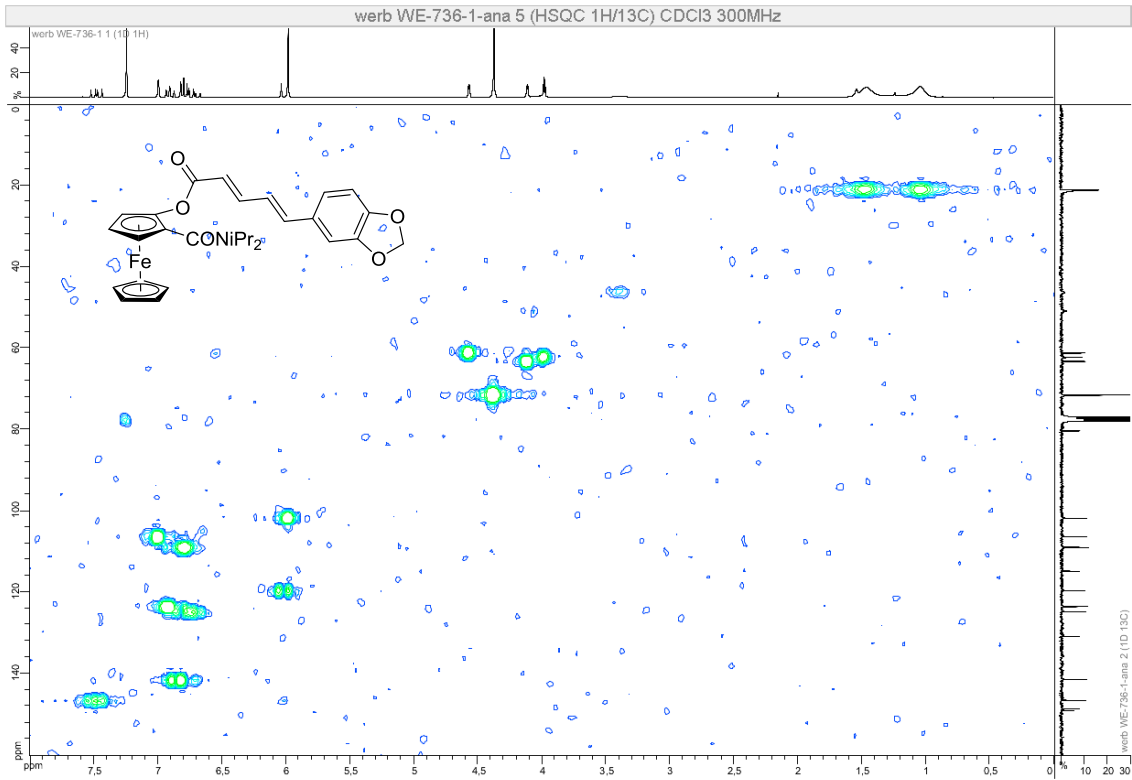




Compound (\pm)-19







Selected NOESY correlations observed by 2D NMR

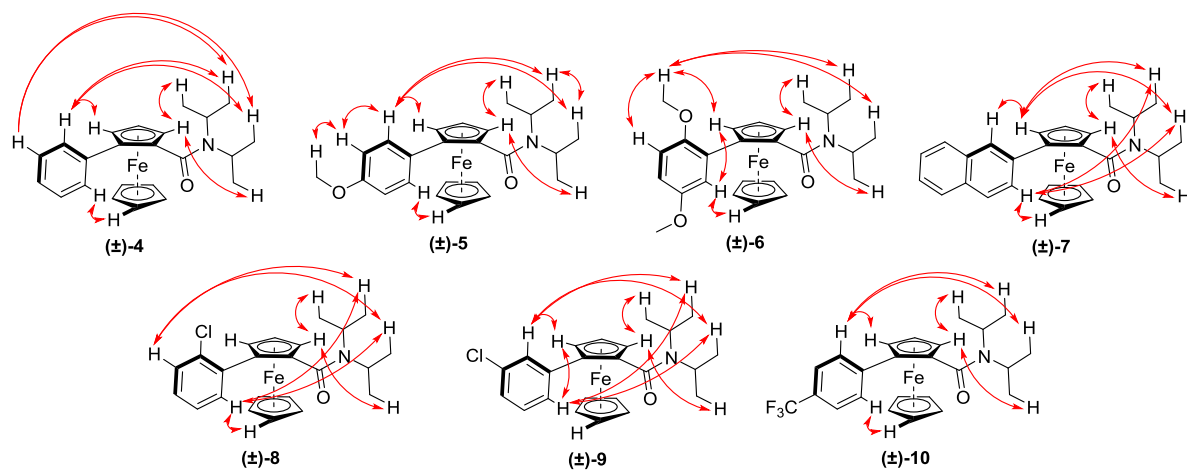
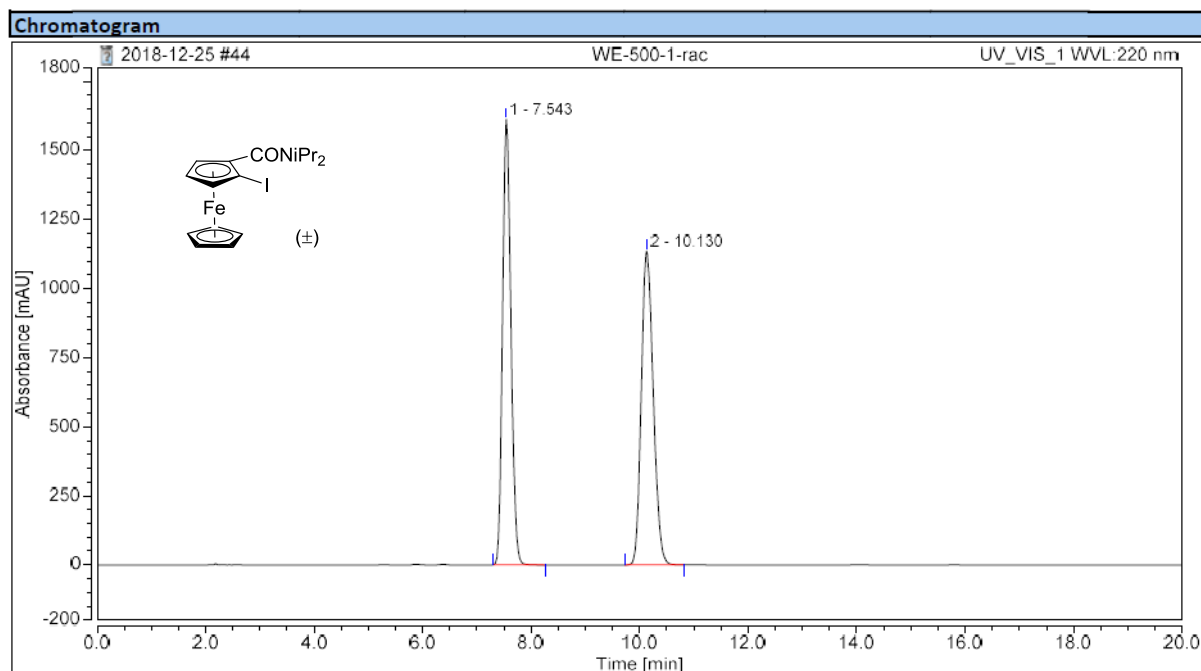


Figure 17.

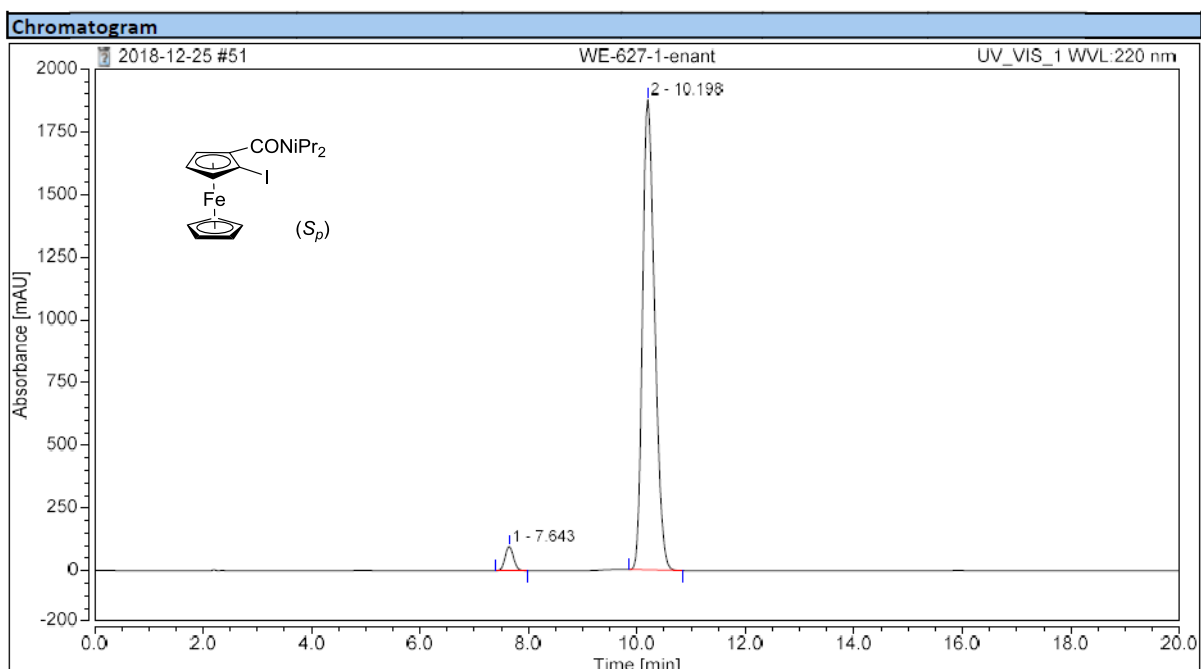
HPLC Chromatograms

Compounds (\pm)- and (S_p)-2



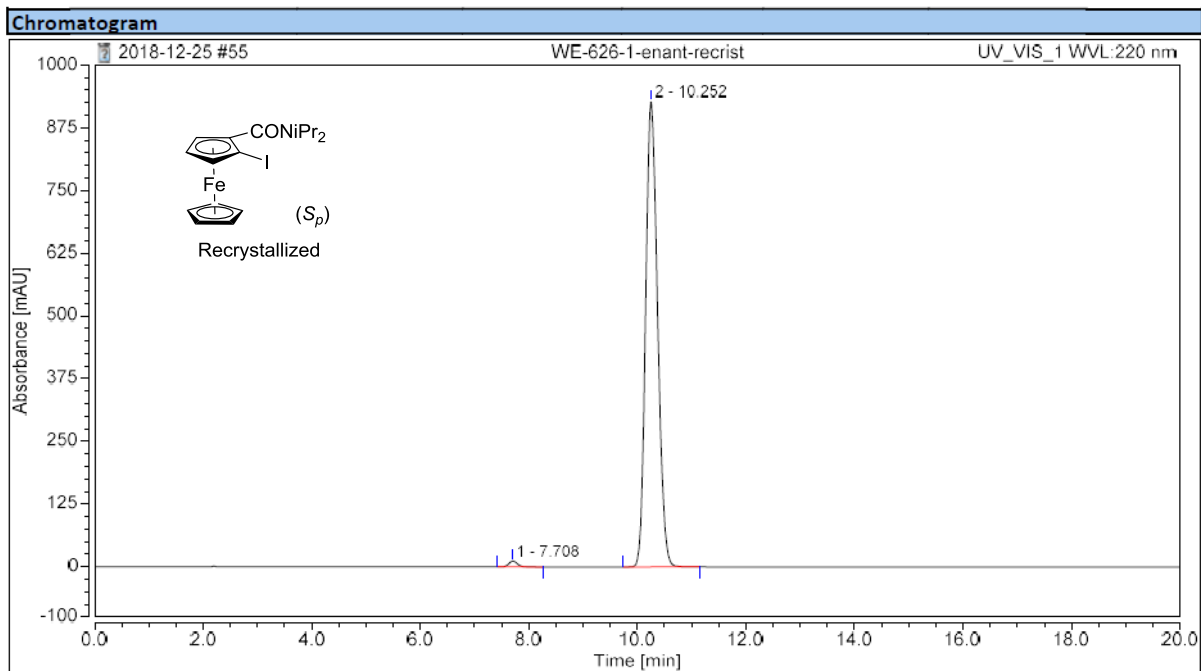
Integration Results

No.	Peak Name	Retention Time min	Area mAU*min	Height mAU	Relative Area %	Relative Height %	Amount n.a.
1		7.543	288.660	1612.105	49.99	58.66	n.a.
2		10.130	288.764	1135.984	50.01	41.34	n.a.
Total:			577.424	2748.089	100.00	100.00	



Integration Results

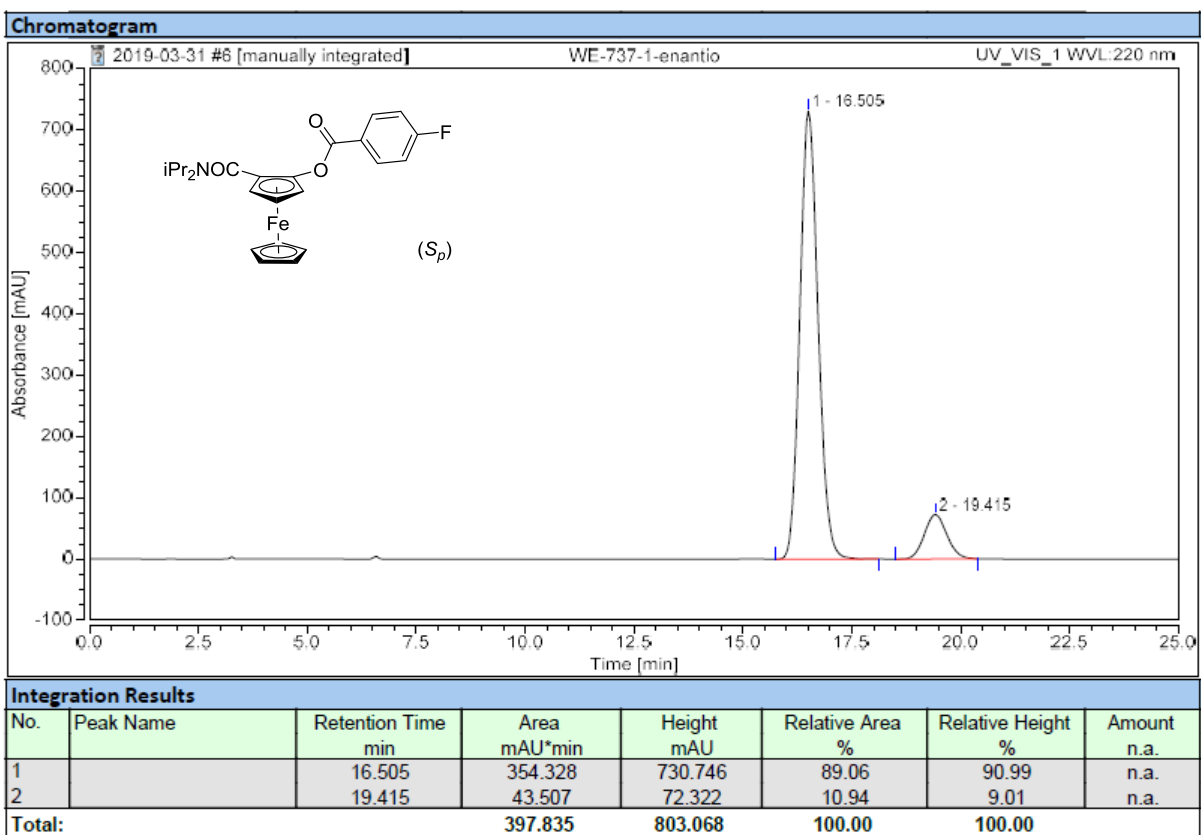
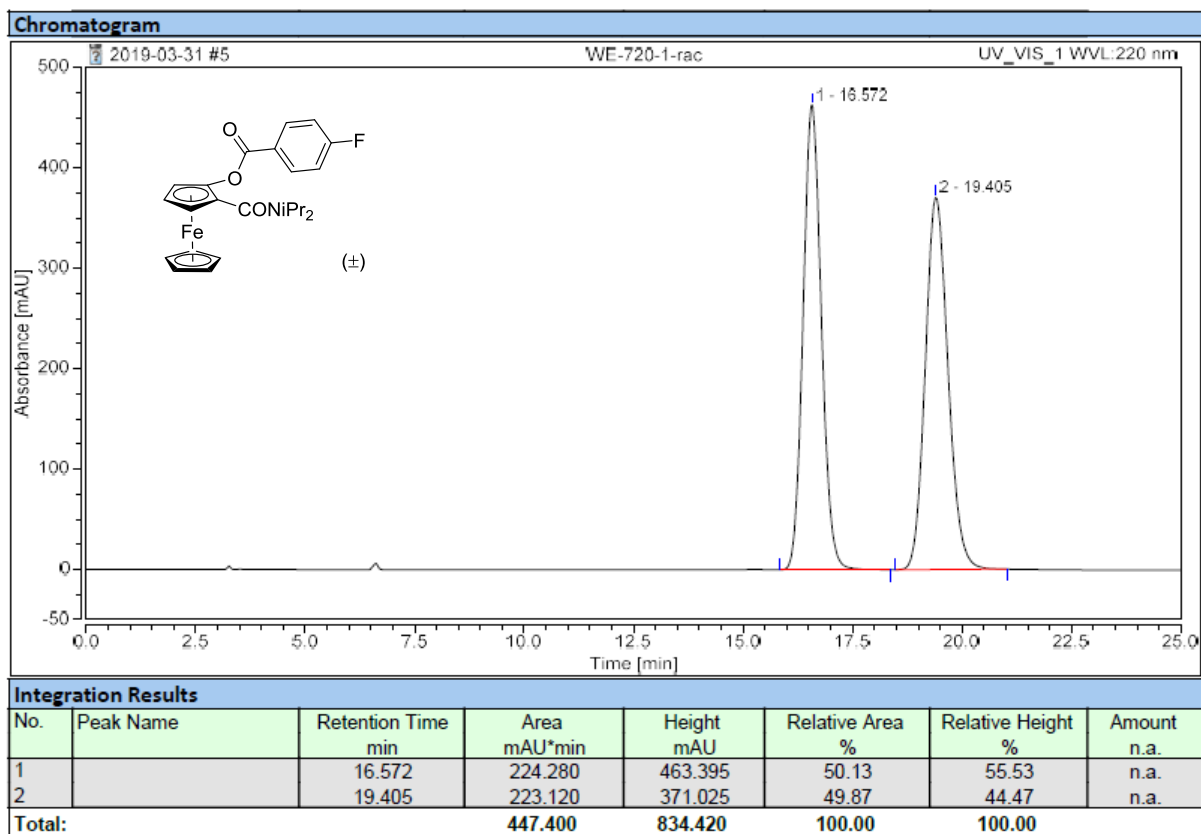
No.	Peak Name	Retention Time min	Area mAU*min	Height mAU	Relative Area %	Relative Height %	Amount n.a.
1		7.643	17.482	97.481	3.48	4.94	n.a.
2		10.198	484.364	1875.323	96.52	95.06	n.a.
Total:			501.846	1972.805	100.00	100.00	



Integration Results

No.	Peak Name	Retention Time min	Area mAU*min	Height mAU	Relative Area %	Relative Height %	Amount n.a.
1		7.708	2.090	11.604	0.88	1.24	n.a.
2		10.252	235.014	927.033	99.12	98.76	n.a.
Total:			237.104	938.637	100.00	100.00	

Compounds (\pm)- and (S_p)-11



References

1. Sheldrick, G. *Acta Crystallogr. Sect. A* **2015**, *71*, 3-8.
2. Sheldrick, G. *Acta Crystallogr. C* **2015**, *71*, 3-8.